

**ARTERIAL RESPONSE TO  
LOCAL MECHANICAL VARIABLES IN ORGAN CULTURE:  
THE EFFECTS OF CIRCUMFERENTIAL AND SHEAR STRESS**

A Thesis  
Presented to  
The Academic Faculty

by

Brian H. Wayman

In Partial Fulfillment  
of the Requirements for the Degree  
Doctor of Philosophy in the  
School of Mechanical Engineering

Georgia Institute of Technology  
May 2007

**COPYRIGHT © 2007 BY BRIAN H. WAYMAN**

**ARTERIAL RESPONSE TO  
LOCAL MECHANICAL VARIABLES IN ORGAN CULTURE:  
THE EFFECTS OF CIRCUMFERENTIAL AND SHEAR STRESS**

Approved by:

Dr. Raymond Vito, Advisor  
School of Mechanical Engineering  
*Georgia Institute of Technology*

Dr. Alexander Rachev  
School of Mechanical Engineering  
*Georgia Institute of Technology*

Dr. Robert Guldberg  
School of Mechanical Engineering  
*Georgia Institute of Technology*

Dr. Todd McDevitt  
School of Biomedical Engineering  
*Georgia Institute of Technology*

Dr. Marc Levenston  
Department of Mechanical Engineering  
*Stanford University*

Date Approved: April 6, 2007

“Hold fast to dreams...”

Langston Hughes

## ACKNOWLEDGEMENTS

There are a number of people whom I would like to thank for their support in helping me achieve this milestone. First, I would like to thank my advisor, Dr. Raymond Vito, for supporting me over the years and guiding me down the path to becoming an independent researcher. To Dr. Alexander Rachev, thank you for working with me diligently to refine my technical skills and challenging me to think critically as a researcher. Additionally, I'd like to thank my committee members for agreeing to serve on my committee and review my work: Dr. Marc Levenston, Dr. Robert Guldberg, and Dr. Todd McDevitt.

I would also like to thank current and former members of the Vito Lab for their many insightful discussions that have helped to improve the quality of my work and for making my time in the lab enjoyable. To Dr. Peter Carnell, I've developed a great friendship with you and I thank you for challenging me both intellectually (through our discussions about research) and physically (by encouraging me to run). I truly appreciate all that you and Nancy have done to help me during the final stages my dissertation process. To Lori Lowder, I really appreciate your friendship over the years and your willingness to help me whenever needed, it has meant a lot to me. Thank you, Dr. Hai-Chao Han, for teaching me the organ culture techniques required to be successful in this project. Thank you, Dr. Pete Davis, for setting the standard for organ culture research in our lab. I appreciate you helping me get started running experiments.

There have been a number of people outside of the lab that have provided technical assistance and contributed greatly to this work. To Dr. Manu Platt, thank you very much for being a patient teacher. You really made learning molecular biology fun

for an engineer. To Tracey Couse, thank you for teaching me so much about histology. To Sha'Aqua Asberry, thank your for your help with histology in the latter stages of my work. To the machine shop, thank you for your excellent work on all of the parts you've made for me over the years. To Tommy Phillips, the USDA inspector, I always looked forward to sharing a laugh with you during my early morning trips to Holifield Farms.

I would like to thank Dr. Freeman Hrabowski, Ms. Earnestine Baker, and Mr. LaMont Toliver of the Meyerhoff Program at the University of Maryland Baltimore County for encouragement during this process. Thank you, Dr. Timmie Topoleski, for exposing me to the world of bioengineering, recognizing my talents, and giving me an opportunity to work in your lab.

I would like to thank the Whitaker Foundation and the National Institutes of Health Research Supplement for Underrepresented Minorities for financial support. In addition, I would like to thank the Georgia Tech STEP Program and Georgia Tech FACES Program for financial and academic support as well as for guidance along the way. This work was supported by National Institutes of Health Grant #R01HL70531. The tissue was generously donated by Holifield Farms.

Special thanks are due to my family and friends for there confidence in me and encouragement during this process. To my parents, Henry and Michele Wayman, thank you for allowing me to dream and then encouraging me pursue those dreams. To my sister, Dawn, thank you for your encouragement and for lending a listening ear when I needed it. To my extended family, thank you for the encouraging words along the way. To my son, Donovan, thank you for the bringing a joy that I never knew life could bring. Finally, to my wife, Dr. Annica Wayman, thank you for your rock solid belief in me and

your constant encouragement. I appreciate your sacrifice and patience during this process.

## TABLE OF CONTENTS

ACKNOWLEDGEMENTS .....	iv
TABLE OF CONTENTS.....	vii
LIST OF TABLES .....	xi
LIST OF FIGURES .....	xii
LIST OF SYMBOLS AND ABBREVIATIONS .....	xvi
SUMMARY .....	xix
INTRODUCTION .....	1
1.1 Cardiovascular Disease .....	1
1.2 Structure and Function of Arteries .....	1
1.3 Arterial Remodeling .....	5
1.4 Organ Culture Studies .....	9
1.5 Mathematical Models of Remodeling .....	15
OBJECTIVES .....	19
METHODS .....	23
3.1 Organ Culture System .....	23
3.2 Artery Preparation .....	25
3.3 Method for Controlling Circumferential and Shear Stress.....	26
3.4 Experimental Protocol .....	29
3.4.1 Beginning of Experiment .....	30
3.4.2 Experimental Conditions .....	30
3.4.3 Development of Method for Controlling Circumferential and Shear Stresses.	31
3.4.4 Method for Controlling Circumferential and Shear Stress.....	35
3.4.5 End of Experiment.....	39
3.5 Data Acquisition.....	40

3.5.1 Cross-Sectional Dimensions.....	40
3.5.2 Outer Diameter .....	42
3.5.3 Calculations of Circumferential and Shear Stress .....	43
3.5.4 Inflation Test .....	44
3.5.5 Peterson's Elastic Modulus .....	45
3.6 Biological Endpoints .....	46
3.6.1 Collagen Synthesis .....	46
3.6.2 Matrix Metalloproteinase Activity .....	49
3.6.3 Cell Proliferation .....	50
3.6.4 Cell Death.....	51
3.6.5 Quantification of Labeled Nuclei .....	52
3.6.6 Tissue Morphology.....	53
3.7 Statistics .....	54
RESULTS .....	55
4.1 Independent Control of Circumferential Stress and Shear Stress .....	55
4.1.1 Change in Geometrical Dimensions .....	55
4.1.2 Estimation of Final No-load Dimensions .....	59
4.1.3 Pressure-Diameter Response .....	61
4.1.4 Structural Responses .....	62
4.1.5 Time course of Circumferential Stress and Shear Stress.....	64
4.1.6 Effect Controlling Local and Global Parameters on Mechanical Environment.....	68
4.2 Effects of Circumferential Stress on Biological Markers of Remodeling.....	70
4.2.1 Tissue Morphology.....	71
4.2.2 Matrix Synthesis.....	71
4.2.3 MMP Activity.....	72



4.2.4 Cell Proliferation .....	73
4.2.5 Cell Death.....	75
4.3 Effects of Shear Stress on Biological Markers of Remodeling.....	76
4.3.1 Tissue Morphology.....	76
4.3.2 Matrix Synthesis.....	77
4.3.3 MMP Activity.....	78
4.3.4 Cell Proliferation .....	79
4.3.5 Cell Death.....	80
DISCUSSION .....	82
5.1 Changes of No-load Dimensions.....	83
5.2 Changes of the Deformed Dimensions and Control of Local Mechanical Environment .....	85
5.3 Changes in Pressure-Diameter Response .....	89
5.4 Changes in Peterson Elastic Modulus .....	91
5.5 Effects of Local Mechanical Environment of Arterial Remodeling .....	93
5.5.1 Circumferential Stress .....	94
5.5.2 Shear Stress .....	98
5.6 Limitations .....	101
CONCLUSIONS AND FUTURE WORK .....	105
6.1 Conclusions .....	105
6.2 Future Work .....	106
EXPERIMENTAL DATA ACQUISITION PROGRAMS .....	110
A.1 C++ Code for Inflation Test .....	111
A.2 C++ Code for Calculating Circumferential Stress and Shear Stress .....	122
PROTOCOLS FOR BIOLOGICAL ENDPOINTS .....	136
B.1 MTT Protocol .....	137

B.2 H & E Stain Protocol .....	138
B.3 <sup>3</sup> H-Proline Incorporation.....	140
B.4 Tissue Homogenization .....	143
B.5 MMP Zymography Protocol.....	144
B.6 Solutions for MMP Assay .....	145
B.7 Protocol for making SDS-PAGE Gels.....	146
B.8 Protocol for Protein Assay.....	148
B.9 BrdU Stain Protocol.....	149
B.10 DAPI Stain Protocol .....	150
B.11 HIER Protocol using Princess Electric Pressure Cooker and Citrate Buffer .....	151
REFERENCES .....	152

## LIST OF TABLES

Table 3-1:	Quantities used to determine the relationship between global and local mechanical parameters.....	28
Table 3-2:	Timeline of experimental protocol.....	30
Table 3-3:	Summary of the experimental conditions explored in this study. All arteries were held at a physiologic axial stretch ratio of 1.5. Cases A and B were run as paired experiments and cases C and D were paired.....	31

## LIST OF FIGURES

Figure 1-1: Cross-sectional view of an artery showing the three distinct layers – the intima, media, and adventitia (Adapted from Davis et al. 2003). .....	3
Figure 3-1: Schematic drawing of the perfusion organ culture system which is based on the design of Davis et al. (2005). .....	25
Figure 3-2: Flow chart describing the process for controlling circumferential stress and shear stress at a fixed axial stretch ratio in perfusion organ culture. ....	32
Figure 3-3: Typical time course of outer diameter for an artery ( $\sigma_\theta = 50$ kPa, $\tau = 1.5$ Pa, $\lambda_z = 1.5$ ) over the first 12 hours of culture. A strong myogenic response, as indicated by the rapid increase and decrease in outer diameter, occurs during the first 2 – 4 h of culture which is followed by stabilization of the outer diameter. To allow the outer diameter to stabilize following the myogenic response, 4 hours was considered to the minimum time period between adjustments of pressure and flow rate. ....	34
Figure 3-4: The change in no-load volume over time for a typical experiment in which arteries were exposed to low and high circumferential stress (Cases A and B in Table 3-3).....	35
Figure 3-5: Flow chart describing the revised method of independently controlling circumferential stress and shear stress in organ culture. ....	38
Figure 3-6: Schematic diagram of an artery showing how the artery was divided for processing of experimental endpoints following culture. ....	40
Figure 3-7: Typical image of an arterial ring segment that was backlit for measurement of cross-sectional dimensions.....	41
Figure 3-8: Time course of $^3\text{H}$ -proline incorporation for static incubation of tissue segments (n=6 for experimental arteries, n=4 for negative controls). The stress conditions for this experiment were $\sigma_\theta = 150$ or 50 kPa, $\tau = 1.5$ Pa, and $\lambda_z = 1.5$ . There were statistically significant ( $p < 0.05$ ) differences between each experimental specimen and its negative control (shown in cross-hatches) at all time points except at 1 h.....	48
Figure 3-9: Representative image of tissue segments incubated in MTT solution from an artery subjected to low circumferential stress conditions (A) and a negative control (B). The experimental artery was cultured statically for 24 hours following the experiment. The negative control was subjected to a series of freeze-thaw cycles to lyse cells.	

The white spots in the arterial wall are an imaging artifact associated with the camera flash. ....	49
Figure 4-1: Comparison of the initial no-load dimensions of arteries subjected to either a low (A) or high (B) circumferential stress to their values following culture. (*p < 0.05, n = 10).....	57
Figure 4-2: Comparison of no-load dimensions of arteries subjected to either a low (A) or high (B) shear stress following culture to their initial values. (*p < 0.05, n = 6) .....	59
Figure 4-3: Comparison of the estimated no-load dimensions with the actual no-load dimensions measured at the conclusion of the experiment. (n = 8 arteries) .....	60
Figure 4-4: Average pressure-diameter curves for an artery cultured under low or high circumferential stress conditions. Measurements were taken at 0 and 15 hours. (n = 10) .....	61
Figure 4-5: Average pressure-diameter curves for arteries cultured under low and high shear stress conditions. Measurements were taken at 0 and 15 hours. (*p < 0.05 for low vs. high shear stress arteries at t = 15 h, n = 6) .....	62
Figure 4-6: Structural response of arteries as measured by Peterson's modulus. Arteries were subjected to either low or high levels of circumferential stress. The modulus was calculated at the onset of the experiment and again after 15 hours of culture. (n = 10).....	63
Figure 4-7: Structural response of arteries as measured by Peterson's modulus. Arteries were subjected to either low or high levels of shear stress. The modulus was calculated at the onset of the experiment and again after 15 hours of culture. (n = 6) .....	64
Figure 4-8: Time course of mechanical parameters for a representative experiment (Case D). The prescribed values of $\sigma_\theta$ , $\tau$ , and $\lambda_z$ were 100 kPa, 2.25 Pa, and 1.5, respectively. Each point represents the average measurement of each parameter over 5 hours. The shaded vertical line indicates the adjustment period during which the current no-load dimensions were determined and the inflation test was conducted. Prior to this period, circumferential and shear stress were calculated using the initial no-load dimensions. Following this period, the stresses were calculated using the updated no-load dimensions. Results are plotted as mean $\pm$ SD. ....	66
Figure 4-9: Detailed view of mechanical parameters during an iterative adjustment of pressure and flow rate for the representative experiment (Case D). ....	67

Figure 4-10: Representative experiment comparing the mechanical environment of arteries in which local parameters ( $\sigma$ and $\tau$ ) were controlled with arteries in which global parameters ( $P$ and $Q$ ) were controlled.....	70
Figure 4-11: Comparison of tissue morphology of transverse sections for arteries cultured for 3 days using hematoxylin and eosin staining. Representative samples of a fresh (A) artery and vessels subjected to low (B) and high circumferential stress (C) are shown. The lumen is on the right in each image.....	71
Figure 4-12: Comparison of $^3\text{H}$ -proline incorporation in arteries subjected to low (Case A) and high (Case B) circumferential stress conditions for 3 days in culture. (* $p < 0.05$ , $n = 10$ ).....	72
Figure 4-13: Effect of circumferential stress on MMP-2/9 gelatinolytic activity measured using SDS-PAGE zymography. A representative zymogram for arteries exposed to low and high levels of circumferential stress are shown (A) with MMP-2 (67 kDa), pro-MMP-2 (72 kDa), and pro-MMP-9 (92 kDa) activity as clear lysis bands. Gelatinase activity was determined by densitometric quantitation of zymograms (B). (* $p < 0.05$ , $n = 9$ ).....	73
Figure 4-14: Percentage of proliferating cells detected by BrdU incorporation. Arteries were subjected to low or high levels of circumferential stress during 3 days of culture. (* $p < 0.05$ , $n = 8$ ) .....	74
Figure 4-15: Representative tissue sections immunostained with BrdU (A) and DAPI (B) to measure cell proliferation. For this artery, the prescribed values of $\sigma_\theta$ , $\tau$ , and $\lambda_z$ were 150 kPa, 1.5 Pa, and 1.5, respectively (Case B). The lumen is on the right in both images. The images are inverted and taken at 10X magnification.....	74
Figure 4-16: Percentage of EthD-positive cells in arteries subjected to low or high levels of circumferential stress during 3 days of culture. (* $p < 0.05$ , $n = 10$ ).....	75
Figure 4-17: Fluorescent microscope images of representative tissue sections stained with EthD (A) and DAPI (B) to measure cell death. The artery was subjected to the prescribed values of $\sigma_\theta$ , $\tau$ , and $\lambda_z$ were 50 kPa, 1.5 Pa, and 1.5, respectively (Case A) for 3 days of culture. The lumen is on the lower right in both images. The images are inverted and taken at 10X magnification. ....	76
Figure 4-18: Comparison of tissue morphology of transverse sections for arteries cultured for 3 days using hematoxylin and eosin staining. Representative samples of a fresh (A) artery and vessels subjected to	

low shear stress (B) and high shear stress (C) are shown. The lumen is on the right in each image. ....	77
Figure 4-19: Comparison of $^3\text{H}$ -proline incorporation in arteries subjected to low (0.75 Pa) and high (2.25 Pa) shear stress conditions for 3 days in culture. (n = 6) .....	78
Figure 4-20: Effect of shear stress on MMP-2/9 gelatinolytic activity measured using SDS-PAGE zymography. A representative zymogram for arteries exposed to low and high levels of shear stress are shown (A) with MMP-2 (67 kDa), pro-MMP-2 (72 kDa), and pro-MMP-9 (92 kDa) activity as clear lysis bands. Gelatinase activity was determined by densitometric quantitation of zymograms (B). (n = 6) .....	79
Figure 4-21: Percentage of proliferating cells detected by BrdU incorporation. Arteries were subjected to low or high levels of shear stress during 3 days of culture. (n = 6) .....	80
Figure 4-22: Percentage of EthD-positive cells in arteries subjected to low or high levels of circumferential stress during 3 days of culture. (n = 6) .....	81
Figure 5-1: Schematic of processes leading to the changes in geometry and mechanical responses of an artery in organ culture. ....	83

## LIST OF SYMBOLS AND ABBREVIATIONS

$\alpha$	Diameter Ratio
$\beta$	Thickness Ratio
$\lambda_z$	Axial Stretch Ratio
$\mu$	Dynamic Viscosity
$\sigma_\theta$	Circumferential Stress
$\tau$	Shear Stress
A	Curve Fit Parameter
B	Curve Fit Parameter
$d_o$	Deformed Outer Diameter
$D_o$	No-Load Outer Diameter
$E_p$	Peterson's Modulus
h	Deformed Thickness
H	No-Load Thickness
$I_b$	Background Image Intensity
$I_f$	Foreground Image Intensity



$I_t$	Threshold Image Intensity
$l$	Deformed Length
$L$	No-Load Length
$P$	Transluminal Pressure
$Q$	Flow Rate
$t$	Time
Circ.	Circumferential
Neg.	Negative
A/D	Analog to Digital
BrdU	Bromodeoxyuridine
BSA	Bovine Serum Albumin
CCD	Charge Coupled Device
DAPI	4'-6-diamidino-2-phenylindole
DMEM	Dulbecco's Modified Eagle's Medium
DNA	Deoxyribonucleic Acid
DPM	Disintegrations per Minute
EthD	Ethidium Homodimer

FCS	Fetal Calf Serum
H & E	Hematoxylin and Eosin
MMP	Matrix Metalloproteinase
MTT	Methylthiazol Tetrazolium
PBS	Phosphate Buffered Saline
SD	Standard Deviation
SEM	Standard Error of the Mean
SMC	Smooth Muscle Cell
SDS-PAGE	Sodium Dodecyl Sulfate Polyacrylamide Gel Electrophoresis

## SUMMARY

The mechanical environment of arteries can be described in terms of *global* parameters (pressure, flow rate, and axial force) or *local* parameters (circumferential stress, shear stress, and axial strain). The global and local parameters are related by the equations of equilibrium, the flow equation, and the pressure-diameter response of the artery. From *in vivo* studies, it is known that arteries respond to changes in global parameters by changing dimensions, tone, and mechanical properties to restore the local parameters to homeostatic levels. This process of remodeling has also been studied in perfusion organ culture. To date, *in vivo* and organ culture studies of remodeling have subjected arteries to controlled changes of a single global parameter. Because arteries change dimensions and mechanical properties to restore the local mechanical environment to baseline levels, the local parameters vary over time. To address this limitation, a new approach has been developed to independently control local parameters by appropriately changing pressure and flow rate in organ culture. To illustrate the method, the effect of circumferential stress and shear stress on several biological markers of remodeling was studied.

Porcine carotid arteries were cultured for 3 days in a perfusion organ culture system to investigate the effects of circumferential stress and shear stress on arterial remodeling. For experiments varying circumferential stress, arteries were subjected to a circumferential stress of either 50 kPa or 150 kPa, while shear stress and axial stretch ratio were held at physiologic levels of 1.5 Pa and 1.5, respectively. For experiments varying shear stress, arteries were subjected to a shear stress of either 0.75 Pa or 2.25 Pa, while circumferential stress and axial stretch ratio were held at physiologic levels of 100

kPa and 1.5, respectively. Arterial remodeling was assessed by measuring biological marker including matrix synthesis, matrix metalloproteinase (MMP) activity, cell proliferation, and cell death.

The results showed that circumferential stress and shear stress have differential effects on arterial remodeling in organ culture. Circumferential stress induced a response in each of the biological markers. Matrix synthesis, as measured by  $^3\text{H}$ -proline incorporation, was significantly greater in arteries exposed to high circumferential stress. In contrast, MMP-2 activity was significantly less in high circumferential stress, while pro-MMP-9 activity was not significantly affected. The proliferation rates of smooth muscle cells and fibroblasts were significantly greater in arteries exposed to high circumferential stress. Smooth muscle cell death was also greater in high circumferential stress arteries. In contrast to circumferential stress, shear stress did not have a significant effect on the biological markers of remodeling measured in this study.

This novel approach can be used for the design and realization of different types of experiments focused on the effects of local mechanical parameters on arterial remodeling. This method can be used to determine the remodeling capacity of arterial cells or establish a ranking of local parameters to determine experimentally-motivated selection of growth laws for use in mathematical models. The results of this method can also be applied to the field of tissue engineering where understanding the effects of local mechanical factors on remodeling can offer a scientific basis for the design of optimal mechanical conditioning for vascular grafts.

# **CHAPTER 1**

## **INTRODUCTION**

This chapter provides the background required to understand the scope of this research project. The chapter begins by discussing the significance of cardiovascular disease which provides the overall motivation for cardiovascular research. The next section describes the structure and function of arteries. The process of arterial remodeling is then described based on the current state of research in the field. Finally, organ culture and analytical approaches to understanding arterial remodeling are reviewed.

### **1.1 Cardiovascular Disease**

Cardiovascular disease is the leading cause of death in the United States. Over 71 million Americans have a form of cardiovascular disease and the annual cost of treatments associated with the disease exceeds \$400 billion (Thom et al. 2006). Given the prevalence and high costs of this disease, there is a great need to better understand its etiology and progression. As the fundamental understanding of the cardiovascular system improves, new clinical solutions – in the form of diagnostic tools, drug therapies, medical devices, and surgical techniques – will be developed to reduce the morbidity and mortality associated with the disease.

### **1.2 Structure and Function of Arteries**

The primary function of arteries is to transport blood, which contains the oxygen and nutrients required for cellular function, from the heart to tissues throughout the body. Blood is pumped from the heart into the aorta and on through a network of arteries with progressively smaller diameters until it reaches the capillaries. The beating heart

generates pressure pulses in the blood flow which are dampened by the compliance of the arterial wall prior to reaching the capillaries. Capillaries have a diameter small enough to restrict flow to the passage of a single cell and walls thin enough to allow oxygen and nutrient transfer to the surrounding tissues (Humphrey 2002).

Arteries are tube-like structures comprised of three distinct layers – the intima, media, and adventitia – as shown in Figure 1-1. The intima is composed of an endothelial cell monolayer that serves as an interface between blood and the vessel wall. Under normal flow conditions, endothelial cells have a flat, cobblestone-like morphology and are elongated in the direction of flow. Endothelial cells have anticoagulant properties that are essential to maintaining normal blood flow. They also sense changes in flow-induced shear stress and regulate the arterial response to these changes through the release of signaling molecules to smooth muscle cells (SMCs) in the medial layer. On their basal surface, endothelial cells adhere to the basal lamina. The basal lamina is a membrane that consists of type IV collagen, cell adhesion molecules including laminin and fibronectin, and proteoglycans. The basal lamina lies on the internal elastic lamina – a fenestrated sheet of elastin that separates the intima and media (Humphrey 2002).

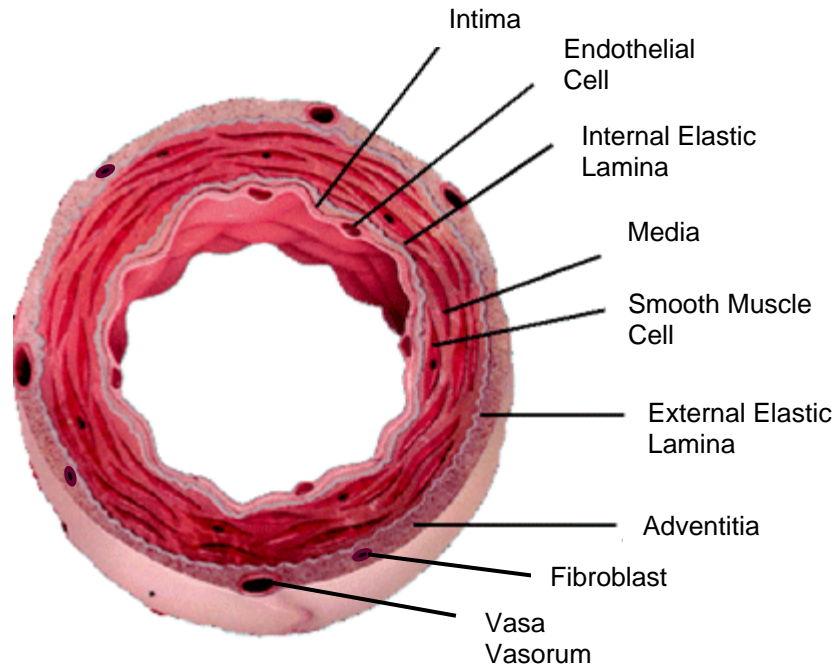


Figure 1-1: Cross-sectional view of an artery showing the three distinct layers – the intima, media, and adventitia (Adapted from Davis et al. 2003).

The media is the central layer of the artery. The media is composed of smooth muscle cells embedded in a fibrous network of collagen (primarily types I, III, and V), elastin, and proteoglycans. SMCs have a spindle-like geometry and are oriented circumferentially or helically at small angles throughout the media (Takamizawa et al. 1992; Liu 1998). They play a primary role in the maintenance of vascular tone as well as the secretion of extracellular matrix constituents (Osol 1995). The network of collagen and elastin within the media are responsible for the artery's mechanical properties. In the absence of pressure, collagen and elastin fibers have a crimped appearance, but upon loading, the fibers straighten as they become stretched circumferentially. The external elastic lamina, a thin fenestrated sheet of elastin, is located on the outer surface of media, separating the media from the adventitia.

The adventitia is the outermost layer of the arterial wall. The adventitia is composed of fibroblasts, type I collagen, and elastin. This layer lacks the organized, lamellar structure of the media. The vasa vasorum, a network of small vessels, runs throughout the adventitia to supply blood to cells in this region that cannot receive oxygen and nutrients by diffusion. While the mechanical significance of the adventitia is not fully understood, it may serve to limit overdistension of the arterial wall (Humphrey 2002).

The primary constituents of arteries are water, collagen, and elastin. For canine carotid arteries, water comprises  $71.1 \pm 0.1\%$  of the tissue wet weight, collagen takes up  $50.7 \pm 2.1\%$  of the tissue dry weight, elastin is  $20.1 \pm 1.0\%$ , and the remaining dry weight is accounted for by a combination of other proteins (Fischer and Llaurodo 1966). This provides an example of the composition of a specific artery, but the relative composition of arteries varies with species and location within the vasculature.

Arteries can be classified as either elastic or muscular based on the relative size of the layers. Elastic arteries tend to have a thick media layer and the adventitia comprises only 10% of the arterial wall. Elastic arteries tend to be larger and more compliant to dampen pressure pulses in the blood flow generated by the beating heart. The aorta is an example of an elastic artery. On the other hand, muscular arteries tend to have a thinner medial layer and the adventitia comprises about 50% of the wall thickness. Muscular arteries are present in the location where fine control of vessel tone is required for systemic control of pressure and flow, such as mesenteric arteries. Note that the distinction between elastic and muscular arteries is not always clear (Humphrey 2002).



Arterial tissue is a heterogeneous material with complex mechanical properties. The heterogeneity arises from the presence of water, cells, and collagen and elastin fibers. Arteries exhibit nonlinear mechanical properties which arise from the fact the collagen and elastin have a crimped structure when unloaded, but gradually straighten and carry proportionally greater loads under elevated pressures. The artery is considered to be a viscoelastic material because it exhibits creep, stress relaxation, hysteresis and its mechanical properties are strain-rate dependent. The anisotropy of the artery arises from the orientation of the collagen and elastin fibers which is generally in the circumferential direction. Therefore, arteries are often modeled as an orthotropic material. Finally, the artery is considered to be incompressible due to its high water content and limited fluid transfer to and from the loaded tissue (Humphrey 2002).

### **1.3 Arterial Remodeling**

Remodeling is the process by which arteries respond to changes in their mechanical environment. The result of remodeling is a change in arterial dimensions and mechanical properties at the macroscopic level. These macroscopic changes are manifest by a series of cellular responses that are triggered by changes in the mechanical environment. Remodeling occurs as a part of normal physiology and is typically a self-limiting process referred to as adaptation. In the case of adaptation, the artery remodels to restore the mechanical environment to its homeostatic state. However, in pathological states, arterial remodeling can be maladaptive and result in the development and progression of disease conditions such as atherosclerosis or aneurysms.

The arterial mechanical environment can be described in terms of *global* and *local* parameters. The *global* mechanical environment is due to blood pressure, flow rate, and

axial stretch, while the *local* mechanical environment is comprised of circumferential stress, shear stress, and axial strain. These *global* and *local* parameters are related by force equilibrium and the flow equation. When changes to the *global* mechanical parameters occur, arteries respond by altering the proliferative, synthetic, and degradative activity of cells in a manner that restores the *local* parameters to normal levels.

Various *in vivo* studies have investigated the effects of changes in global parameters on arterial remodeling. In studies of hypertension, arteries were shown to increase wall thickness in response to elevated pressure in order to restore circumferential stress to homeostatic levels in as little as 2 weeks (Liu and Fung 1989; Vaishnav et al. 1990; Matsumoto and Hayashi 1994; Fridez et al. 2001). This macroscopic response was achieved through a series of events that occur on a cellular level. Sustained hypertension induces an acute myogenic response in smooth muscle cells such that vascular tone increases in order to preserve the luminal diameter (Fridez et al. 2002). This myogenic response is followed by a chronic response characterized by SMC hypertrophy (Olivetti et al. 1980) and an increase in matrix synthesis. These responses contribute to the observed increase in wall thickness, which, in turn, restores circumferential stress and SMC tone to normal levels. In the chronic response, the increase in wall thickness is associated with the preservation of luminal diameter (Liu and Fung 1989; Matsumoto and Hayashi 1994). Therefore, assuming the flow rate is unchanged, the artery responds in a manner that maintains shear stress, which is sensed by endothelial cells, at baseline levels. Further, by increasing wall thickness, the artery also remodels to restore circumferential stress, which is sensed by SMCs, to normal levels.

Arteries respond to changes in flow rate by adjusting luminal diameter in order to restore shear stress to normal levels (Kamiya and Togawa 1980; Zarins et al. 1987; Masuda et al. 1989; Brownlee and Langille 1991). On a cellular level, endothelial cells sense changes in shear stress, although the precise mechanisms of the mechanotransduction remain unknown. In the case of increased flow, endothelial cells sense increased shear stress and acutely upregulate vasodilators, including nitric oxide, which cause SMCs to relax and results in an increase in luminal diameter (Kaiser et al. 1986). This acute response is followed by a chronic response. The chronic response is characterized by the migration and proliferation of SMCs combined with an increase in matrix synthesis that ultimately increases the luminal diameter and wall thickness (Masuda et al. 1989). Because of these responses, shear stress, average circumferential stress, and muscular tone are restored to baseline levels. In addition, increased endothelial cell proliferation maintains a constant density of endothelial cells lining the luminal surface of the artery (Masuda et al. 1989). The arterial response to increased flow-induced shear stress is a slower process than the hypertensive response, taking several months or more (Kamiya and Togawa 1980; Zarins et al. 1987; Masuda et al. 1989).

The artery also responds to reductions in blood flow in a manner that restores shear stress to normal levels (Langille and O'Donnell 1986; Langille et al. 1989). In response to reduced flow, endothelial cells acutely release vasoconstrictors that cause SMCs to contract and reduce luminal diameter. In the chronic response, the matrix is reorganized such that the luminal diameter is reduced to restore shear stress to normal levels and, in addition, the wall thickness is altered to maintain circumferential stress at

normal levels (Langille and O'Donnell 1986; Langille et al. 1989). This response is also associated with a net reduction in the number of endothelial cells in order to maintain a constant endothelial cell density. The arterial response to reduced flow rate was found to take approximately 2 weeks (Langille and O'Donnell 1986; Langille et al. 1989).

Additional studies have been performed that provide further insights into the flow-induced remodeling response. Langille and O'Donnell (1986) conducted a set of experiments demonstrating that endothelial cells are responsible for initiating the flow-induced remodeling response. In this study, rabbit carotid arteries were denuded of endothelium and did not exhibit a diameter decrease in response to reduced flow rates. To support this finding, others have also shown that the flow-induced remodeling response is endothelium dependent (Melkumyants et al. 1989).

The hypothesis that shear stress, as opposed to flow rate, regulates the remodeling response was strengthened by a study by Melkumyants and Balashov (1990). In this study, the viscosity of blood was changed by varying hematocrit levels and then feline femoral arteries were subjected to several different flow rates. In the end, regardless of flow rate or viscosity, the arteries adjusted diameter to restore shear stress to normal levels.

In a study by Langille et al. (1989), the remodeling response to flow-induced shear stress was found to vary with age. When subjected to reduced blood flow, adult rabbit carotid arteries decreased luminal diameter, but there were no changes in vessel mass or extracellular matrix content. However, for young rabbits, the arteries had a reduced luminal diameter in addition to changes in the composition and structure of the arterial wall.

Recently, a study investigated the role of axial strain in arterial remodeling. Jackson et al. (2002) lengthened a rabbit carotid artery by approximately 25% and after seven days the axial strain in the artery was restored to normal levels. This response was associated with increases in cell proliferation, collagen content, and elastin content. In addition, axial strain was normalized in arteries denuded of endothelium which suggest that smooth muscle cells regulate the remodeling response to axial loads. These results suggest that axial strain is the local parameter responsible for regulating arterial remodeling due to axial stretch. The axial stretch-induced remodeling response is consistent with that observed for pressure-induced and flow-induced remodeling. Taken together, the results of the pressure-induced, flow-induced, and axial stretch-induced remodeling studies strengthen the view that arteries remodel to changes in global parameters to restore the local mechanical environment to its homeostatic state.

#### **1.4 Organ Culture Studies**

As described in the previous section, *in vivo* studies have provided much of the basis for the current understanding of how the mechanical environment affects arterial remodeling. However, to further the understanding of arterial remodeling, studies have been conducted in organ culture and cell culture environments. Each experimental approach has advantages and disadvantages. On one end of the spectrum, *in vivo* studies maintain the artery in its native, physiologic environment, but the mechanical environment cannot be precisely controlled. At the other end of the spectrum, cell culture provides control over cells in a well-defined mechanical and biochemical environment, but the cells are not in their native environment and thus, the physiological relevance of the results may be limited. Organ culture provides a balance between *in vivo* and cell

culture studies. Organ culture studies provide more control of the mechanical and biochemical environment than *in vivo* studies and a more physiologically relevant environment than cell culture. In addition, organ culture studies provide information on short-term responses of arteries that cannot readily be observed in animal studies. This review will focus on organ culture studies on arterial remodeling since they are most relevant to this study.

In organ culture studies, an arterial segment is explanted from a donor and maintained in an experimental system where mechanical loads can be applied while cellular function is supported with essential nutrients using culture media. Organ culture studies have been conducted under conditions with no flow (static) or flow (perfusion) of culture medium through the lumen of a blood vessel. The simplicity of static organ culture make it an attractive experimental tool (Gotlieb and Boden 1984; De Mey et al. 1989; Koo and Gotlieb 1991; Voisard et al. 1999). Static culture experiments have been reported to range in duration from seven to fifty-six days, with regular changes of culture media (Gotlieb and Boden 1984; De Mey et al. 1989; Voisard et al. 1999). Static culture experiments have examined the structural and cellular response of arteries to various mechanical stimuli and have examined various biochemical pathways involved in arterial remodeling (Gotlieb and Boden 1984; De Mey et al. 1989; Boonen et al. 1991; Koo and Gotlieb 1991; Holt et al. 1992; Lindqvist et al. 1997; Earley et al. 1998; Binko et al. 1999; Lindqvist et al. 1999; Voisard et al. 1999; Wilson et al. 1999; Del Rizzo et al. 2001).

Perfusion organ culture studies have also been developed and used to study the effects of mechanical stimuli on vascular biology (Matsumoto et al. 1999; Han and Ku

2001; Clerin et al. 2002; Gleason et al. 2004; Davis et al. 2005). Since the presence of pressure and flow in perfusion organ culture more closely mimics the native arterial environment, these studies tend to yield more physiologically relevant results than static organ culture experiments. To date, perfusion organ culture studies have typically controlled pressure, flow rate, and axial strain in experiments investigating the effects of mechanical parameters on arterial remodeling. The hemodynamic conditions have incorporated pulsatile pressure and flow waveforms that mimic physiologic conditions (Brant et al. 1987; Labadie et al. 1996; Schwartz et al. 1996; Vorp et al. 1996; Bakker et al. 2000; Surowiec et al. 2000; Han and Ku 2001). While the effects of axial strain have been studied by several groups (Clerin et al. 2003; Han et al. 2003; Gleason et al. 2007), Davis et al. (2005) were the first to control axial stress in an perfusion organ culture experiment.

To an extent, shear stress has been controlled in organ culture experiments. However, in most studies, the flow rate is typically determined based on the artery's initial dimensions and then held constant throughout the experiment (Chesler et al. 1999; Han and Ku 1999; Clerin et al. 2003; Davis et al. 2005). Shear stress is inversely proportional to the cube of the inner diameter, therefore small changes in inner diameter can lead to large variations in shear stress. Since arterial dimensions do not typically remain constant throughout the culture period (Han and Ku 1999), significant errors in shear stress are likely in such studies.

Perfusion organ culture studies have been shown to maintain the functionality of arteries for seven to nine days (Han and Ku 1999; Clerin et al. 2002; Davis et al. 2005). In one study, viability was maintained for 27 days in porcine carotid arteries cultured

under subphysiologic pressure and flow conditions (Clerin et al. 2002), although studies of such duration are rare.

The effect of hypertension on arterial remodeling has been studied extensively in perfusion organ culture. Matsumoto et al. (1999) showed that the wall thickness was significantly greater while inner diameter was not changed in rabbit carotid arteries cultured under elevated pressure for six days. Although these increases in wall thickness were not sufficient to restore circumferential stress to physiologic levels, they are qualitatively consistent with the responses observed *in vivo*. Han and Ku (2001) showed that hypertension causes increased luminal diameter and contractile responses in porcine carotid arteries after 7 days in culture. In a study of hyper- and hypotension, Zulliger et al. (2002) found that the cross-sectional area of the arterial wall did not change during culture for either group of porcine carotid arteries cultured for 3 days. In addition, for the hypotension case, the elastic modulus and contraction was reduced while, for the hypertensive artery, peak contractility was observed at higher pressures (Zulliger et al. 2002). Collectively, these studies provide evidence that remodeling responses occur on short time scales, although changes in geometrical dimensions cannot always be observed. Therefore, organ culture studies have investigated the effect of hypertension on biological markers of remodeling, including the synthesis and expression of various proteins (Bardy et al. 1996; Birukov et al. 1997; Birukov et al. 1998).

Organ culture studies on flow-induced remodeling are limited possibly due to the longer timeframe required for remodeling. In a study of the differential effects of pressure-induced and flow-induced remodeling, Chesler et al. (1999) found that that matrix metalloproteinase-2 (MMP-2) activity was greater in normotensive porcine carotid



arteries than in hypertensive arteries after 48 hours of culture. In contrast, they found that MMP-9 activity was greater in hypertensive vessels. Further, both MMP-2 and MMP-9 activity were not affected by changes in flow rate. Recently, Gambillara et al. (2006) studied the effect of flow conditions on endothelial cell function. In this study, porcine carotid arteries were subjected to a high or low unidirectional shear stress or an oscillatory shear stress. They found that oscillatory shear stress, which is found in disease-prone locations, leads to reduced vasoactive responses and reduced eNOS protein expression.

Recently, a number of studies have reported the effects of axial strain on arterial remodeling. Han et al. (2003) investigated the effects of fixed axial strain on arterial adaptation by comparing porcine carotid arteries held at an axial stretch ratio of 1.8 to controls held at a physiologic stretch ratio of 1.5 for five days in perfusion organ culture. This study found that axial stretch promotes cell proliferation while maintaining arterial functionality. In another study, porcine carotid arteries were continually elongated under a constant axial stress of 250 kPa or greater under physiologic pressure and flow conditions for a period of seven days (Davis et al. 2005). Davis and colleagues found that increases in unloaded length could be achieved when the loaded axial stretch ratio exceeded 2.14. When this critical stretch ratio was achieved, the unloaded length of arteries increased by approximately 13%. This increase in length was associated with a decrease in axial stiffness and a significant increase in the total number of cells in the medial layer of stretched arteries. In another study on axial strain, Clerin et al. (2003) gradually elongated juvenile porcine carotid arteries to an axial stretch ratio greater than 2.0 over nine days. They found that approximately 20% increases in unloaded length

could be achieved when the arteries were cultured under subphysiologic pressure and flow conditions. This group later found that the increases in unloaded length were less dramatic when the artery was cultured under physiologic pressure and flow rates (Nichol et al. 2005). Gleason et al. (2007) studied the mechanical responses wild-type mice carotid arteries subjected to low, medium, and high axial strains for 2 days in culture. They found that, although there were changes there were changes in structural responses (i.e. pressure-axial force and axial-force length), there were no significant differences in the material responses (i.e. circumferential stress-strain or axial stress-strain) following culture. To study the effects of cyclic axial loads on arterial remodeling, Vorp and colleagues (1996; 1999) developed a device and found that cyclic flexure downregulated expression of MMP-1 and E-selectin in porcine femoral arteries in just 4 hours of culture.

In conclusion, organ culture provides a well-defined biochemical and mechanical environment for studying arterial remodeling. In general, perfusion organ culture studies have been shown to maintain cell functionality for up to nine days. Because this timeframe may not always be sufficient to observe macroscopic changes in geometry and mechanical properties, biological markers are often used to indicate trends in the remodeling responses that occur on a cellular level. Organ culture studies typically control pressure, flow rate, and axial strain when studying the role of the mechanical environment on arterial remodeling. The resultant studies have shown that arteries remodel in response to changes in the global mechanical environment by changing geometry, cell proliferation, cell death, protein expression, and enzymatic activity.

## 1.5 Mathematical Models of Remodeling

Because remodeling is driven by local mechanical parameters, mathematical models have been developed to analytically investigate the process of arterial remodeling. The objective of these models is to predict the geometrical and mechanical response of arteries to changes in the mechanical environment. Mathematical models complement the findings of experiments and offer several benefits such as the ability to investigate phenomenon that are not feasible to study experimentally, offering insights into processes that cannot be observed experimentally, and providing a rationale for conducting future experiments. These models have been developed to describe the process of arterial remodeling using the principles of continuum mechanics coupled with phenomenological observations of geometrical and mechanical changes in arterial behavior.

In general, mathematical models study arterial remodeling using one of three approaches: finite volumetric growth, global growth, or constrained mixture. In the finite volumetric growth approach, the artery is assumed to be a collection of elements that grow differentially that change their zero-stress state (Skalak et al. 1982; Rodriguez et al. 1994; Taber and Eggers 1996). In the global growth approach, models focus on the description of the kinematics of the zero-stress configuration of the vessel as a whole (Rachev 1997; Rachev et al. 1998; Rachev 2000). Lastly, constrained mixture models combine a rule-of-mixtures structural model with a kinetic model of the production and removal of arterial constituents (Humphrey 1999; Gleason et al. 2004; Gleason and Humphrey 2005).

Regardless of the approach, the selection of a growth stimulus and growth laws must be considered when developing a mathematical model. The growth stimulus is the

local mechanical parameter (i.e. stress or strain) that initiates the remodeling response. However, growth laws describe the relationship between the growth stimulus and the remodeling response of the artery. For example, Fung (1990) proposed a nonlinear mass-stress growth law which states that mass is either produced or resorbed when the stress deviates from the physiologic homeostatic stress state. The growth stimulus and growth laws are based on an intuitive selection of the mechanical factors driving remodeling. The output of the mathematical model typically the geometry, arterial mass, or mechanical properties resulting from the application of the growth stimulus.

Finite growth models have been proposed by several authors to study arterial remodeling. Rodriguez et al. (1994) developed a general continuum model for finite volumetric growth of soft tissues that accounts for residual stresses and stress-dependent tissue growth. Building on this model, Taber and Eggers (1996) modeled the artery as a pseudoelastic tube composed of two layers representing the intima/media and the adventitia. The model predictions for aortic growth and the time course of vessel radii and residual strain in arteries were in close agreement with published experimental results. Since the mechanical growth stimulus for arteries is not well understood, Cowin (1996) extended the theory of Rodriguez et al. to include strain and deformation rate as growth stimuli. The work of Rodriguez et al. has been extended by others in developing more intricate models of arterial remodeling using a finite volumetric growth model (Chen and Hoger 2000; Epstein and Maugin 2000).

Global growth models have been proposed which describe pressure-induced and flow-induced remodeling. In a study of pressure-induced remodeling, Rachev et al. (1996) consider the artery to be a thick-walled tube made of a nonlinear elastic

incompressible material using a global growth model. Hypertension was modeled as step increase in pressure and, as a result, the geometrical dimensions changed asymptotically to restore circumferential stress and shear stress to normal levels. In addition, the opening angle changed in a biphasic manner. Both findings were in close agreement with experimental evidence. In a later study, Rachev (1997) considered the artery as a thick-walled two-layer tube. The model predicted that, when subjected to hypertension, remodeling causes the artery to increase in wall thickness and inner diameter, and retain residual stresses even after the unloaded artery is subjected to a radial cut, results that were also in agreement with experimental findings. Rachev has developed models of flow-induced remodeling to further the understanding of this process (Rachev et al. 1998; Rachev et al. 2000).

Constrained-mixture models have been developed to describe pressure-induced, flow-induced, and axial strain-induced remodeling. Gleason et al. (2004) developed a two-dimensional constrained mixture model to study the remodeling of a cylindrical artery in response to sustained alterations in flow rate. The authors found that, upon perturbation, the dimensions of the artery changed in order to restore circumferential stress and axial stress to homeostatic values. However, when elastin turnover was considered to be negligible, the artery was not able to completely restore the stresses to homeostatic level. These results suggest that arterial remodeling can be limited by biological constraints, a result that is consistent with previous experimental observations. Gleason and Humphrey (2005) later developed a two-dimensional constrained mixture model to study the arterial response to a sustained increase in axial extension. Their

finding that axial strain returns to homeostatic levels following axial extension qualitatively agrees with *in vivo* observations.

## CHAPTER 2

### OBJECTIVES

Both *in vivo* and organ culture studies performed so far have revealed many aspects of the normal and pathologic remodeling of arteries from different species, age groups, and locations within the vasculature (Zarins et al. 1987; Glagov et al. 1988; Langille et al. 1989; Matsumoto et al. 1999; Clerin et al. 2002). However, the methodology used in these studies cannot address several important issues. Past studies cannot quantify the remodeling response caused by a controlled change in a single parameter of the local mechanical environment such as circumferential stress, flow-induced shear stress, or axial strain while keeping the remaining local parameters unchanged. In general, a change in a single global parameter, which is the experimental design used in past investigations, leads to a change of several local parameters and, therefore, the remodeling response is a result of the combined changes of all local parameters. For instance, a change in the mean arterial pressure causes changes in circumferential stress, pulsatile circumferential strain, and shear stress at the endothelium. Though under physiological conditions, the arterial pressure, flow, or longitudinal stretch might vary, understanding the contribution solely of a single local mechanical factor to which the endothelial and smooth muscle cells are exposed can provide insights on the mechanisms of arterial remodeling. Quantification of the independent effects of altered shear stress, circumferential stress, and circumferential pulsatile strain can reveal which parameter has a major remodeling effect, whether they synergistically contribute to the remodeling outputs, and whether there exists a causal

link between a deviation from the baseline value of certain local mechanical parameter and observed remodeling outputs.

Focusing on the effects on remodeling caused by the alterations in global mechanical parameters, past studies did not sufficiently analyze the contributions of arterial dimensions and mechanical properties to remodeling outputs. The size and the mechanical properties of the vascular tissue relate the changes in global mechanical environment of an artery to the changes in local mechanical environment of arterial cells via equations of equilibrium. Therefore, past studies could not determine the extent of the “remodeling capacity” of endothelial and smooth muscle cells or the amount and reorganization of the extracellular matrix responsible for an observed mode of remodeling.

The results from the proposed approach can be beneficial for tissue engineering of arterial grafts. Understanding the effects of local mechanical factors on remodeling can offer a scientific basis for a design of optimal mechanical conditioning in bioreactors of constructs with embedded cells. In addition, the results obtained can be useful for mathematical modeling of arterial remodeling. Mathematical modeling of arterial remodeling requires motivated choice of local mechanical parameters, for which deviations from homeostatic values are assumed to elicit specific modes of remodeling. So far, the proposed stress-growth laws (Taber and Eggers 1996; Humphrey 1999) and remodeling rate equations (Rachev et al. 1998) are based on an intuitive selection of the driving mechanical factors, rather than on their experimentally motivated ranking. The results of the novel experimental design used here can identify which are the significant



mechanical parameters that should be taken into account when growth laws are postulated.

It is not possible to realize independent control of the local mechanical environment of the endothelial and smooth muscle cells in animal experiments. However, a novel approach in design and performance investigations in organ culture systems can address the issues mentioned above. This study illustrates this approach by studying the effects of circumferential and shear stress on arterial remodeling of porcine carotid arteries.

The hypothesis of this work is that arterial remodeling can be evaluated on the basis of independent changes in circumferential stress and shear stress in perfusion organ culture. To test this hypothesis, the following specific aims were identified:

**Specific Aim 1:** *To develop a method of independently controlling circumferential stress and shear stress in organ culture.*

By simultaneously adjusting pressure and flow rate, it is possible to independently control circumferential stress and shear stress. This approach can be uniquely achieved in organ culture where pressure and flow rate can be adjusted in response to changes in arterial dimensions to maintain target values of circumferential stress and shear stress.

**Specific Aim 2:** *To evaluate the effects of an independent change of circumferential stress on arterial remodeling.*

Using the method developed in Specific Aim 1, circumferential stress can be independently varied while shear stress is held constant by appropriately adjusting

pressure and flow rate. Arterial responses to circumferential stress are evaluated by measuring mechanical behavior and biological markers of remodeling.

**Specific Aim 3:** *To evaluate the effects of an independent change of shear stress on arterial remodeling.*

Using the method developed in Specific Aim 1, shear stress can also be independently varied while circumferential stress is held constant by appropriately adjusting pressure and flow rate. Arterial responses to shear stress are evaluated by measuring mechanical behavior and biological markers of remodeling.

## **CHAPTER 3**

### **METHODS**

This chapter describes the materials and methods used in this research. First, the details of organ culture system and preparation of arteries are described. Then, the method for independently controlling circumferential and shear stress in organ culture is discussed. A description of the experimental protocol and the stress conditions used for this research is given next. The chapter concludes with descriptions of the methods used to measure arterial dimensions and chosen biological endpoints.

#### **3.1 Organ Culture System**

The organ culture system (Figure 3-1) used in this research is based on the design of Davis et al. (2005). The flow loop consists of a medium reservoir and a vessel chamber connected by PharMed tubing (Cole-Parmer). Two thin-walled stainless steel cannulae are mounted on each end of the chamber and are connected to the flow loop. Grooves were machined on the surface of one end of each cannula to allow vessel mounting. Prior to each experiment, the flow loop and culture chamber were sterilized by autoclave. The media reservoir and vessel chamber is filled with sterile perfusion medium (~ 500 ml) and bathing medium (~150 ml), respectively.

Perfusion and bathing media were composed of Dulbecco's Modified Eagles Medium (DMEM, Sigma) supplemented with sodium bicarbonate (3.7 g/L, Sigma), L-glutamine (2 mM, Sigma), L-proline (0.4 mM, Sigma), ascorbic acid (50 mg/L, Sigma), antibiotic-antimycotic solution (1%, Sigma), and calf serum (10%, HyClone). Dextran

(6.5%, Sigma) was added to the perfusion media increase its viscosity to physiologic levels (4 cP).

After assembly under a laminar flow hood, the flow loop was transferred to an incubator (Forma Scientific). The incubator maintained the temperature of the organ culture system at 37 °C and the carbon dioxide levels at 5%. The pH (7.4) of the perfusion and bathing media was maintained through gas exchange in the vessel chamber and the medium reservoir.

A charge-coupled device (CCD) camera (Marshall Electronics) with an adjustable zoom lens (Leica) was used to image the vessel during experiments for use in measuring the outer diameter. A computer program was written to calculate vessel outer diameter using images acquired by a framegrabber (Data Translation) as described in Section 3.5.2.

Flow rate was controlled using a peristaltic roller pump (Cole-Parmer). A pulse dampener (Cole-Parmer) was used to achieve steady flow by minimizing the pulsatility produced by the roller pump. Mean perfusion pressure was controlled by resistance clamps which were located between the pressure port and media reservoir. A pressure transducer (Harvard Apparatus) measured perfusion pressure. The pressure transducer was connected to an A/D board (Data Translation) for data acquisition.

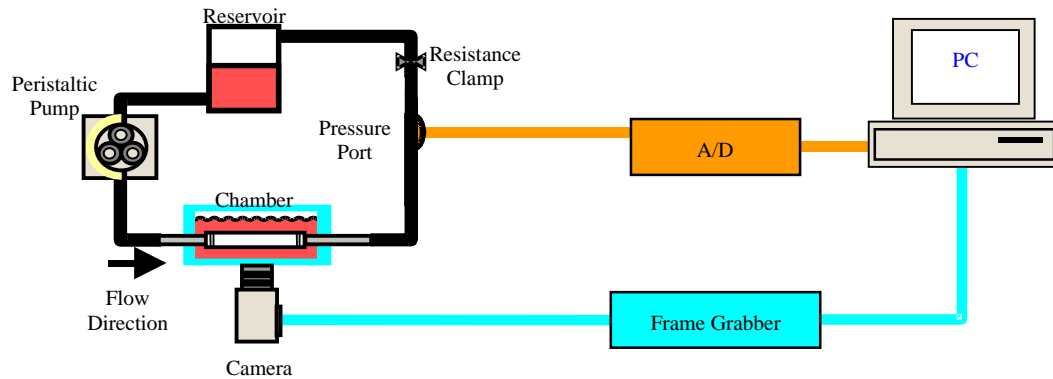


Figure 3-1: Schematic drawing of the perfusion organ culture system which is based on the design of Davis et al. (2005).

### 3.2 Artery Preparation

Bilateral porcine common carotid arteries were harvested from 6 to 7-month-old farm pigs (100 – 150 kg) at a local abattoir. Arterial segments were rinsed with Dulbecco's phosphate buffered saline (PBS, Sigma) and were transported to the laboratory in ice-cold PBS.

Arterial segments were prepared for each experiment in a laminar flow hood. Artery preparation involved removing excess connective tissue, gentle inflation with air to identify leaks, and ligating side branches, if necessary. Leak-free segments that were 3 – 5 cm in length at the no-load state were used in the experiment. A 2 mm wide segment was cut from each end of the vessel in order to measure the cross-sectional area, outer diameter, and wall thickness. The arteries were then mounted on each cannula using a single purse-string suture and oriented in the *in vivo* flow direction. Warm (37 °C) bath and perfusion medium were added to the vessel chamber and flow loop. The entire flow loop was then transferred to the incubator for the duration of the experiment.

### 3.3 Method for Controlling Circumferential and Shear Stress

The global mechanical environment of arteries is defined by blood pressure, flow rate, and axial stretch. However, the cells within the artery sense the local mechanical environment which is comprised of circumferential stress and axial strain in the media and flow-induced shear stress at the intima. By simultaneously adjusting pressure and flow rate while the artery is held at a constant axial stretch ratio, it is possible to independently control circumferential stress and shear stress in perfusion organ culture experiments. The global and local parameters are related by the equations of equilibrium, the flow equation, and the pressure-diameter response of the artery.

Based on overall equilibrium in the radial direction, the mean circumferential stress within the arterial wall at a given time  $t$  is

$$\sigma_{\theta} = \frac{P(d_o - 2h)}{2h} \quad 3-1$$

where  $P$  is the transmural pressure,  $d_o$  is the outer diameter at the loaded state, and  $h$  is the loaded thickness of the arterial wall. This equation applies for both thick- and thin-walled tubes and for cases when residual stresses are considered.

Assuming the culture medium to be a Newtonian fluid and to develop Poiseuille flow, the mean shear stress along the luminal surface of an artery at time  $t$  is

$$\tau = \frac{32\mu Q}{\pi(d_o - 2h)^3} \quad 3-2$$

where  $\mu$  is the viscosity of the culture medium and  $Q$  is the average flow rate.

Of the variables used in Equations 3-1 and 3-2, the values of  $P$ ,  $Q$ , and  $d_o$  can be measured using the experimental system. To calculate the wall thickness of the loaded vessel, the artery was assumed to behave as an incompressible material (Carew et al.

1968; Nichols and O'Rourke 1998). Considering the artery as a circular cylinder of constant thickness, it follows from incompressibility that at time  $t$  the volume of the no-load and deformed configurations are equal

$$(D_o - H)H = (d_o - h)h\lambda_z \quad 3-3$$

where  $D_o$  is the no-load outer diameter of the vessel,  $H$  is the no-load wall thickness of the artery, and  $\lambda_z$  is the axial stretch ratio. The axial stretch ratio,  $\lambda_z$ , is defined as  $l/L$ , where  $l$  is the *in situ* vessel length and  $L$  is the no-load length.

A functional relationship between pressure and outer diameter can be determined by conducting a pressure-diameter test while the artery is held at a fixed  $\lambda_z$ . An interpolation function can then be used to fit this data and determine the pressure-diameter relationship. For this study, the outer diameter was measured at three pressures as described later. The resulting measurements were then fit to a quadratic curve, which took the following general form

$$P = Ad_o^2 + Bd_o + C \quad 3-4$$

where A and B are coefficients determined by the curve fit.

Table 3-1 categorizes each of the quantities used in Equations 3-1 to 3-4. The prescribed parameters,  $\sigma_\theta$ ,  $\tau$ , and  $\lambda_z$ , are defined by the experimental design. The known parameters,  $D_o$  and  $H$ , are measured at the onset of the experiment. Given the target values of  $\sigma_\theta$ ,  $\tau$ , and knowing the undeformed dimensions,  $D_o$  and  $H$ , as well as the axial stretch ratio,  $\lambda_z$ , Equations 3-1 to 3-4 can be solved for  $P$ ,  $Q$ ,  $d_o$ , and  $h$ . For this study, a code was written in MAPLE 10 (Maplesoft, see Appendix A.2) to solve these equations.

The resulting pressure and flow rate are accepted as a first guess to achieve the prescribed values of circumferential and shear stress. Once the artery is subjected to this

pressure and flow rate, it is possible to measure the deformed outer diameter and to calculate the existing circumferential and shear stress from Eqs. 3-1 to 3-3. At this point, the realized values of circumferential and shear stress may not equal their target values due to the conditions under which the pressure-diameter relationship, Eq. 3-4, is obtained. The mechanical behavior of the artery *in vivo* is a result of the passive response of the elastin and collagen as well as the active response of vascular smooth muscle cells. In this study, we performed the inflation test in the absence of flow. Though Eq. 3-4 might account for the myogenic response of the vascular muscle, it does not account for the effect of flow on the muscular tone. It is well known that flow-induced shear stress modulates the vascular tone through release of relaxing or constricting factors by the endothelial cells (Ligush et al. 1992). Provided the difference between the existing and target values of the stresses is greater than the admissible error, pressure and flow rate are iteratively adjusted to achieve the target values of circumferential stress and shear stress.

Table 3-1: Quantities used to determine the relationship between global and local mechanical parameters.

Prescribed	Known	Unknown
$\sigma_\theta$	$D_o$	$P$
$\tau$	$H$	$Q$
$\lambda_z$		$d_o$
		$h_o$

In general, remodeling leads to changes in arterial dimensions and mechanical properties. Therefore, to maintain the prescribed values of circumferential and shear stress over time, the pressure and flow in organ culture system must vary accordingly.



The approach depends on the technical ability to determine the deformed outer diameter and wall thickness of the artery during an organ culture experiment. If it is possible to monitor the outer diameter and the wall thickness, the actual values of the circumferential and shear stress can be calculated at any moment and the pressure and flow can be iteratively adjusted as described above. A similar procedure is applicable if the duration of the experiment is relatively short and no significant changes in undeformed dimensions (i.e. no mass is added or removed) of the cultured artery are observed. Then, the current wall thickness is calculated from the measured outer diameter using the condition of material incompressibility, Eq. 3-3. This is typically the case in the experiments performed in this study. Finally, if the arterial dimensions vary but wall thickness cannot be continuously recorded, it is necessary to interrupt the experiment after a certain time interval and to directly measure the current undeformed wall thickness and outer diameter. This is the case during first 15 hours of experiments performed in this study.

### **3.4 Experimental Protocol**

Table 3-2 provides an overview of the experimental protocol and lists each step of the protocol in chronological order. The details of each event are described in greater detail throughout this chapter.

Table 3-2: Timeline of experimental protocol.

Day	Experimental Event
0	Harvest and prepare artery
	Measure no-load dimensions of artery
	Mount artery in culture chamber
	Conduct inflation test
	Begin stress control
1	Measure no-load dimensions of artery
	Conduct inflation test
	Resume stress control
2	Conduct inflation test
	Continue stress control
	Add BrdU to flow loop
3	Stop stress control
	Measure no-load dimensions of artery
	Begin proline incorporation assay
	Begin cell death assay
	Prepare samples for histology
	Snap freeze samples for zymography
4	Stop proline incorporation assay
	Stop labeling dead cells

### 3.4.1 Beginning of Experiment

After the flow loops were placed in the incubator, the peristaltic pumps were turned on and the flow rate was set at the minimum flow rate of 30 mL/min for approximately one hour to allow the vessels to become acclimated to the organ culture environment. During this time, the no-load outer diameter was measured and wall thickness of the vessels computed as described in Section 3.5.1. The vessels were then elongated to a physiologic stretch ratio of 1.5 over a period of 30 minutes. Following this period, the method for controlling circumferential and shear stresses was initiated.

### 3.4.2 Experimental Conditions

All experiments were run for 3 days. At the onset of the experiment, the target values for circumferential stress and shear stress are determined. The target values of circumferential stress and shear stress used in this study are shown in Table 3-3. To

investigate the effects of circumferential stress on remodeling, bilateral porcine common carotid arteries were subjected to a circumferential stress of 50 kPa (Case A in Table 3-3) or 150 kPa (Case B), values that are 50% below and above the physiologic level of circumferential stress (100 kPa) (Vaishnav et al. 1990; Matsumoto and Hayashi 1994). Shear stress and the axial stretch ratio were held at physiologic levels of 1.5 Pa (Kamiya and Togawa 1980; Brownlee and Langille 1991) and 1.5 (Han and Ku 2001), respectively.

For shear stress experiments, bilateral porcine common carotid arteries were subjected to a shear stress of 0.75 Pa (Case C) or 2.25 Pa (Case D). Circumferential stress and the axial stretch ratio were held at physiologic levels of 100 kPa and 1.5, respectively.

Table 3-3: Summary of the experimental conditions explored in this study. All arteries were held at a physiologic axial stretch ratio of 1.5. Cases A and B were run as paired experiments and cases C and D were paired.

$\tau$ (Pa) \ $\sigma$ (kPa)	0.75	1.50	2.25
50		A	
100	C		D
150		B	

### 3.4.3 Development of Method for Controlling Circumferential and Shear Stresses

The flow chart shown in Figure 3-2 describes the first approach used to control circumferential stress and flow-induced shear stress in organ culture. This method tacitly assumed that the no-load dimensions change during culture.

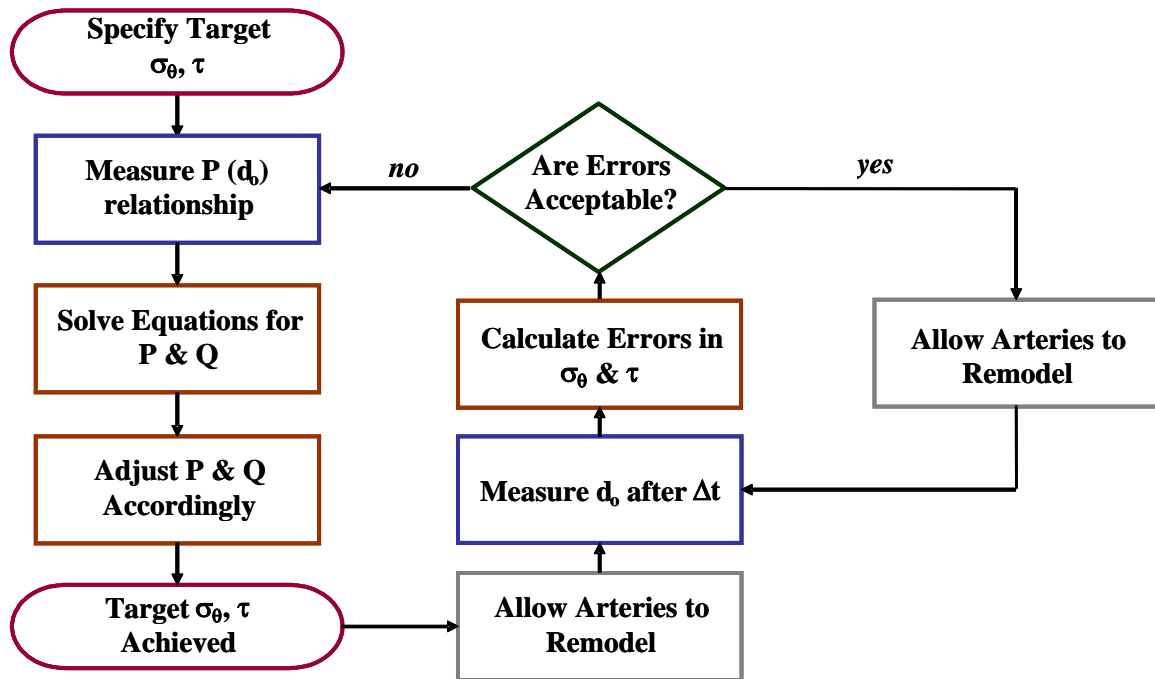


Figure 3-2: Flow chart describing the process for controlling circumferential stress and shear stress at a fixed axial stretch ratio in perfusion organ culture.

After identifying the target values, the next step in controlling the local environment was to determine the pressure-diameter relationship for the artery. The flow to the vessels was stopped in order to conduct the inflation test as described in Section 3.5.4. Following the inflation test, flow was restored to the vessels at the minimum rate of 30 ml/min while the data was being processed. The results of the inflation test, along with the no-load dimensions of the vessel and the prescribed values of stress, were then input into the MAPLE program. Using this program, Equations 3-1 to 3-4 were solved for the values of pressure and flow rate required to achieve the prescribed circumferential stress and flow-induced shear stress. The pressure and flow rate were then gradually adjusted to these values over a 30 minute period.

As shown in Figure 3-2, the outer diameter of the artery is measured at regular time intervals,  $\Delta t$ , after the target values of circumferential and shear stresses have been achieved. Theoretically, the pressure and flow rate would be adjusted continuously to maintain the target circumferential and shear stresses. However, in practice, achieving closed-loop control of circumferential stress and shear stress was not feasible because pressure and flow rate could not automatically be adjusted using the current instrumentation. Therefore, adjustments of pressure and flow rate were done in discrete increments. The lower bound for the time interval between adjustments was determined to be 4 hours. As shown in Figure 3-3, it was found that the arteries undergo a vasoactive response that lasts for 2 – 4 hours following the large increase in pressure and flow rate that occurs after the inflation test. The upper bound of the time interval was 24 hours based on previous studies which show that changes in arterial outer diameter can occur after 24 hours in culture (Han and Ku 2001; Davis 2002). The actual time interval between adjustments of pressure and flow rate was chosen to be 24 hours to allow sufficient time for remodeling while limiting changes in outer diameter.

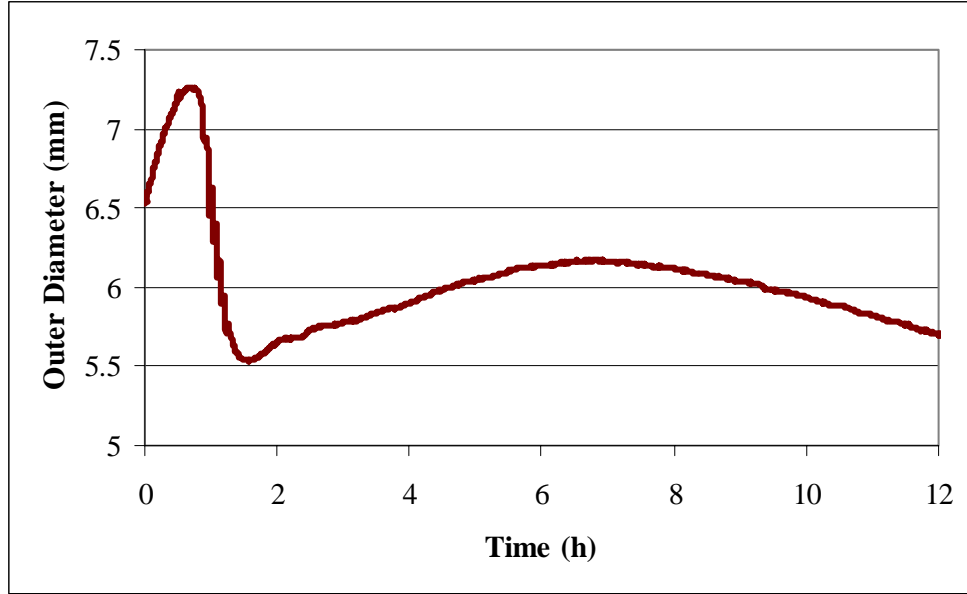


Figure 3-3: Typical time course of outer diameter for an artery ( $\sigma_\theta = 50$  kPa,  $\tau = 1.5$  Pa,  $\lambda_z = 1.5$ ) over the first 12 hours of culture. A strong myogenic response, as indicated by the rapid increase and decrease in outer diameter, occurs during the first 2 – 4 h of culture which is followed by stabilization of the outer diameter. To allow the outer diameter to stabilize following the myogenic response, 4 hours was considered to be the minimum time period between adjustments of pressure and flow rate.

Three 3 – 5 cm segments from bilateral porcine carotid arteries were cultured under typical experimental conditions of low circumferential stress ( $\sigma_\theta = 50$  kPa,  $\tau = 1.5$  Pa, and  $\lambda_z = 1.5$ ) and high circumferential stress ( $\sigma_\theta = 150$  kPa,  $\tau = 1.5$  Pa, and  $\lambda_z = 1.5$ ). Every 24 hours, the flow to one of the vessels was stopped and its no-load dimensions were measured. Figure 3-4 shows that the greatest changes in no-load volume occur during the first 24 hours of culture, after which, the volume remains relatively constant. This trend is consistent for arteries under all loading conditions.

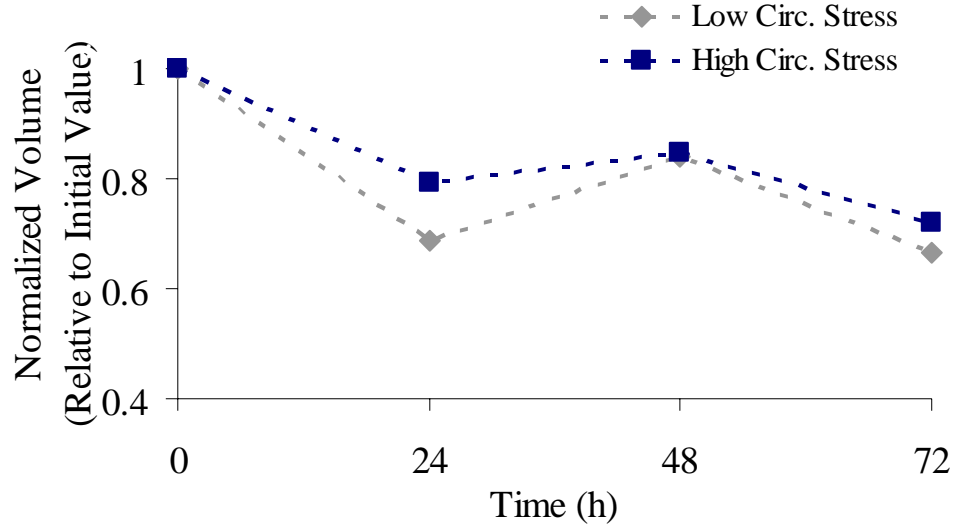


Figure 3-4: The change in no-load volume over time for a typical experiment in which arteries were exposed to low and high circumferential stress (Cases A and B in Table 3-3).

In conclusion, these preliminary studies revealed that the changes in no-load dimensions occur during the early stage of culture. After this period, it is reasonable to assume that the no-load dimensions remain constant. Therefore, it is important to account for the changes in no-load dimensions when applying the incompressibility assumption (Equation 3-3) in organ culture experiments.

#### 3.4.4 Method for Controlling Circumferential and Shear Stress

Using the results of the preliminary method, the experimental approach was slightly modified to improve the control of circumferential stress and shear stress. For this study, three 3 – 5 cm segments were cut from a pair of bilateral porcine carotid arteries. Of the three segments, two were considered experimental arteries and were subjected to a set of the experimental conditions listed in Table 3-3. As described in the previous section, the no-load dimensions of the artery change during culture. Ideally, the

experiment would be stopped after 24 hours and the no-load dimensions of the experimental arteries would be measured directly. However, this approach is not practical due to the risk of contaminating the sterile culture environment. Therefore, an additional arterial segment was cultured in order to estimate changes in no-load dimensions. Only one additional artery was required to estimate the changes in no-load dimensions of both experimental arteries because similar changes in volume were observed in arteries regardless of loading conditions as shown in Figure 3-4. The additional vessel was subjected to high stress conditions for all experiments.

The previous experiments revealed that changes in no-load dimensions occur within 24 hours. Ideally, the exact time required for the changes in no-load dimensions to occur would be known in order to minimize the errors in estimating the wall thickness. Although the precise time required for these changes to occur was not identified, it was determined that the changes occur within 15 hours of culture. Therefore, the additional artery was cultured for approximately 15 hours and then the no-load dimensions of the vessel were measured.

The ratio of the no-load diameter after 15 hours in culture to the initial no-load diameter was determined as:

$$\alpha = \frac{D_o(t = 15 \text{ h})}{D_o(t = 0 \text{ h})} \quad 3-5$$

Similarly, the ratio of the wall thickness at the no-load state after 15 hours in culture to the initial no-load wall thickness was determined as:

$$\beta = \frac{H(t = 15 \text{ h})}{H(t = 0 \text{ h})} \quad 3-6$$



Because all arterial segments were from the same animal source and have similar dimensions, it was reasonable to assume that the values of  $\alpha$  and  $\beta$  were the same for all segments. Therefore, the values of  $D_o(t = 15 \text{ h})$  and  $H(t = 15 \text{ h})$  for the experimental arteries were calculated from Equations 3-5 and 3-6 using the values of  $\alpha$  and  $\beta$  determined from the additional artery. The values of  $D_o(t = 15 \text{ h})$  and  $H(t = 15 \text{ h})$  were assumed to remain constant for the remainder of the experiment as described earlier. After the values of  $D_o(t = 15 \text{ h})$  and  $H(t = 15 \text{ h})$  were calculated, the inflation test was conducted to determine the pressure-diameter relationship of the artery. Using the values of  $D_o(t = 15 \text{ h})$  and  $H(t = 15 \text{ h})$ , Equations 3-1 to 3-4 were solved for the pressure and flow rate required to achieve the target values of circumferential stress and shear stress. The pressure and flow rate were then adjusted accordingly and the control of circumferential and shear stress was resumed.

The method proposed in the previous section was modified to incorporate this process of estimating the no-load dimensions of cultured arteries. In addition, the method was modified to include more frequent adjustments of pressure and flow rate, which will be described later in this section. An overview of the revised method for controlling circumferential stress and shear stress is shown in Figure 3-5.

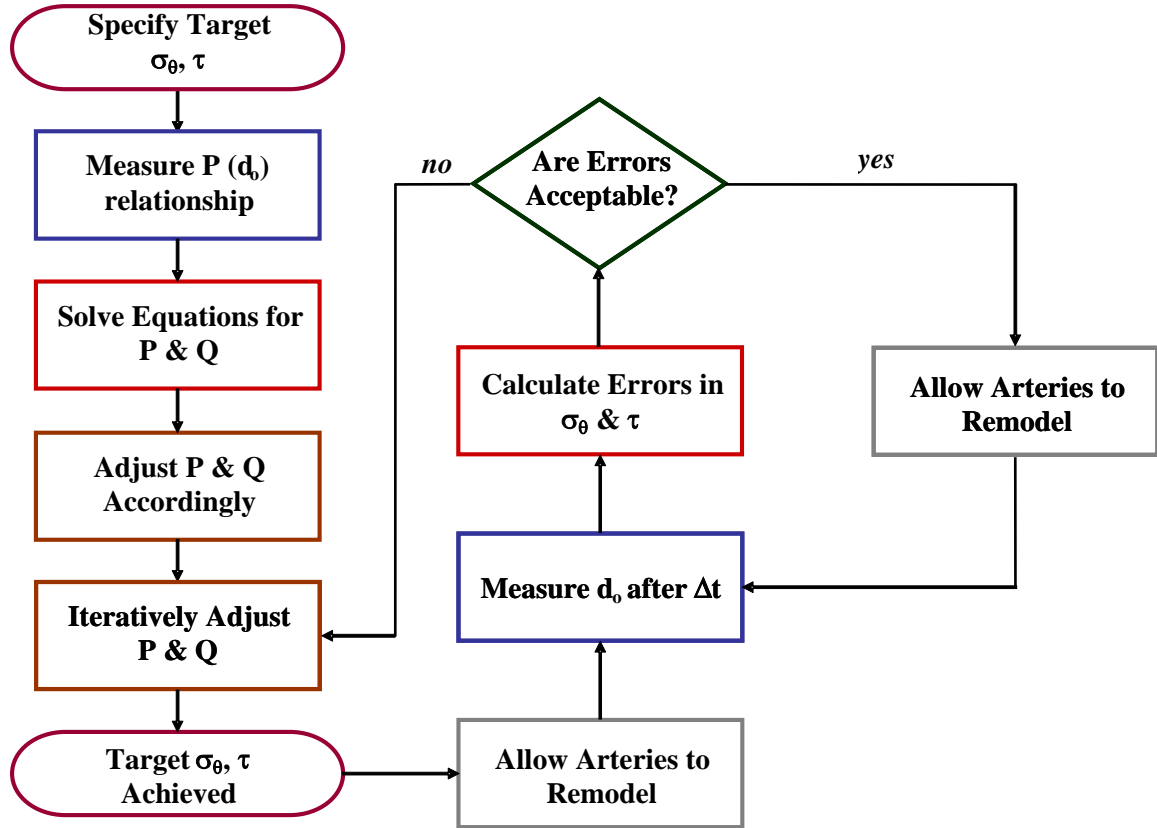


Figure 3-5: Flow chart describing the revised method of independently controlling circumferential stress and shear stress in organ culture.

In the revised method, the no-load dimensions are measured at the onset of the experiment and again after approximately 15 hours of culture. Because the no-load dimensions remain relatively constant after the early-stage of culture, it is possible to accurately estimate the wall thickness using the condition of incompressibility after the first 15 hours (Equation 3-3). Therefore, it is also possible to more frequently calculate circumferential stress and shear stress using the condition of incompressibility.

The revised method described in Figure 3-5 includes an iterative procedure for adjusting the pressure and flow rate in order to maintain the target stress values. The time interval,  $\Delta t$ , between measurements of the deformed outer diameter was reduced to

30 seconds. In turn, the values of circumferential and shear stress were calculated every 30 seconds and then displayed on the computer monitor and recorded using a C++ program described in Section 3.5.3. The experiment was monitored regularly and pressure and flow rate were adjusted when the errors in circumferential stress or flow-induced shear stress exceed 5%. Because the values of circumferential and shear stress were monitored more frequently, only minor adjustment of pressure and flow rate were required to restore the stresses to their target values. The benefit of making minor adjustments of pressure and flow rate is that these more subtle changes in mechanical environment minimize the active responses of the vessel observed when the artery was subjected to large step changes in pressure and flow rate as shown in Figure 3-3.

#### **3.4.5 End of Experiment**

At the end of culture, the flow of perfusion medium was stopped. The culture chambers were quickly removed from the flow loop and the artery was cut free from the cannulae. Approximately 5 mm of each end of the vessel was discarded to avoid end effects and possible tissue damage due to suturing the tissue on the cannulae. The artery was then divided into sections for the desired experimental endpoints as shown in Figure 3-6. Each experimental endpoint is described in detail in Section 3.6.

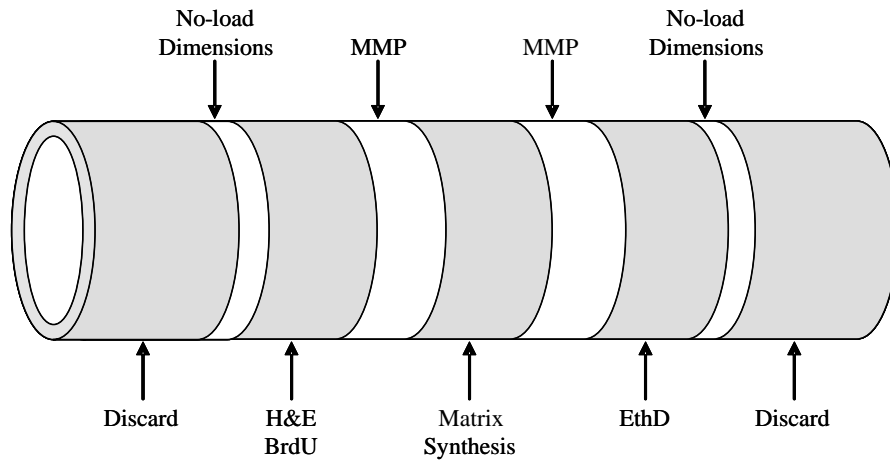


Figure 3-6: Schematic diagram of an artery showing how the artery was divided for processing of experimental endpoints following culture.

### 3.5 Data Acquisition

#### 3.5.1 Cross-Sectional Dimensions

Ring segments of an artery were used to measure the cross-sectional area, inner diameter, and outer diameter of each artery. For the measurement, approximately 2 mm thick segments were cut from each end of the vessel. Ring segments were placed in a petri dish and were lit from below using a backlight (QVABL, Dolan-Jenner Industries) with a variable light intensity fiber optic illuminator (Fiber-Lite, Dolan-Jenner Industries). Images were acquired by a CCD camera (V-1070, Marshall Electronics) fitted with an adjustable zoom lens (MonoZoom-7, Leica). The magnification was increased to maximize the size of the ring segment in the field of view. The intensity of the backlight was adjusted to maximize the contrast between the ring segment and the white background produced by the backlight. Images were captured using DT Acquire

software (Data Translation). A representative image of a ring segment used to measure the cross-sectional dimensions is shown in Figure 3-7.

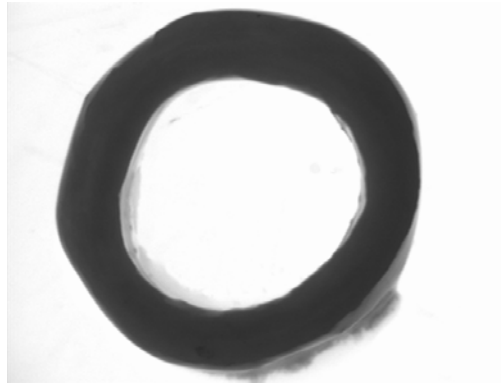


Figure 3-7: Typical image of an arterial ring segment that was backlit for measurement of cross-sectional dimensions.

Image-Pro Plus (Media Cybernetics) was used to calculate the cross-sectional dimensions of the artery. First, the image was thresholded and total cross-sectional area (in pixels<sup>2</sup>) of each ring was measured. The luminal area was then measured and used to calculate the inner diameter (in pixels) of the ring segment by assuming that the inner diameter was circular. Similarly, the outer diameter (in pixels) was calculated using the sum of the luminal and cross-sectional areas. These measurements were taken for two ring segments and then averaged to give the no-load cross-sectional area, inner diameter, and outer diameter for the artery.

The measurements were calibrated by taking an image of a round stainless steel dowel pin of known dimensions (2 mm) under the same lighting and magnification conditions as the ring segments. The pin was oriented horizontally in the field of view and the diameter of the dowel pin was measured in pixels along the vertical camera axis. Since the difference in resolution when calibration was done with the pin oriented along the horizontal or vertical camera axis was approximately 1%, the diameter was only

measured along one axis, which in for this work was the vertical camera axis. The calibration factor, in units of mm/pixel, was calculated by dividing the known diameter of the pin (in mm) by the measured diameter (in pixels). This value was used to convert the units of the cross-sectional dimensions to mm or mm<sup>2</sup>. The resolution depended on the magnification and ranged from approximately 0.011 mm to 0.026 mm. The outer diameters of five adjacent segments of an artery were measured to estimate errors in diameter measurement that may occur due to cutting imperfections and the presence of loose adventitia. This error was approximately 1 - 2% depending on the magnification.

### **3.5.2 Outer Diameter**

The outer diameter was measured during culture using a C++ subroutine (Microsoft Visual Studio 6.0, see Appendix A.2), CCD camera, and framegrabber (DT 3130, Data Translation). The C subroutine was similar to that used by Davis et al. (2002). During culture, the artery was illuminated from below the culture chamber using a variable-intensity fiber optic backlight and a CCD camera was positioned above the artery to capture images. The use of backlighting created an image (640 X 480 X 8-bit resolution) in which the artery was dark and the background was light. At the onset of the experiment, the image magnification was set such that the loaded artery would take up approximately 80% of the field of view.

Thresholding was used to segment the artery from the background. The subroutine was written to automatically determine the threshold intensity. The threshold intensity,  $I_t$ , was

$$I_t = I_b - 0.25(I_b - I_f) \quad 3-7$$

where  $I_b$  is the average background intensity and  $I_f$  is the average foreground (artery) intensity as described by Davis (2002).  $I_b$  was computed by averaging the intensity of a row of pixels near the top or bottom of the field of view that are out of the range of where the artery would be located.  $I_f$  was computed by averaging the intensity of a row of pixels near the center of the field of view where the artery is definitely located.

For each image, 20 equally spaced vertical line scans were used to measure the diameter. For each line, pixels were counted if their intensity was less than or equal to the threshold intensity and the total number of counted pixels were taken as the local diameter for that column. The local diameter was measured for each line scan and the average of these local diameters was recorded as the diameter for each image.

Diameter calibration was achieved using the stainless steel cannula which had a known outer diameter of 5.16 mm. The diameter of the cannula, in pixels, was measured as described above. A conversion factor, in mm/pixel, was then computed and used to convert all diameter measurements into units of millimeters. Following each measurement, the diameter data was written to a text file for later analysis.

The resolution of diameter measurements depended on the magnification and ranged from approximately 0.012 to 0.022 mm. To estimate the measurement error, the diameter of the cannula was measured five times. The resulting measurement error was approximately 0.5%.

### **3.5.3 Calculations of Circumferential and Shear Stress**

A C++ subroutine (see Appendix A.2) was written to continuously calculate circumferential and shear stress for experiments using the revised stress control method described in Section 0. The parameters required to make these calculations are pressure,

flow rate, outer diameter, and wall thickness of the artery. The pressure was acquired from the pressure transducer which was connected to a data acquisition board (DT300, Data Acquisition). The flow rate was input manually by the user. The outer diameter was measured as described above. The wall thickness was then calculated by assuming incompressibility as shown in Equation 3-3. Once the data was acquired, the subroutine calculated circumferential and shear stress using Equations 3-1 and 3-2, respectively.

Circumferential and shear stress values were calculated every 30 seconds and displayed on the monitor and written to a text file. If adjustments to pressure and flow were required, data acquisition was paused while adjustments were made and resumed afterwards. The subroutine was run for the duration of the experiment.

#### **3.5.4 Inflation Test**

For the inflation test, flow was stopped and the tubing of the flow loop was clamped such that the vessel and the pressure transducer were isolated. A 10 mL syringe (Becton Dickinson) with a 0.22  $\mu\text{m}$  filter (Millipore) was mounted in a hand-driven pump and connected to the isolated portion of the flow loop to regulate the pressure. Arteries were preconditioned by increasing pressure from 50 mmHg to 200 mmHg for 10 cycles. For the inflation test, diameter measurements were taken at pressures of 50, 125, and 200 mmHg while the artery was held at a constant axial stretch ratio of 1.5. If the pressure required to achieve the target stress condition was outside of this range, the inflation test was repeated over a wider range of pressures. For each reading, the pressure was slowly adjusted to the desired level by moving the syringe pump. The outer diameter measurement was acquired using a C++ program (see Appendix A.1) and the data were written to a text file as described in the Section 3.5.2. The pressure data were



simultaneously acquired using Quick DataAcq software (Data Acquisition) and were written to an Excel file.

### 3.5.5 Peterson's Elastic Modulus

The pressure-diameter results obtained from the inflation tests were used to calculate the Peterson's elastic modulus for cultured arteries. Peterson's modulus is a measure of the overall mechanical response of the artery around a defined deformed mechanical state. It includes the effects of geometry and the mechanical properties of vascular tissues.

In general, Peterson's modulus is given as:

$$E_p = \frac{\Delta P d_{o,mean}}{\Delta d_o} \quad 3-8$$

where  $P$  is the transmural pressure,  $d_o$  is the outer diameter, and  $d_{o,mean}$  is the mean outer diameter over the pressure range of interest.

In this study, Peterson's modulus was calculated over the entire pressure range measured during the inflation test (50 mmHg – 200 mmHg) as:

$$E_p = \frac{(P_{200mmHg} - P_{50mmHg})(d_{o,200mmHg} + d_{o,50mmHg})}{2(d_{o,200mmHg} - d_{o,50mmHg})} \quad 3-9$$

The subscripts indicate the pressure at which each measurement was taken.

## 3.6 Biological Endpoints

### 3.6.1 Collagen Synthesis

Collagen synthesis was measured using a  $^3\text{H}$ -proline incorporation assay based on the method of Peterkofsky and Prockop (1962). Proline, an amino acid highly conserved in collagen, is incorporated into cells during the early stages of fiber formation (Alberts et al. 1994). Therefore, the amount of radiolabeled proline incorporated into cells is a marker of collagen synthesis.

For the  $^3\text{H}$ -proline incorporation assay, ring segments, approximately 4 mm in length, were cut from the artery following culture and statically incubated in DMEM supplemented with  $^3\text{H}$ -proline (10  $\mu\text{Ci/ml}$ ). Pilot studies were conducted to determine the appropriate time period for incubation in radiolabeled media and will be described later. Although it would have been ideal to add the  $^3\text{H}$ -proline to the perfusion media, the potential for radioactive contamination and the expense associated with using such large volumes of  $^3\text{H}$ -proline precluded its use during culture. Following radiolabeling, tissue segments were washed in quench solution four times for 30 minutes. The quench solution consisted of PBS supplemented with sodium sulfate (0.8 mM, Sigma) and L-proline (1.0 mM, Sigma). Samples were then lyophilized and the dry weight was measured. Samples were digested in 0.2 – 0.4 mg/ml proteinase K (Sigma) in 100 mM ammonium acetate solution (Sigma) overnight at 60 °C. The radioactivity was measured using a scintillation counter (Tri-Carb, PerkinElmer) and results were normalized to the tissue sample's dry weight.

Because the radiolabeling occurred post-culture, the synthetic response of cells could change over time following the removal of the mechanical stimulus. Therefore,

pilot studies were conducted to determine the optimal incubation period following culture. Tissue segments, along with negative controls, were incubated for times ranging from 1 – 24 hours. Negative controls were used to confirm that the  $^3\text{H}$ -proline was incorporated into the cells rather than being retained by the tissue following incubation. The negative controls were tissue segments taken from the experimental artery and subjected to a series of three freeze-thaw cycles to lyse the cells and, thus, inhibit any synthetic activity.

Figure 3-8 shows the results for proline incorporation at various incubation periods. As expected, after a short incubation of one hour there was little differentiation in proline incorporation between the high and low circumferential stress conditions, presumably because there had not been sufficient time for differences in incorporation rates to become apparent. However, at later time points, the difference between the two stress conditions became more pronounced with statistically significant differences occurring at 3, 18, and 24 hours of incubation. Based on these results, we decided to incubate the tissue segments in radiolabeled media for 18 h following culture as mentioned earlier.

Figure 3-8 also shows that the incorporation levels for the negative controls were much less than the experimental samples. Therefore, the protocol is effective in measuring the  $^3\text{H}$ -proline that is actively incorporated by cells and in washing away  $^3\text{H}$ -proline in the matrix.

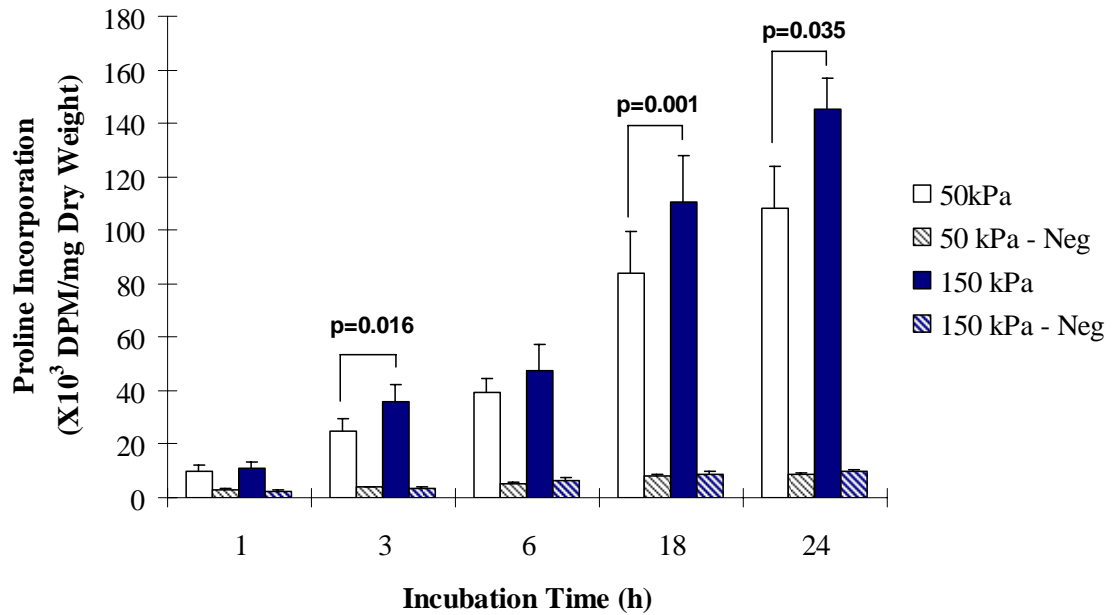


Figure 3-8: Time course of  $^3\text{H}$ -proline incorporation for static incubation of tissue segments ( $n=6$  for experimental arteries,  $n=4$  for negative controls). The stress conditions for this experiment were  $\sigma_0 = 150$  or  $50$  kPa,  $\tau = 1.5$  Pa, and  $\lambda_z = 1.5$ . There were statistically significant ( $p<0.05$ ) differences between each experimental specimen and its negative control (shown in cross-hatches) at all time points except at 1 h.

To further demonstrate that arteries were viable after the static incubation period following culture, arteries were incubated in methylthiazol tetrazolium (MTT). Following culture, tissue segments, approximately 3 mm in length, were statically incubated for 24 hours at  $37^\circ\text{C}$ . These tissue segments, along with segments from the negative controls, were incubated in 10 mg/ml MTT in deionized water for one hour at  $37^\circ\text{C}$ . MTT is a yellowish solution that is converted to a dark blue color by the mitochondria of viable cells.

Figure 3-9 shows the color of a tissue segment of an artery cultured under low circumferential stress conditions compared to that of a negative control. As seen in Figure 3-9, the experimental artery has a dark blue color which indicates that the tissue is

viable, while the negative control retains its natural color which suggests that the tissue is not viable. These results demonstrate that arterial cells retain viability in static incubation as occurs during the  $^3\text{H}$ -proline incorporation assay.

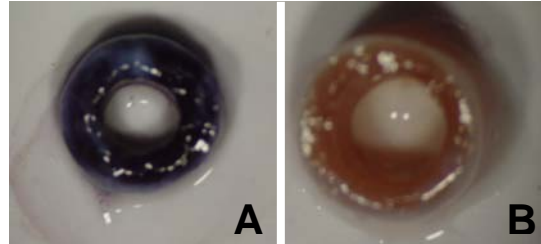


Figure 3-9: Representative image of tissue segments incubated in MTT solution from an artery subjected to low circumferential stress conditions (A) and a negative control (B). The experimental artery was cultured statically for 24 hours following the experiment. The negative control was subjected to a series of freeze-thaw cycles to lyse cells. The white spots in the arterial wall are an imaging artifact associated with the camera flash.

### **3.6.2 Matrix Metalloproteinase Activity**

The activity of matrix metalloproteinases (MMPs)-2 and -9 were measured using SDS-PAGE zymography. Using this method, the gelatinolytic activity of MMPs-2 and -9 can be detected following electrophoretic migration due to their ability to degrade the gelatin incorporated in the SDS-PAGE gels (Kleiner and Stetler-Stevenson 1994).

Following culture, a ring segment of tissue, approximately 3 mm in length, was cut from the artery, snap frozen in liquid nitrogen and stored at  $-80\text{ }^{\circ}\text{C}$  for subsequent analysis. Frozen samples were homogenized in ice-cold lysis buffer (10 mM sodium phosphate pH 7.2, 150 mM sodium chloride, 1% Triton X-100, 0.1% SDS, 0.5% sodium deoxycholate, 0.2% sodium azide (Sigma)) using a mechanical tissue homogenizer (Ultra-Turrax 25, IKA). The protein concentrations of the samples were measured using a modified Lowry protein assay (Lowry et al. 1951). Equal amounts of protein were loaded in each lane of the gel. The gels were 10% polyacrylamide with 1.0 mg/ml of gelatin. The electrophoretic migration was carried out at  $4\text{ }^{\circ}\text{C}$ . Following migration, the

proteins in the gel were renatured in a series of 2 incubations in 2.5% Triton X-100 for 15 minutes each. The gels were then incubated overnight at 37 °C in an assay buffer (50 mM Tris-HCL pH 7.4, 10 mM calcium chloride, 50 mM sodium chloride, and 0.05% Triton X-100). Following incubation, the gels were washed in deionized water and stained with Coomassie Brilliant Blue (Sigma). Proteins having gelatinolytic activity were visualized as clear lysis bands while the rest of the gel was stained blue. Prestained molecular weight markers were used to determine the molecular weight of the lysis bands. ScionImage was used to quantify the zymography results based on the pixel intensity and size of the lysis band.

### **3.6.3 Cell Proliferation**

Cell proliferation was measured by using a 5-bromo-2'-deoxy-uridine (BrdU, BrdU Labeling and Detection Kit I, Roche) incorporation assay. In this assay, cells that have incorporated BrdU into deoxyribonucleic acid (DNA) can be detected using a monoclonal antibody against BrdU and a fluorescently labeled secondary antibody (Alberts et al. 1994).

For these experiments, BrdU was added to the perfusion media at a final concentration of 10  $\mu$ M for the last 24 hours of culture. Following culture, a 4 mm segment of tissue was fixed in formalin overnight. The sample was then stored in 70% isopropyl alcohol and later processed for histologic analysis. The tissue was embedded in paraffin and cut into 5  $\mu$ m thick sections which were mounted on Superfrost Plus microscope slides. Slides were deparaffinized and then boiled for 15 minutes in 10mM citrate buffer (pH = 6.0) in a pressure cooker for antigen retrieval (Shi et al. 1993). The slides were then allowed to cool at room temperature for 20 minutes. Following cooling,

the slides were washed in PBS for five minutes. Cell membranes were permeabilized using 0.5% Triton X-100 in PBS for 20 minutes at 37 °C. Slides were then washed in PBS for five minutes. Sections were covered with 1% bovine serum albumin (BSA) for five minutes to prevent non-specific binding of the primary antibody.

The detection of BrdU was achieved using an antibody kit. Following blocking, sections were covered with approximately 100 µl of anti-BrdU mouse monoclonal antibody which was diluted 1:10 in an incubation buffer (66 mM Tris buffer, 0.66mM MgCl<sub>2</sub>, 1mM 2-mercaptoethanol) included in the kit for 30 minutes at 37 °C. Slides were then washed twice in PBS for five minutes per wash. Sections were then covered with approximately 100 µl of anti-mouse-Ig-fluorescein antibody diluted 1:10 in incubation buffer for 30 minutes at 37 °C. Slides were then washed twice in PBS for five minutes per wash. Slides were incubated in 0.25 µg/ml 4'-6-diamidino-2-phenylindole (DAPI, Sigma) in PBS for five minutes. DAPI was used as a counterstain to visualize all of the cell nuclei in the tissue section. Slides were washed in deionized water for five minutes. Coverslips were then mounted on the slides using Gel/Mount (Biomed), an aqueous mounting agent. Sections were later visualized using fluorescent microscopy and cell proliferation was quantified as described Section 3.6.5.

#### **3.6.4 Cell Death**

Cell death was measured using an ethidium homodimer-1 (EthD) dye binding assay. EthD is a fluorescent dye that has a high affinity for DNA and low membrane permeability (Alberts et al. 1994). Therefore, EthD cannot permeate the intact membranes of viable cells. However, since nonviable cells have ruptured membranes, EthD readily binds the exposed DNA.

The protocol for this assay was derived from that of Merrilees et al. (1995). For this protocol, short arterial segments (approximately 4 mm in length) were incubated in culture medium supplemented with 10% calf serum and 5  $\mu$ M EthD (Invitrogen) for 24 hours at 37 °C following the experiment. Although EthD could have been added to the flow loop during the experiment, such an approach would have been expensive due to the large amount of EthD required. The current method is well established and has been reported previously (Han and Ku 2001; Han et al. 2003; Davis et al. 2005).

Following incubation, the tissue segments were fixed in formalin, embedded in paraffin, and sectioned as described in Section 3.6.3. After deparaffinization, slides were incubated in 0.25  $\mu$ g/ml DAPI in PBS for five minutes. DAPI was used as a counterstain to visualize all of the cell nuclei in the tissue section. Slides were washed in deionized water for five minutes. Coverslips were then mounted on the slides using Gel/Mount. Sections were later visualized using fluorescent microscopy and cell death was quantified as described in Section 3.6.5.

### **3.6.5 Quantification of Labeled Nuclei**

The ratio of BrdU-positive nuclei to total cell nuclei and EthD-positive nuclei to total cell nuclei was used to quantify cell proliferation and cell death, respectively. Monochrome fluorescent images were acquired at 10X magnification using a Nikon Eclipse E800 fluorescent microscope. Samples were first imaged using the DAPI filter cube (EF-4 UC-2E/C, Nikon) to capture total nuclei and then, the same field of view was imaged using the FITC filter cube (41001, Chroma Technology Corporation) for BrdU-labeled nuclei or the TRITC filter cube (EF-4 G-2A, Nikon) for EthD-labeled nuclei. Images were acquired at four different circumferential locations (0°, 90°, 180°, and 270°)



on two non-adjacent cross-sections for each artery. For BrdU samples, two sets of images were acquired at each circumferential location – one set that captured the intima and media and another set that capture the adventitia. For EthD samples, images were only captured in the media because it was generally difficult to distinguish between labeled and unlabeled nuclei in the intima and adventitia due to the autofluorescence of elastin in the internal and external elastic lamina.

The total nuclei for each field of view were counted using Image Pro. The threshold for each field of view was manually adjusted to segment the nuclei. The number of objects in the field of view was then counted using Image Pro. Labeled nuclei were counted by hand or by manually setting a threshold and automatically counting if there was a large quantity of labeled nuclei. The average ratio of labeled nuclei to total nuclei for each artery was computed by dividing the sum of labeled nuclei by the sum of the total nuclei. This ratio was computed for each cell type – endothelial cells, smooth muscle cells, and fibroblasts – within the arterial wall. The cell type was based on the location of the cell within the arterial wall since endothelial cells primarily reside in the intima, smooth muscle cells in the media, and fibroblasts in the adventitia.

### **3.6.6 Tissue Morphology**

Hematoxylin and eosin (H&E) staining was used to compare the morphology of arterial tissues used in this study. Transverse sections, 5  $\mu\text{m}$  thick, from each sample were deparaffinized and stained for H&E using an auto-stainer (Leica). Hematoxylin stains cell nuclei purple and eosin stains connective tissue pink. Following staining, coverslips were mounted over the sections using Cytoseal 60 mounting medium

(Richard-Allan Scientific). Sections were imaged using a Nikon Eclipse E800 microscope.

### **3.7 Statistics**

Results are plotted as mean  $\pm$  standard error of the mean (SEM) unless otherwise noted. Paired student's t-tests were used to compare the difference between the means of the experimental groups. A p-value of less than 0.05 was considered statistically significant.

## **CHAPTER 4**

### **RESULTS**

Experiments were conducted to examine the effects of independent changes of circumferential or shear stress on biological markers of remodeling using the method described in the previous chapter. This chapter is separated into two major sections - the first section includes results related to the method of controlling the local mechanical environment and the second section includes results related to the effect of circumferential stress and shear stress on biological markers of remodeling. The first section begins by presenting results for the changes in the no-load dimensions that occurred during the culture period for both sets of experiments. Next, the results for pressure-diameter and structural responses of cultured arteries are presented. This is followed with a characterization of the method developed to independently control circumferential and shear stress in organ culture. The first major section concludes with a comparison of the method for controlling the local mechanical environment with the traditional organ culture approach of controlling the global mechanical environment. The second major section of this chapter presents results on the effects of circumferential stress and shear stress on tissue morphology,  $^3\text{H}$ -proline incorporation, MMP activity, BrdU incorporation, and EthD incorporation.

#### **4.1 Independent Control of Circumferential Stress and Shear Stress**

##### **4.1.1 Change in Geometrical Dimensions**

Typically, the no-load dimensions of cultured arteries changed during the course of the experiment. In the previous section, Figure 3-4 showed that the majority of the changes in no-load volume occurred within the first 24 hours of culture. In this section,

we further explore this phenomenon by comparing the magnitude of the changes of each no-load dimension before and after culture.

Figure 4-1 shows the no-load outer diameter, wall thickness, and area measured before and after culture for arteries subjected to low (Case A in Table 3-3) and high levels (Case B) of circumferential stress. In general, the outer diameter and volume decreased during culture and the wall thickness increased slightly. For the artery subjected to low circumferential stress, the outer diameter was significantly reduced from  $5.06 \pm 0.26$  mm to  $3.84 \pm 0.21$  mm ( $p < 0.002$ ) over the culture period ( $n = 10$ ). The difference in wall thickness before and after culture was not statistically significant. The area significantly decreased from an initial value of  $12.65 \pm 1.13$  mm<sup>2</sup> to a final value of  $9.60 \pm 1.10$  mm<sup>2</sup> ( $p < 0.03$ ).

A similar trend for the changes in no-load dimensions occurred in arteries exposed to high circumferential stress. The no-load outer diameter significantly decreased from  $4.86 \pm 0.25$  mm before culture to  $4.23 \pm 0.21$  mm ( $p < 0.05$ ) following culture. There was a significant increase in wall thickness with the initial and final values being  $0.92 \pm 0.05$  mm and  $1.08 \pm 0.07$  mm ( $p < 0.03$ ), respectively. There was no significant difference in area before and after culture.

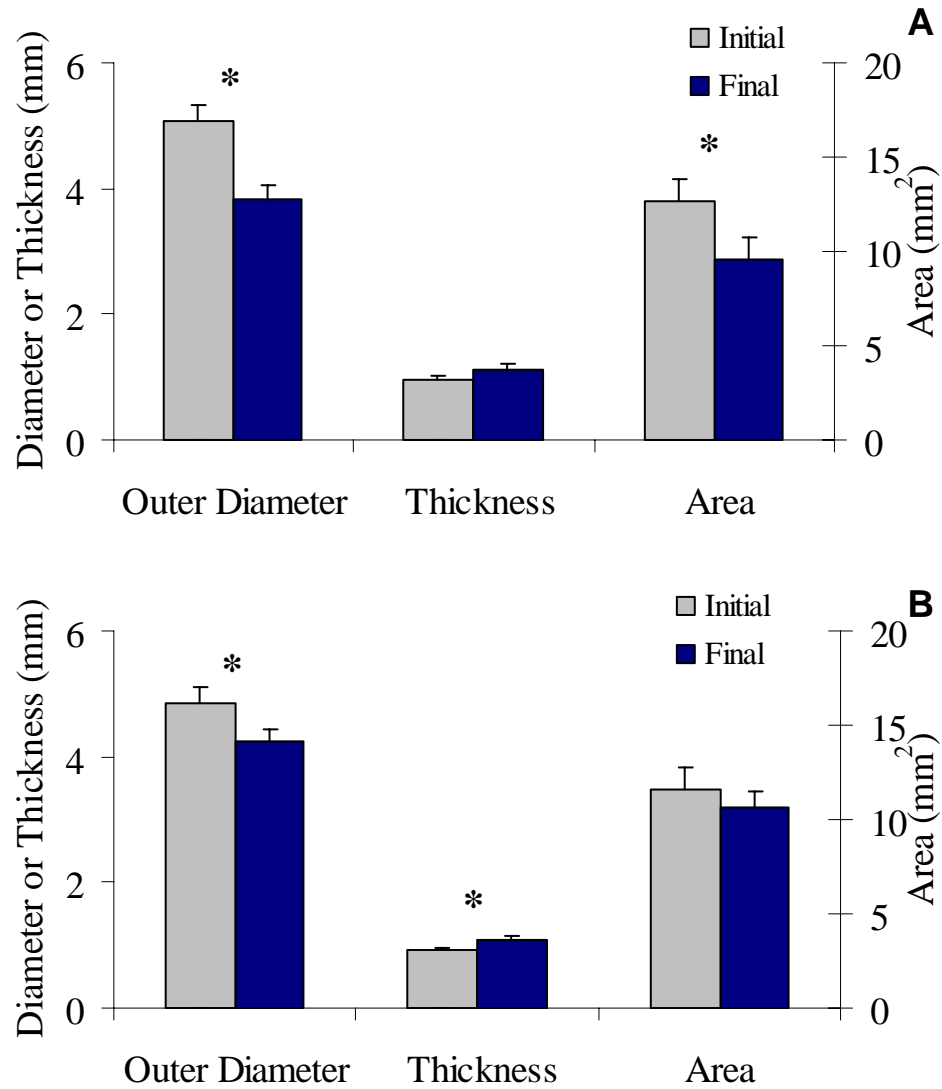


Figure 4-1: Comparison of the initial no-load dimensions of arteries subjected to either a low (A) or high (B) circumferential stress to their values following culture. (\* $p < 0.05$ ,  $n = 10$ )

Figure 4-2 shows the no-load outer diameter, wall thickness, and area measured before and after culture for arteries subjected to low (Case C in Table 3-3) and high levels (Case D) of shear stress. As observed in the circumferential stress experiments, the outer diameter and volume generally decreased during culture and the wall thickness increased slightly in the shear stress studies. For the arteries subjected to low shear stress, the outer diameter was significantly reduced from  $5.40 \pm 0.20$  mm to  $3.77 \pm 0.34$  mm ( $p < 0.02$ )

over the culture period ( $n = 6$ ). The difference wall thickness before and after culture was not statistically significant. The volume significantly decreased from an initial value of  $14.92 \pm 0.91 \text{ mm}^2$  and a final value of  $9.80 \pm 1.39 \text{ mm}^2$  ( $p < 0.05$ ).

For the arteries subjected to high shear stress, all of the no-load dimensions changed significantly over the culture period. The initial and final values of outer diameter were  $5.24 \pm 0.120 \text{ mm}$  to  $3.82 \pm 0.21 \text{ mm}$  ( $p < 0.01$ ), respectively. The wall thickness significantly increased from an initial value of  $1.04 \pm 0.02 \text{ mm}$  to a final value of  $1.19 \pm 0.04 \text{ mm}$  ( $p < 0.03$ ), respectively. The area significantly reduced from an initial value of  $13.69 \pm 0.76 \text{ mm}^2$  to a final value of  $9.78 \pm 0.71 \text{ mm}^2$  ( $p < 0.01$ ).

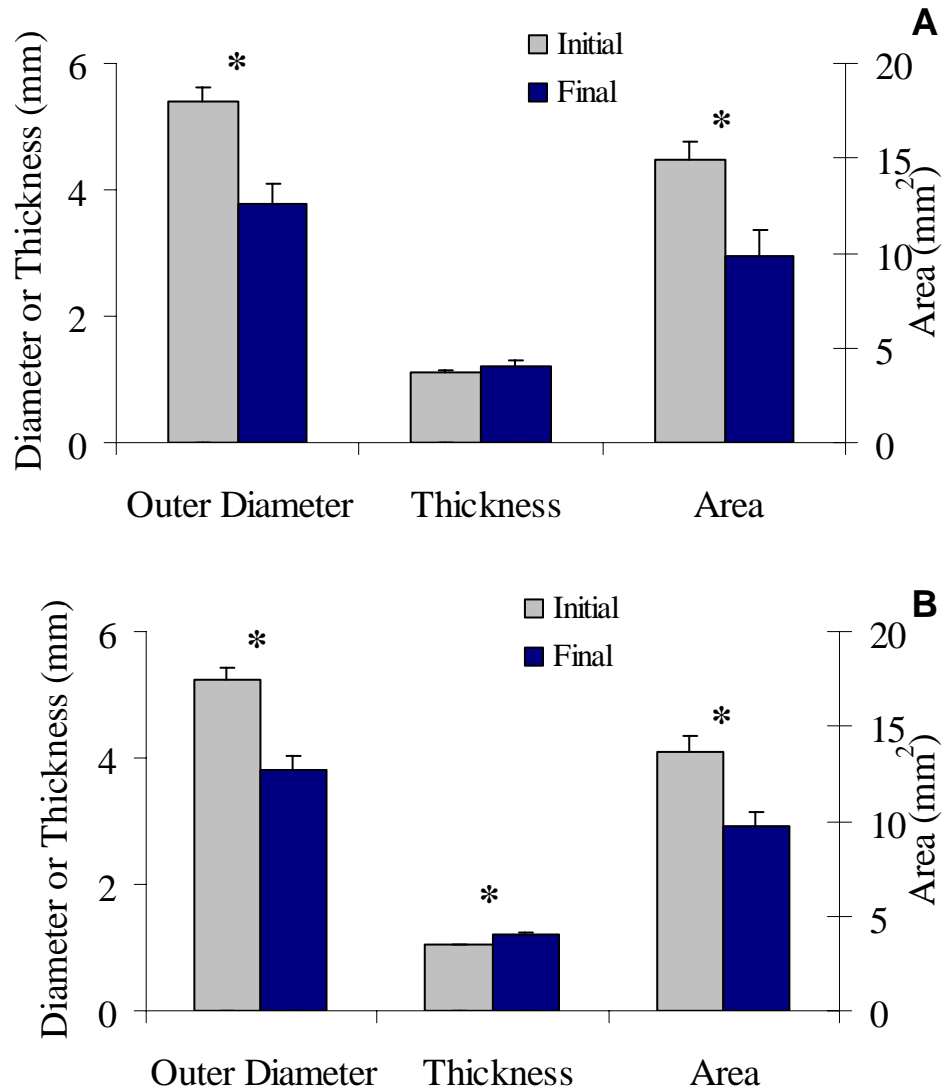


Figure 4-2: Comparison of no-load dimensions of arteries subjected to either a low (A) or high (B) shear stress following culture to their initial values. (\* $p < 0.05$ ,  $n = 6$ )

#### 4.1.2 Estimation of Final No-load Dimensions

An approach that accounts for the changes in no-load dimensions that occur during the early stage of culture was described in the previous chapter (Section 3.3). In order to evaluate the accuracy of this approach, the actual no-load dimensions measured

following culture were compared to the no-load dimensions estimated using the method in this section.

The measurements of the no-load dimensions for two circumferential stress (with a pair of arteries per experiment) and two shear stress experiments (with a pair of arteries per experiment) were combined for this analysis. Because loading conditions should not affect estimates of the no-load dimensions, combining the results of arteries under different loading conditions was a valid approach. Figure 4-3 shows how the estimated no-load dimensions compare to the actual no-load dimensions measured at the conclusion of the experiment ( $n = 8$  arteries). As shown in Figure 4-3, the estimated values of the no-load dimensions were in close agreement with the actual no-load dimensions measured following culture. Further, there were no significant differences between the estimated no-load dimensions and the no-load dimensions measured at the conclusion of the experiment.

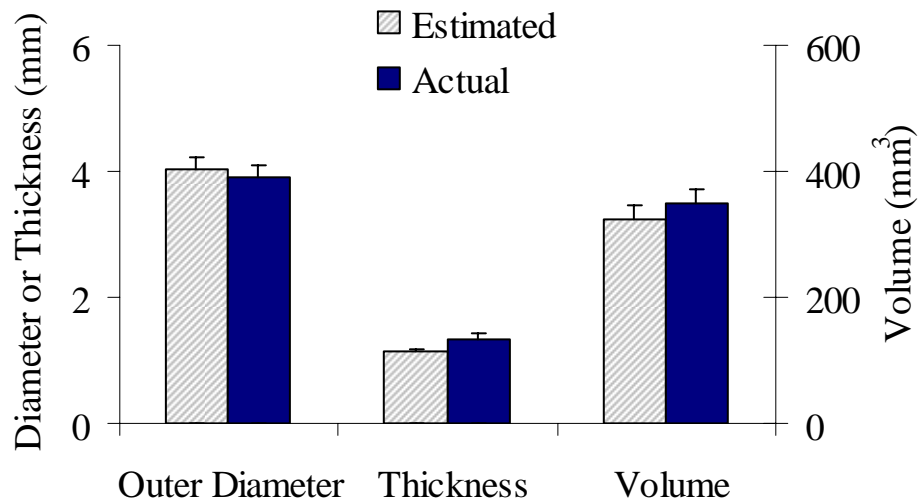


Figure 4-3: Comparison of the estimated no-load dimensions with the actual no-load dimensions measured at the conclusion of the experiment. ( $n = 8$  arteries)



### 4.1.3 Pressure-Diameter Response

Figure 4-4 shows average pressure-diameter curves for arteries subjected to low and high circumferential stress. Measurements were taken at the onset of the experiment and again after the adjustment period, which occurred at approximately 15 hours. The outer diameter measurement was normalized to the outer diameter measured at 50 mmHg, which was the lowest pressure measured for the inflation test. The results show that arteries tended to be less distensible over the range of pressures measured at 15 hours compared to the pressure-diameter relationship measured at the onset of the experiment for both sets of arteries (Figure 4-4).

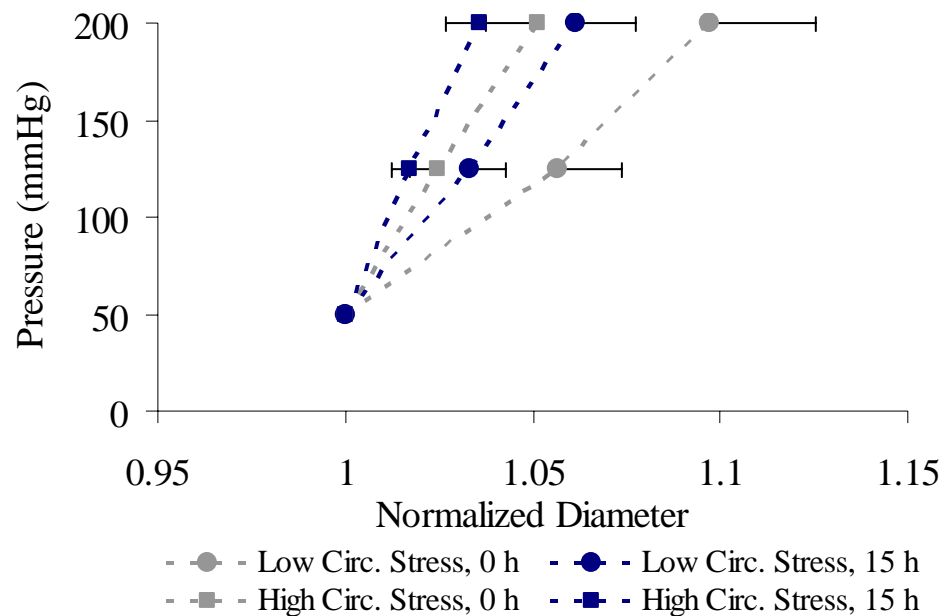


Figure 4-4: Average pressure-diameter curves for an artery cultured under low or high circumferential stress conditions. Measurements were taken at 0 and 15 hours. (n = 10)

The pressure-diameter response observed in the shear stress experiments displayed a trend similar to that observed in arteries exposed to different levels of shear

stress. For both low and high shear stress vessels, the arteries tended to become less distensible over the measured pressure range after 15 hours of culture (Figure 4-5). There was a significant difference in the normalized diameter of low and high shear stress arteries at 200 mmHg at 15 hours.

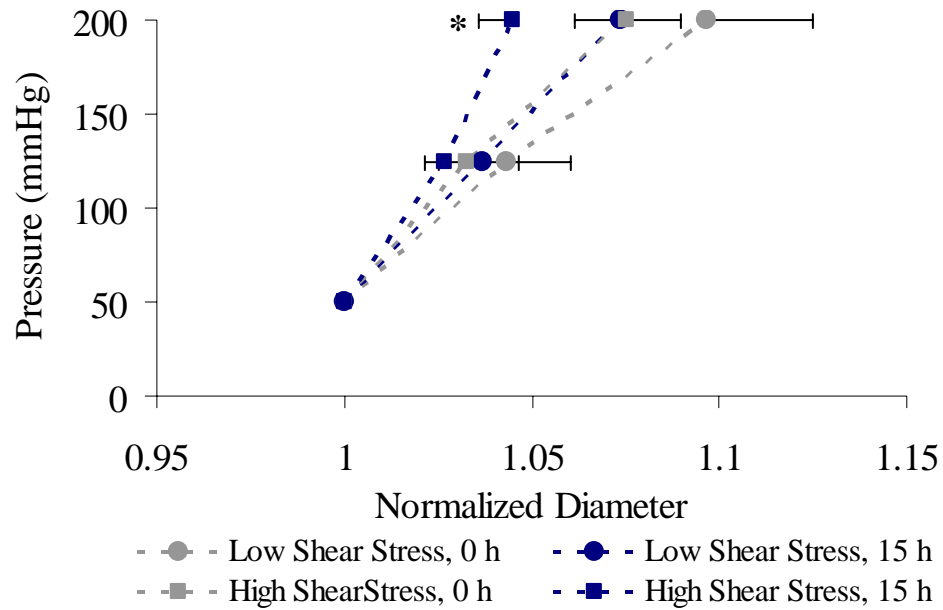


Figure 4-5: Average pressure-diameter curves for arteries cultured under low and high shear stress conditions. Measurements were taken at 0 and 15 hours. (\* $p < 0.05$  for low vs. high shear stress arteries at  $t = 15$  h,  $n = 6$ )

#### 4.1.4 Structural Responses

The structural response of arteries was determined using Peterson's elastic modulus as described in Section 3.5.5. There was no significant difference in Peterson's modulus calculated at the onset and at 15 hours for arteries exposed to either low or high circumferential stress (Figure 4-6).

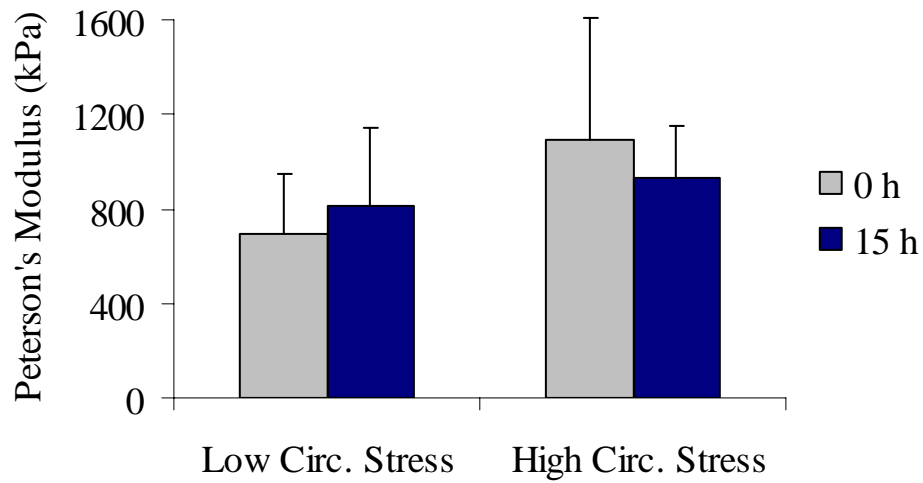


Figure 4-6: Structural response of arteries as measured by Peterson's modulus. Arteries were subjected to either low or high levels of circumferential stress. The modulus was calculated at the onset of the experiment and again after 15 hours of culture. (n = 10)

For the arteries subjected to low or high shear stress, there was also no significant difference in Peterson's modulus calculated at the onset and at 15 hours (Figure 4-7). However, at  $t = 15$  h, the modulus of the high shear stress arteries ( $566.3 \pm 105.4$  kPa) was significantly greater than the modulus of the low shear stress arteries ( $318.3 \pm 51.5$  kPa) ( $p < 0.02$ ).

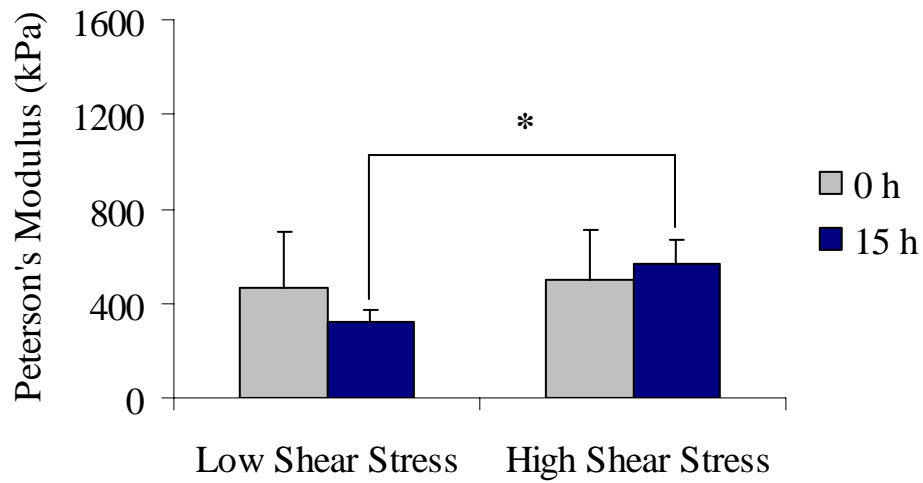


Figure 4-7: Structural response of arteries as measured by Peterson's modulus. Arteries were subjected to either low or high levels of shear stress. The modulus was calculated at the onset of the experiment and again after 15 hours of culture. (n = 6)

#### 4.1.5 Time course of Circumferential Stress and Shear Stress

Figure 4-8 shows the time course of each mechanical parameter for a representative case to demonstrate the method of controlling the local mechanical environment. The prescribed values of circumferential stress and shear stress were 100 kPa and 2.25 Pa, respectively (Case D). The no-load dimensions and pressure-diameter relationship of the artery were determined at the onset of the experiment and again after approximately 15 hours of culture. This process, referred to as the adjustment period, is shown in Figure 4-8 as a shaded vertical line at 15 hours. For the case presented (Figure 4-8), the no-load diameter and wall thickness of the artery reduced by 36.3% and 1.7%, respectively, after 15 hours of culture. Analysis of the results will be focused on data recorded after the adjustment period because, prior to this, observed changes in geometry may result from the transient changes of the no-load dimensions.

The vessel experienced non-monotonic changes in outer diameter during culture. Following the adjustment period, artery underwent a period of vasodilation for about 15 hours followed by vasoconstriction for the remainder of the experiment. To account for these changes in outer diameter, pressure and flow rate were adjusted up to 12.7% and 20.7% to maintain circumferential and shear stress. As a result, circumferential stress and shear stress were maintained within 3.8% of their prescribed values.

The time course of mechanical parameters measured continuously are shown during an iterative adjustment of pressure and flow rate (Figure 4-9) for the representative experiment (Case D). The progressive increase in arterial outer diameter resulted in deviations of circumferential stress and shear stress from their prescribed values. In order to restore circumferential and shear stress, pressure was reduced by approximately 6.3% and flow rate was increased by 7.5%. During this iterative adjustment, circumferential stress was reduced by approximately 6.8% and shear stress was increased by approximately 8.6%, which restored the stresses to their prescribed values. The outer diameter of the artery reduced rapidly for approximately 20 minutes following adjustment of pressure and flow rate and, then the outer diameter continued to increase as it did prior to the iterative adjustment.

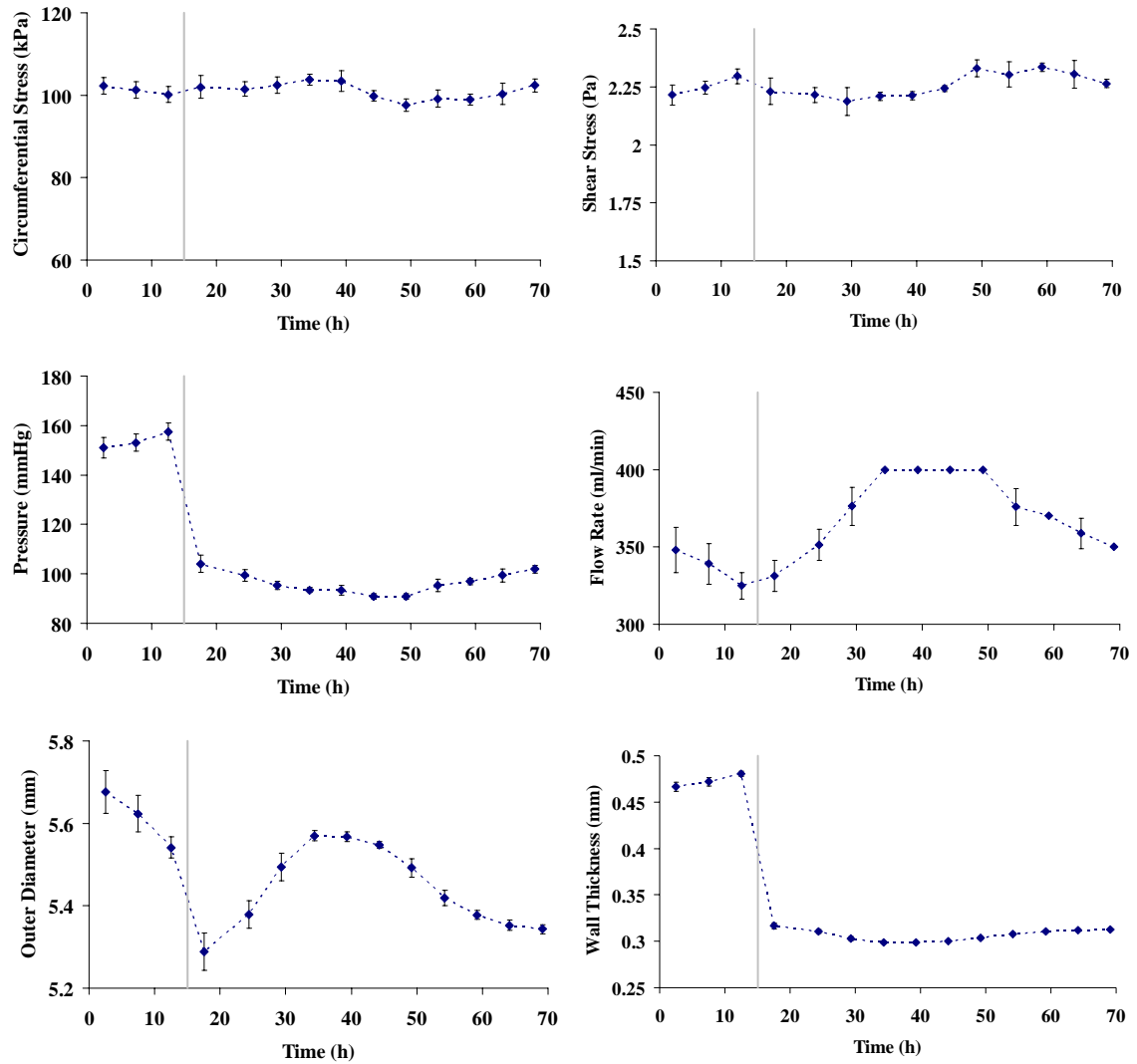


Figure 4-8: Time course of mechanical parameters for a representative experiment (Case D). The prescribed values of  $\sigma_\theta$ ,  $\tau$ , and  $\lambda_z$  were 100 kPa, 2.25 Pa, and 1.5, respectively. Each point represents the average measurement of each parameter over 5 hours. The shaded vertical line indicates the adjustment period during which the current no-load dimensions were determined and the inflation test was conducted. Prior to this period, circumferential and shear stress were calculated using the initial no-load dimensions. Following this period, the stresses were calculated using the updated no-load dimensions. Results are plotted as mean  $\pm$  SD.

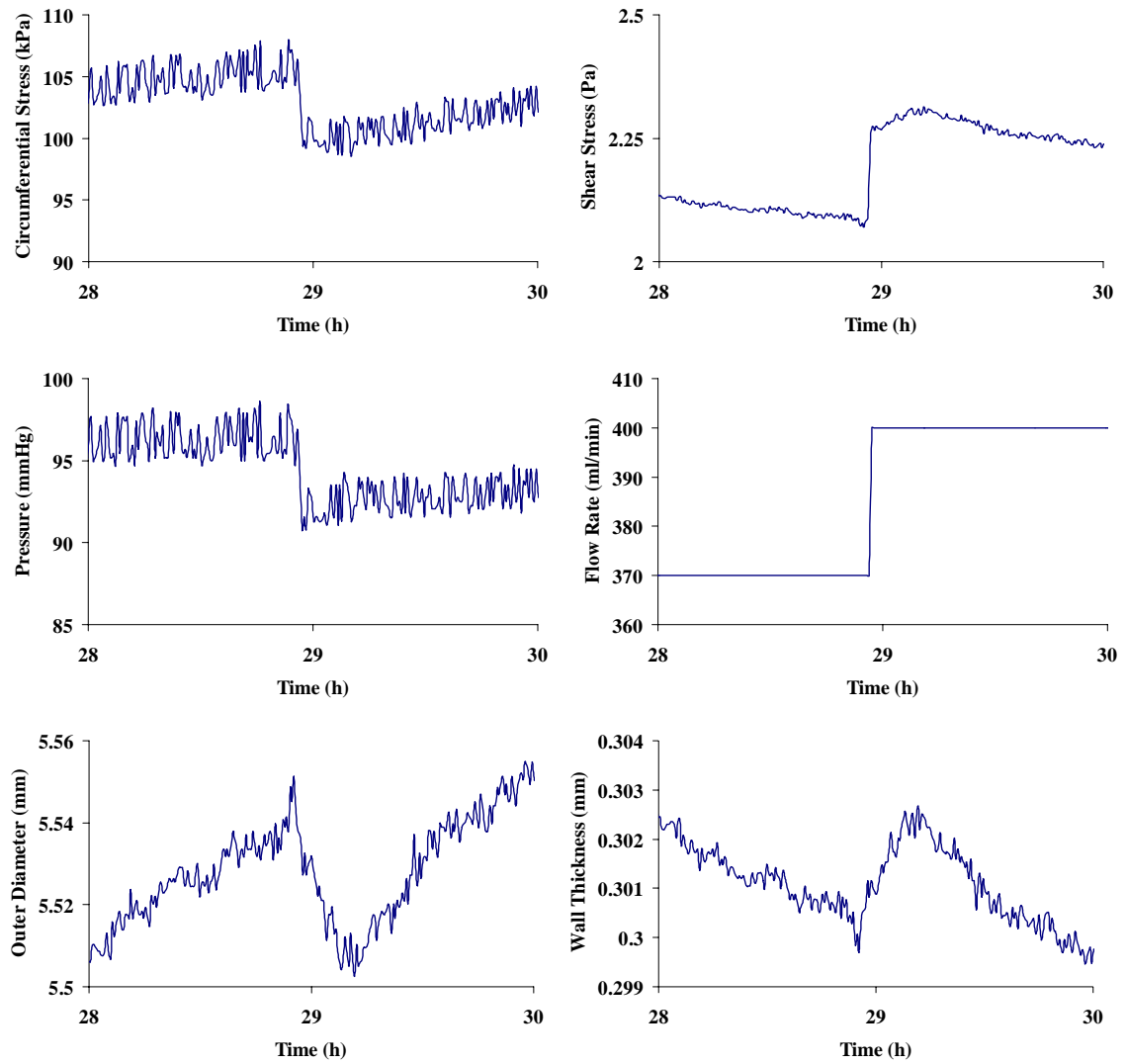


Figure 4-9: Detailed view of mechanical parameters during an iterative adjustment of pressure and flow rate for the representative experiment (Case D).

#### **4.1.6 Effect of Controlling Local and Global Parameters on Mechanical**

##### **Environment**

An experiment was conducted to compare the mechanical environment of arteries in which local parameters ( $\sigma$  and  $\tau$ ) were controlled with that of arteries in which global parameters ( $P$  and  $Q$ ) are controlled (Figure 4-10). The latter control scheme typically occurs in current organ culture experiments. At the onset of the experiment, the arteries were subjected to identical values of circumferential stress and shear stress. In the representative experiment presented, the initial values of circumferential stress and shear stress were 150 kPa and 1.5 Pa, respectively. For the vessel in which the global parameters were controlled, the outer diameter was measured daily because this experiment was conducted at the same time other experiments and only a limited number of cameras could be run simultaneously to measure diameter. For the vessel in which the local parameters were controlled, the outer diameter was measured continuously and adjustments to pressure and flow rate were made as described previously. However, for consistency, the mechanical parameters for the vessel under local control are only plotted in Figure 4-10 at times corresponding to the daily measurement of outer diameter for the vessel under global control.

At the onset of the experiment, the values of circumferential stress and shear stress were calculated using Eqs. 1-1 to 1-3 based on the initial no-load dimensions. However, after the adjustment period ( $t = 15$  h), the values of circumferential stress and shear stress were calculated using the updated no-load dimensions that were determined using the method described earlier in Section 3.4.4. These changes in no-load dimensions contributed to the dramatic change in circumferential stress and shear stress



observed just after the adjustment period in the artery under global control ( $t = 17$  h). For the vessel under local control, the changes in no-load dimensions contributed to the dramatic changes in pressure and flow rate required to maintain the stresses at their target values. Further analysis of the mechanical environment will be focused on the time points following the adjustment period. Prior to this, changes in outer diameter could result from transient changes in no-load dimensions and are most likely not induced by remodeling processes as described in the previous section.

Following the adjustment period, circumferential stress and shear stress were controlled within 3.4% and 4.5% of their target values, respectively, for the artery under local control. In order to maintain these stresses at their target values, pressure and flow rate were changed in response to changes in outer diameter. The outer diameter of the local control artery decreased progressively following the adjustment period and was reduced by 4.1% by the end of culture. In order to maintain circumferential stress, pressure was increased by 5.6% following the adjustment period. Further, the flow rate was reduced by 13.5% to maintain shear stress at its target values.

For the artery under global control, pressure was maintained within 3.9% following the adjustment period and flow rate was held constant. In this case, the outer diameter changed non-monotonically with the outer diameter increasing by 4.3% at  $t = 42$  h and then returning to its value immediately following adjustment by the end of the culture period. These changes in outer diameter led to changes in the local mechanical parameters. The values of circumferential stress and shear stress varied by as much as 7.1% and 15.5%, respectively, following the adjustment period.

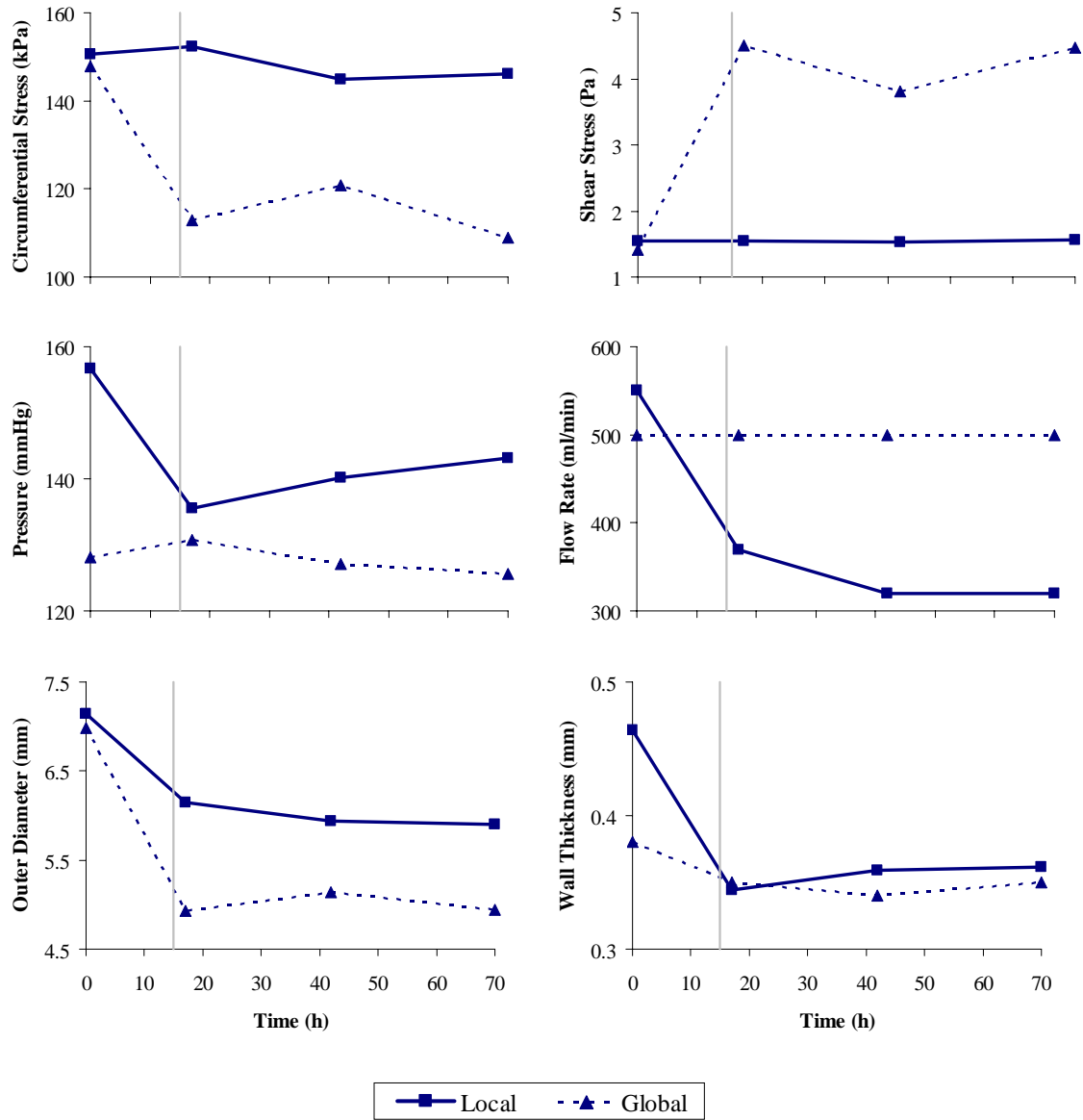


Figure 4-10: Representative experiment comparing the mechanical environment of arteries in which local parameters ( $\sigma$  and  $\tau$ ) were controlled with arteries in which global parameters ( $P$  and  $Q$ ) were controlled.

## 4.2 Effects of Circumferential Stress on Biological Markers of Remodeling

To examine the effects of circumferential stress on remodeling, arteries were subjected either a low (Case A) or high (Case B) circumferential stress while shear stress

and the axial stretch ratio were maintained at physiologic levels of 1.5 Pa and 1.5, respectively.

#### 4.2.1 Tissue Morphology

Figure 4-11 compares the morphology of arteries cultured under low and high circumferential stress conditions with that of fresh tissue. As shown in Figure 4-11, the morphologies of both experimental arteries were similar to that of fresh arteries. For each loading condition, the arteries generally maintained an intima comparable to that of fresh arteries with an intact endothelial cell layer and internal elastic lamina. In the media, the smooth muscle cells were oriented circumferentially and the extracellular matrix retained its structural integrity, free of any ruptures.

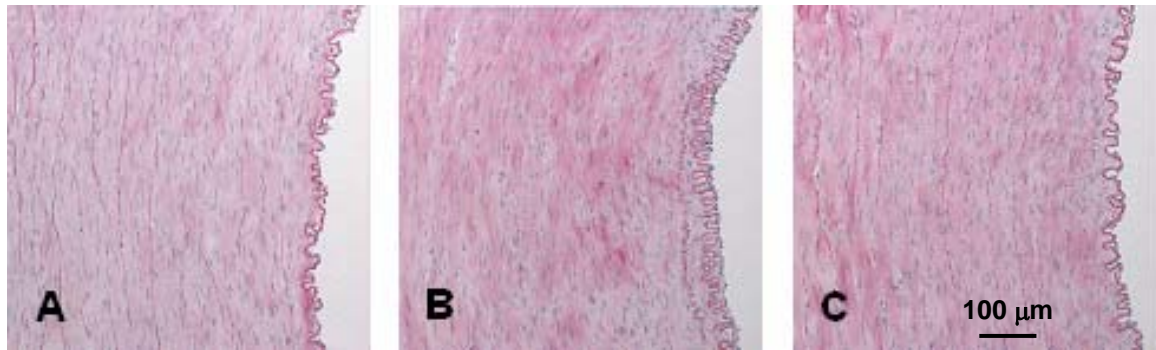


Figure 4-11: Comparison of tissue morphology of transverse sections for arteries cultured for 3 days using hematoxylin and eosin staining. Representative samples of a fresh (A) artery and vessels subjected to low (B) and high circumferential stress (C) are shown. The lumen is on the right in each image.

#### 4.2.2 Matrix Synthesis

Figure 4-12 shows the effect of circumferential stress on  $^3\text{H}$ -proline incorporation. The  $^3\text{H}$ -proline incorporation level in the high circumferential stress artery ( $124.0 \pm 15.7 \times 10^3$  DPM/mg) was significantly greater than in the low circumferential stress artery ( $104.2 \pm 12.7 \times 10^3$  DPM/mg) ( $n = 10$ ,  $p < 0.05$ ). Since  $^3\text{H}$ -proline incorporation is a marker of extracellular matrix synthesis, the increased levels of  $^3\text{H}$ -proline incorporation

indicates that the rate of matrix synthesis was greater in the artery subjected to high circumferential stress.

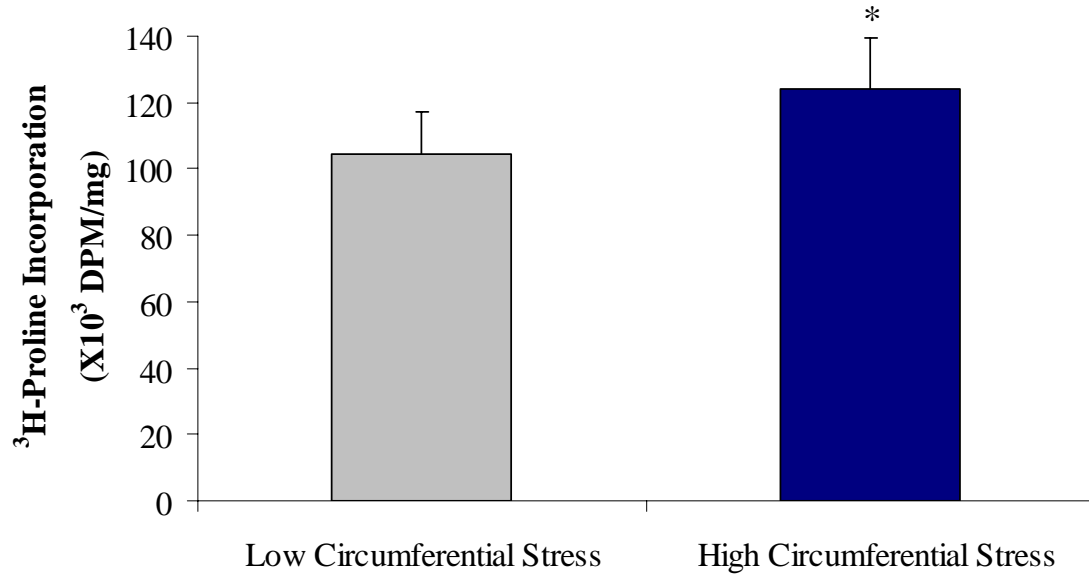


Figure 4-12: Comparison of <sup>3</sup>H-proline incorporation in arteries subjected to low (Case A) and high (Case B) circumferential stress conditions for 3 days in culture. (\*p < 0.05, n = 10)

#### 4.2.3 MMP Activity

Figure 4-13 shows the results of MMP activity in arteries exposed to low and high levels of circumferential stress. Mean MMP-2 and pro-MMP-2 activity in arteries exposed to high circumferential stress were 22.2% (p < 0.05) and 21.9% (p < 0.03) less than the relative activity observed in arteries exposed to low circumferential stress, respectively. Changes in circumferential stress did not significantly affect the levels of pro-MMP-9 activity.

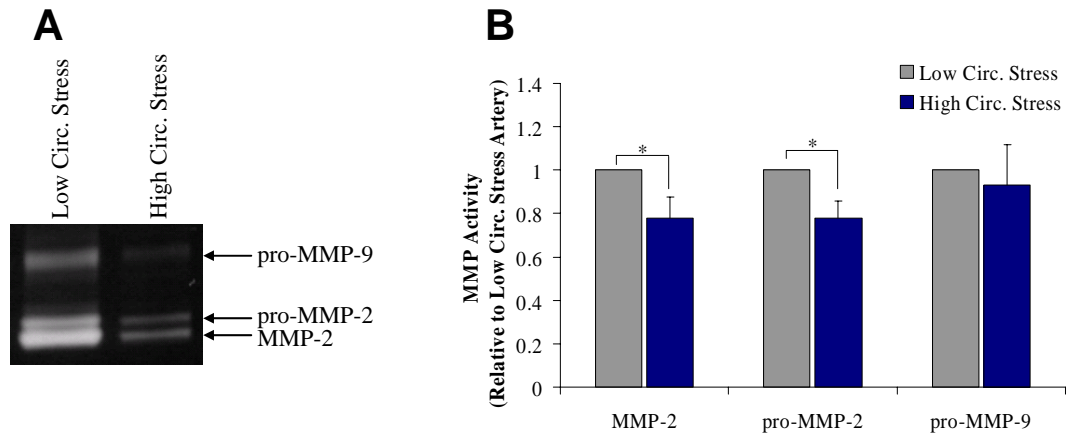


Figure 4-13: Effect of circumferential stress on MMP-2/9 gelatinolytic activity measured using SDS-PAGE zymography. A representative zymogram for arteries exposed to low and high levels of circumferential stress are shown (A) with MMP-2 (67 kDa), pro-MMP-2 (72 kDa), and pro-MMP-9 (92 kDa) activity as clear lysis bands. Gelatinase activity was determined by densitometric quantitation of zymograms (B). (\* $p < 0.05$ ,  $n = 9$ )

#### 4.2.4 Cell Proliferation

Figure 4-14 shows the effect of circumferential stress on cell proliferation. For both levels of circumferential stress, the percentage of proliferating cells was greater for endothelial cells and fibroblasts than for smooth muscle cells. There was an approximately four-fold increase in proliferation for smooth muscles cells and a 49.7% increase in proliferating fibroblasts at high circumferential stress relative to low circumferential stress arteries ( $p < 0.05$ ). In addition, there was no statistically significant difference in endothelial cell proliferation between arteries exposed low or high circumferential stress.

Figure 4-15 shows images taken using fluorescent microscopy of a representative section of an artery under the low circumferential stress condition. The images show a higher concentration of BrdU-positive cells in the intima and adventitia compared to the media. In general, proliferating cells were evenly distributed throughout the media. The

distribution of proliferating cells was similar in arteries cultures under high circumferential stress as well.

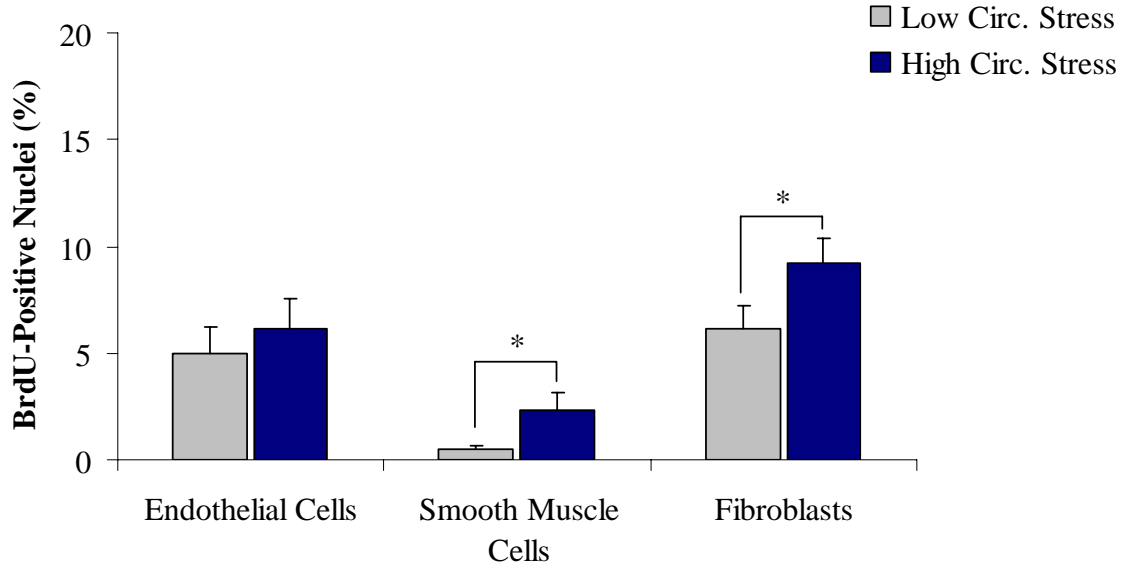


Figure 4-14: Percentage of proliferating cells detected by BrdU incorporation. Arteries were subjected to low or high levels of circumferential stress during 3 days of culture. (\* $p < 0.05$ ,  $n = 8$ )

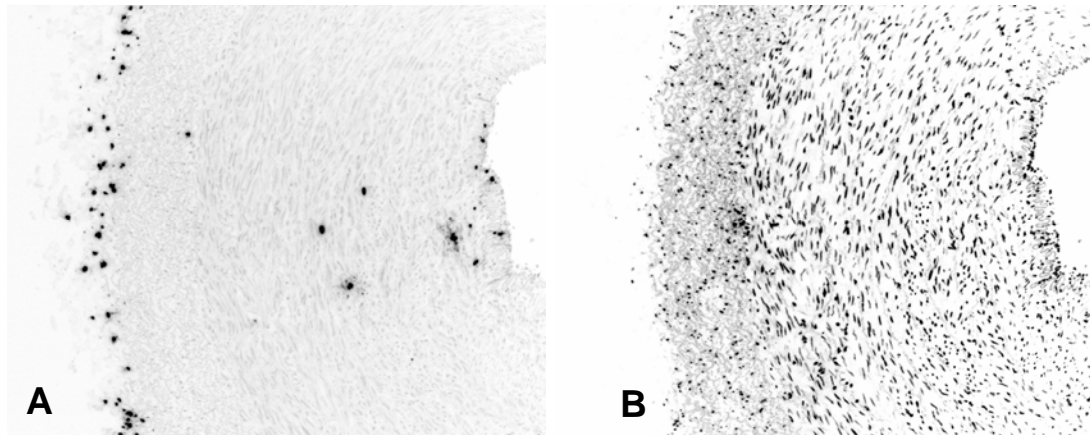


Figure 4-15: Representative tissue sections immunostained with BrdU (A) and DAPI (B) to measure cell proliferation. For this artery, the prescribed values of  $\sigma_\theta$ ,  $\tau$ , and  $\lambda_z$  were 150 kPa, 1.5 Pa, and 1.5, respectively (Case B). The lumen is on the right in both images. The images are inverted and taken at 10X magnification.

#### 4.2.5 Cell Death

Figure 4-16 shows the percent of EthD-positive cells in response to varying levels of circumferential stress. The percentage of dead cells, as measured by EthD incorporation, in arteries exposed to high circumferential stress was significantly greater than in arteries under low circumferential stress ( $p < 0.02$ ). Figure 4-17 shows images of the nuclei of dead and total smooth muscle cells taken by fluorescent microscopy. In general, the EthD-positive cells were evenly distributed throughout the media in both sets of arteries.

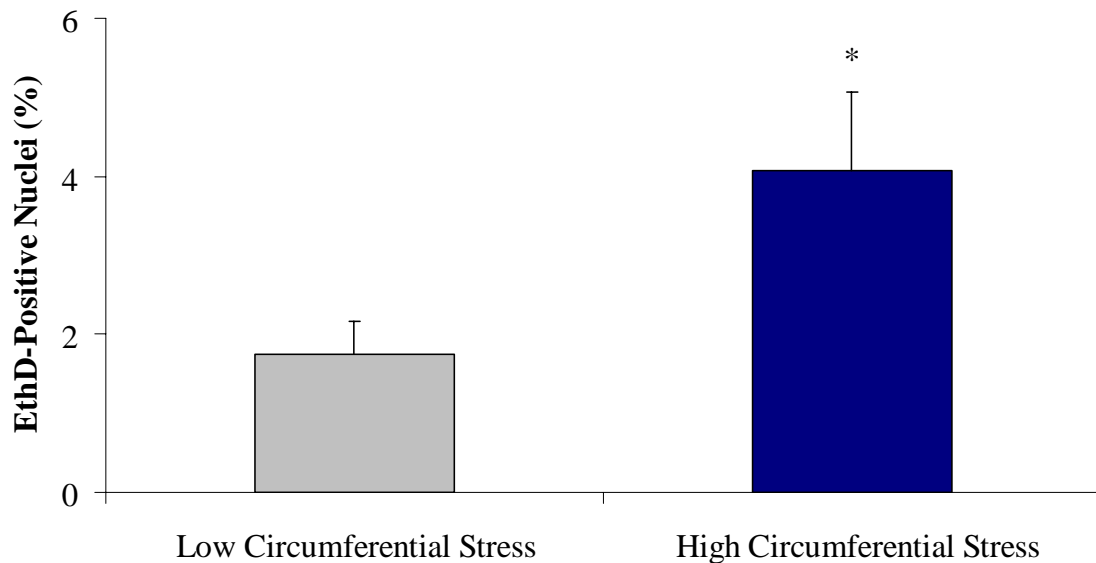


Figure 4-16: Percentage of EthD-positive cells in arteries subjected to low or high levels of circumferential stress during 3 days of culture. (\* $p < 0.05$ ,  $n = 10$ )

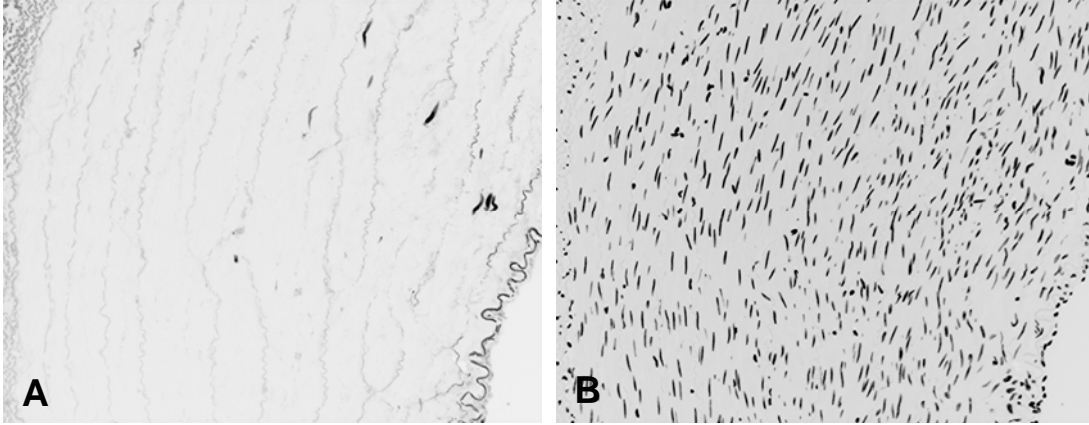


Figure 4-17: Fluorescent microscope images of representative tissue sections stained with EthD (A) and DAPI (B) to measure cell death. The artery was subjected to the prescribed values of  $\sigma_\theta$ ,  $\tau$ , and  $\lambda_z$  were 50 kPa, 1.5 Pa, and 1.5, respectively (Case A) for 3 days of culture. The lumen is on the lower right in both images. The images are inverted and taken at 10X magnification.

### 4.3 Effects of Shear Stress on Biological Markers of Remodeling

To examine the effects of shear stress on remodeling, arteries were subjected either a low (Case C) or high (Case D) circumferential stress while circumferential stress and the axial stretch ratio were maintained at physiologic levels of 100 kPa and 1.5, respectively.

#### 4.3.1 Tissue Morphology

Figure 4-18 compares the morphology of arteries cultured under low and high shear stress conditions with that of fresh tissue. As occurred for circumferential stress, the arteries under both shear stress conditions generally maintained healthy intimal and medial layers that were comparable to that of fresh arteries. The fact that the morphologies of the experimental arteries were comparable to that fresh suggests that the arteries maintained structural integrity under the applied mechanical loads.



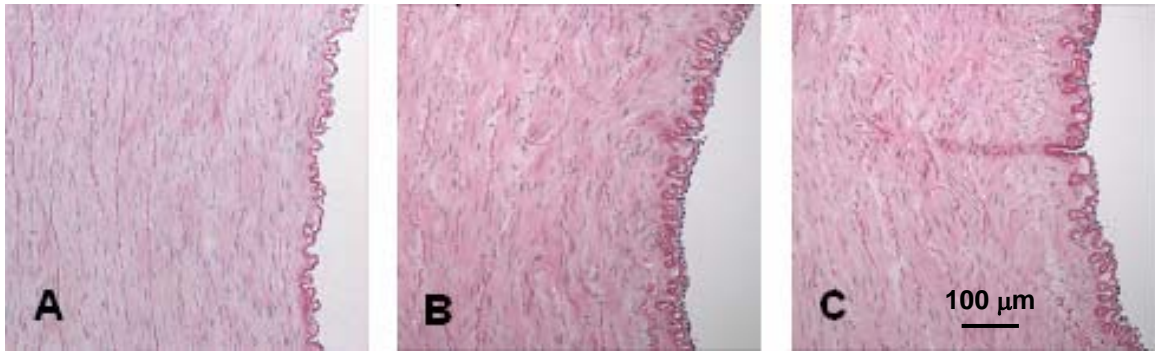


Figure 4-18: Comparison of tissue morphology of transverse sections for arteries cultured for 3 days using hematoxylin and eosin staining. Representative samples of a fresh (A) artery and vessels subjected to low shear stress (B) and high shear stress (C) are shown. The lumen is on the right in each image.

#### 4.3.2 Matrix Synthesis

Figure 4-12 shows the effect of circumferential stress on  $^3\text{H}$ -proline incorporation. The  $^3\text{H}$ -proline incorporation levels in the low and high shear stress arteries were not significantly different ( $n = 6$ ). Since  $^3\text{H}$ -proline incorporation is a marker of extracellular matrix synthesis, the results indicate that the rate of extracellular matrix synthesis was not affected by shear stress.

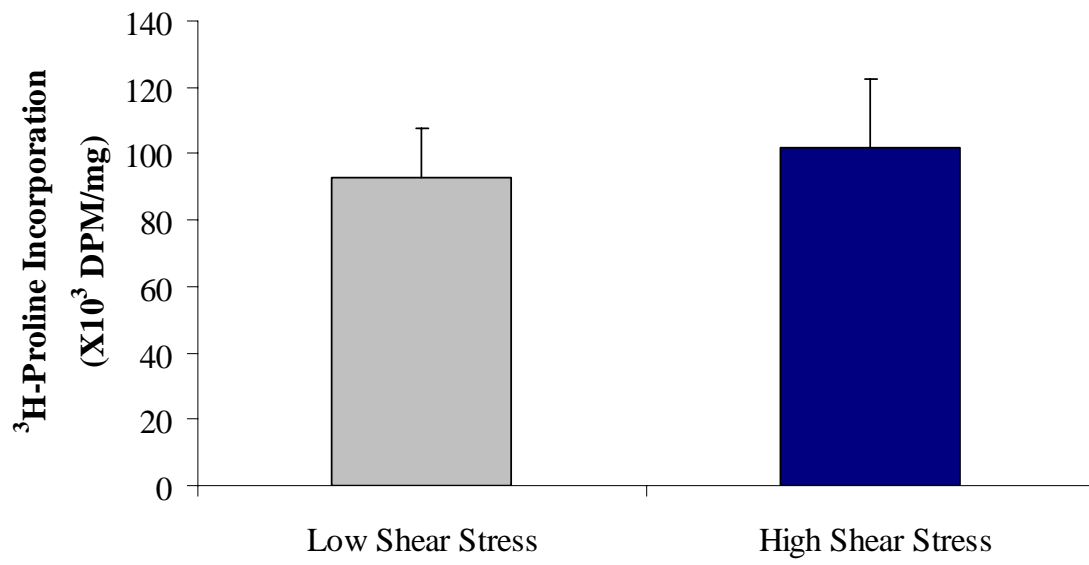


Figure 4-19: Comparison of <sup>3</sup>H-proline incorporation in arteries subjected to low (0.75 Pa) and high (2.25 Pa) shear stress conditions for 3 days in culture. (n = 6)

#### 4.3.3 MMP Activity

Figure 4-20 shows the results of MMP activity in arteries exposed to low and high levels of shear stress. Changes in shear stress did not significantly affect the levels of MMP-2, pro-MMP-2, or pro-MMP-9 activity.

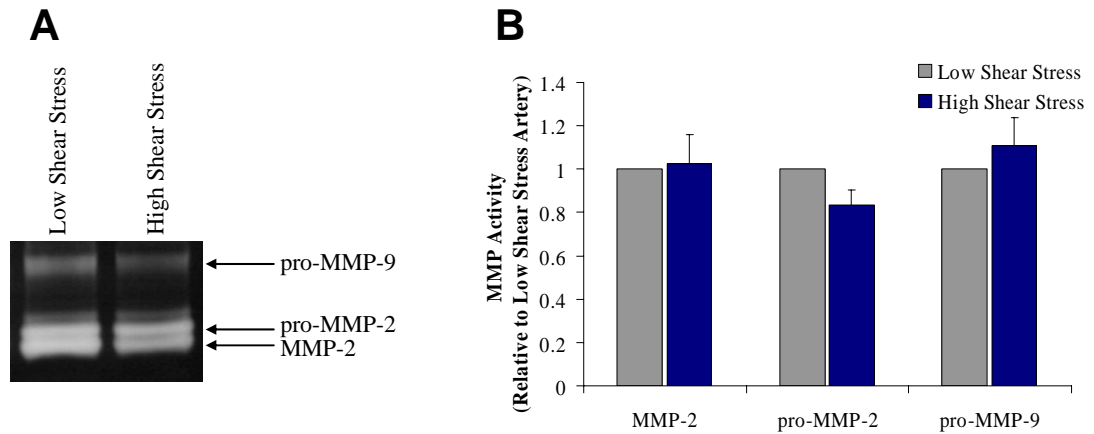


Figure 4-20: Effect of shear stress on MMP-2/9 gelatinolytic activity measured using SDS-PAGE zymography. A representative zymogram for arteries exposed to low and high levels of shear stress are shown (A) with MMP-2 (67 kDa), pro-MMP-2 (72 kDa), and pro-MMP-9 (92 kDa) activity as clear lysis bands. Gelatinase activity was determined by densitometric quantitation of zymograms (B). (n = 6)

#### 4.3.4 Cell Proliferation

Figure 4-21 shows the proliferative response of cells within arteries exposed to different levels of shear stress. As observed in arteries exposed to different levels of circumferential stress, proliferation rates for endothelial cells and fibroblasts were greater than for smooth muscle cells. As shown in Figure 4-21, shear stress had no significant effect on proliferation of endothelial cells, smooth muscle cells, or fibroblasts. Proliferating smooth muscle cells were evenly distributed through the media as observed in circumferential stress arteries (Figure 4-15).

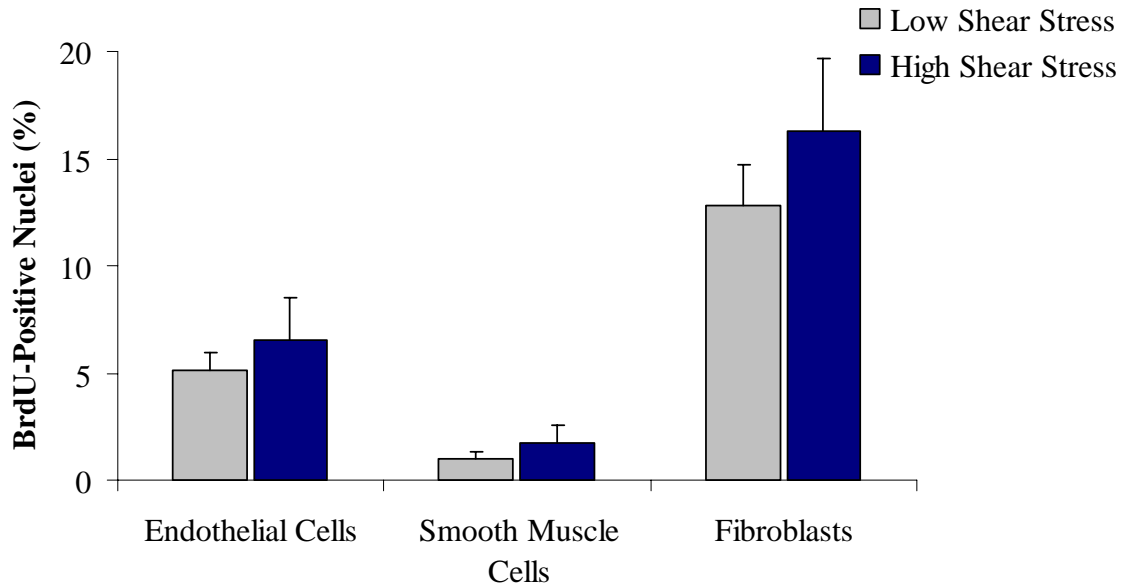


Figure 4-21: Percentage of proliferating cells detected by BrdU incorporation. Arteries were subjected to low or high levels of shear stress during 3 days of culture. (n = 6)

#### 4.3.5 Cell Death

Figure 4-22 shows how shear stress affects cell death. As shown in Figure 4-22, the percentage of dead cells was not significantly different in arteries exposed to low and high shear stress (n = 6). As observed in arteries subjected to different levels of circumferential stress, the EthD-positive cells were evenly distributed through the media in arteries at both levels of shear stress as described earlier for circumferential stress arteries (Figure 4-17).

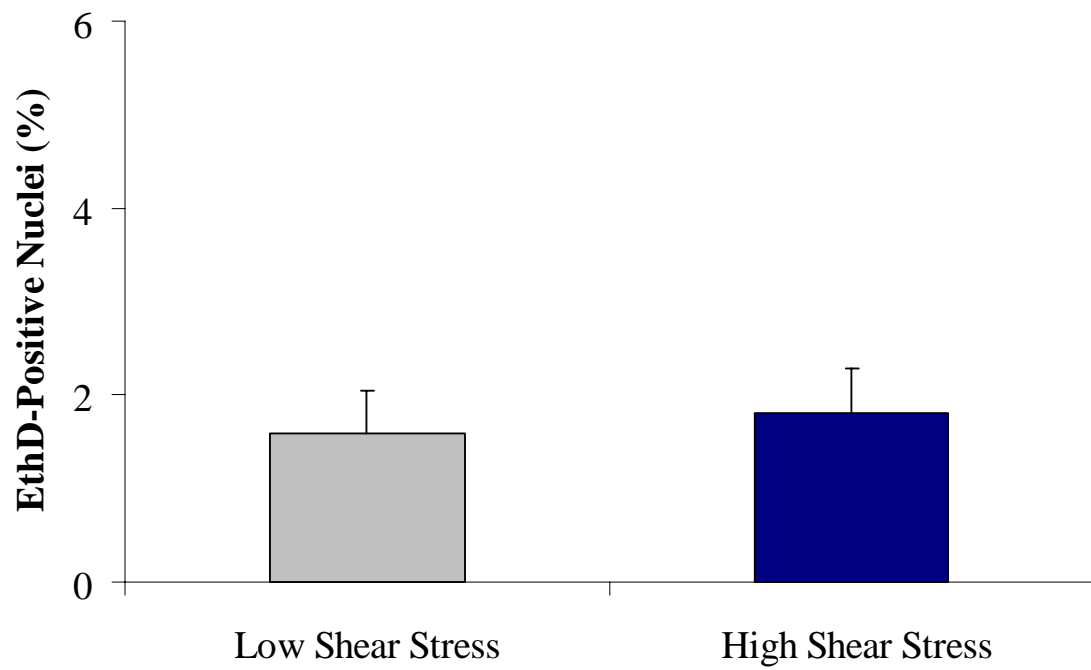


Figure 4-22: Percentage of EthD-positive cells in arteries subjected to low or high levels of circumferential stress during 3 days of culture. (n = 6)

## **CHAPTER 5**

### **DISCUSSION**

The motivation for this work is the need to better understand the role of the local mechanical environment in arterial remodeling, which cannot be fully achieved using existing experimental approaches. Therefore, a novel approach to independently controlling circumferential stress and shear stress in perfusion organ culture was developed. To illustrate this method, the effect of circumferential stress and shear stress on the response of several biological markers was studied.

The method of controlling of the mechanical environment is an important distinction between the approach used in this study and the used in previous studies of arterial remodeling. In this study, a single local parameter was changed and held constant throughout the duration of the experiment. In response, the artery was forced to continually remodel because it could not restore the local mechanical environment to baseline levels. In previous studies of remodeling, the artery was subjected to a change of a global parameter which induced remodeling. Remodeling in these studies is due to the coupled changes of multiple local parameters and will continue until the local mechanical environment is restored to baseline levels. Due to this fundamental difference in the two methods, results from this study should be compared to the results occurring well before the local mechanical environment is restored in traditional studies.

As described in the Introduction, arteries respond to changes in mechanical environment by changing arterial dimensions and mechanical processes in a two stage process. The first stage involves vasomotor responses that adjust vascular tone and occurs quickly, on the order of minutes. The second stage of the arterial response

involves remodeling and requires a week to several months to manifest. The results of this work revealed that the organ culture environment can also contribute to changes in arterial responses. An overview of this process is shown schematically in Figure 5-1 which will serve as the basis for discussing the data presented in the Results chapter. This chapter also discusses limitations of the method.

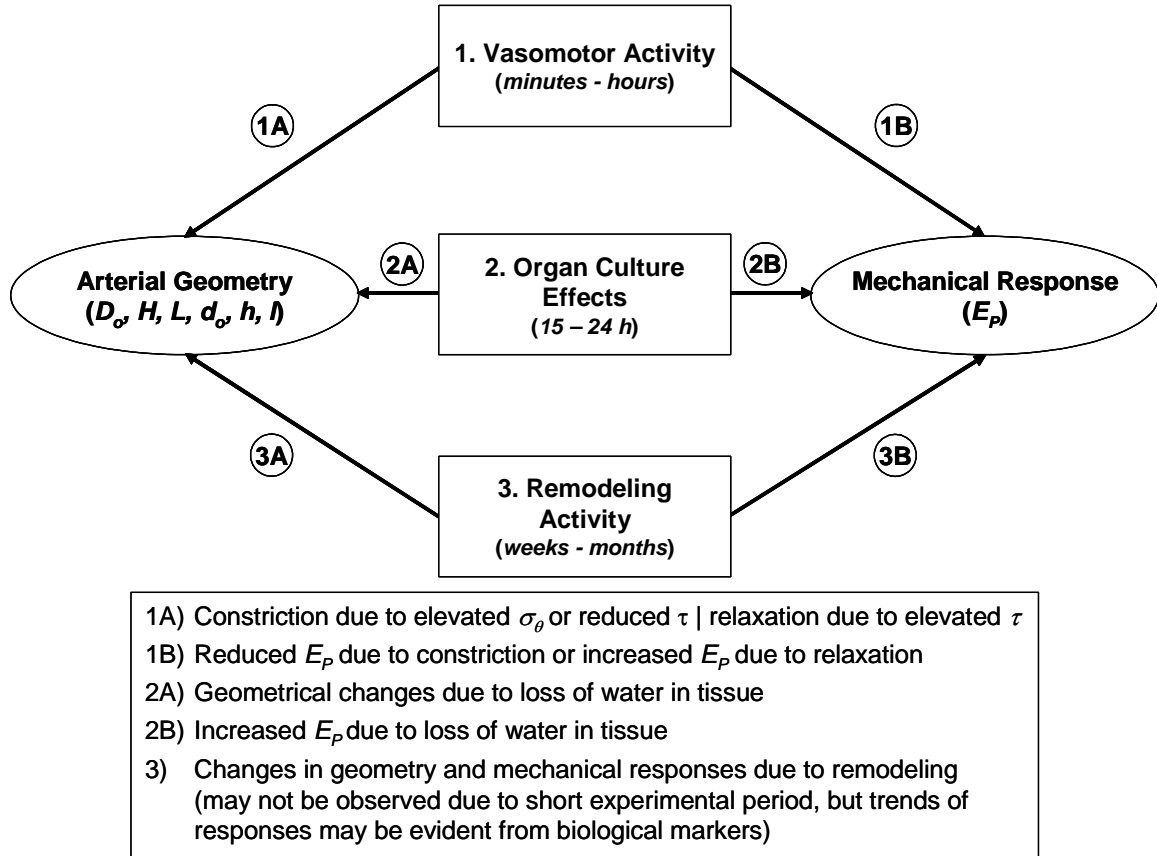


Figure 5-1: Schematic of processes leading to the changes in geometry and mechanical responses of an artery in organ culture.

## 5.1 Changes of No-load Dimensions

The no-load dimensions were found to change during the early stage of culture. The no-load outer diameter and area were both decreased during this period, while there

was a slight increase in the no-load wall thickness. These changes were present for all loading conditions.

Only a limited number of organ culture studies have reported results related to the change of no-load dimensions during culture. Davis (2002) found that the no-load volume of porcine carotid arteries reduced by 16 – 27% following 7 days of culture when subjected to varying levels of axial stretch. However, the author did not investigate the time course of the changes in no-load dimensions. By further studying the time course of this response, we determined that the changes in no-load dimensions occur during the first 15 hours of culture and stabilize thereafter. The magnitude and direction of the changes of no-load dimensions of this study are in close agreement with the results of Davis.

The changes of no-load arterial dimensions that occurred during the early stage of culture were probably not caused by remodeling due to the short timeframe, but likely due to other processes that take place during culture. These changes probably result from the loss of water content due to forced diffusion in a manner similar to that described by Chuong and Fung (1984) in which water extrusion occurred when a vessel was subjected to radial compression. Because the loss of no-load volume was found for all loading conditions, this response is an artifact of perfusion organ culture, and not a response that depends on the local mechanical environment (*Process 2A* in Figure 5-1).

To address the change of no-load dimensions during culture, future experiments by our lab could include a method of non-destructively measuring the wall thickness of arteries during culture. Such an approach has been used by Zulliger et al. (2002) who used an ultrasonic transducer to measure wall thickness in organ culture.



## 5.2 Changes of the Deformed Dimensions and Control of Local Mechanical Environment

The time course of circumferential stress and shear stress, along with the pressure, flow rate, outer diameter and wall thickness for a representative experiment was presented in the Results chapter (Figure 4-8). The time course was presented for this experiment to demonstrate our ability to control the local mechanical environment. The ability to control the local environment for all other experiments (Table 3-3) was similar so their time courses were not shown. This section will discuss the mechanisms contributing to the observed changes in deformed dimensions that occurred during culture. These changes likely result from the competing effects of vasomotor responses (*Process 1A* in Figure 5-1) and organ culture artifacts (*Process 2A*) as will be described in detail. While the discussion focuses in detail on the mechanism of diameter change for a specific case, the mechanism discussed in this section explain the diameter changes observed in arteries under different experimental conditions.

For the representative experiment, the artery was subjected to an elevated shear stress while circumferential stress and axial stretch ratio were held at physiologic levels (Figure 4-8). Under these loading conditions, the artery is expected to dilate in order to restore shear stress to physiologic levels according to the macroscopic view of remodeling described in the Introduction (Section 1.3). In this case, shear stress is fixed and cannot be restored to baseline levels, therefore, the diameter is expected to continually increase until the SMCs fully relax. The deviations of the observed changes in outer diameter and the expected diameter response will be discussed in this section. The discussion will focus separately on the periods before  $t = 15$  h, when transient

changes in no-load dimensions occur, and after  $t = 15$  h, when the no-load dimensions are stabilized.

In contrast to the expected dilation response, the artery actually undergoes a sustained reduction in loaded outer diameter during the first 15 hours of culture. This observation is likely due to structural changes experienced by the artery due to the loss of water described earlier in Section 5.1 (*Process 2A* in Figure 5-1). Alternatively, the observed response may result from the presence of FCS in the culture media in accordance with the finding that an addition of 10% FCS in the culture media induces a vasoconstrictive response in arteries in perfusion culture for four days (Bakker et al. 2000). Further, the sustained reduction in diameter may result from the combined effects of both factors, the forced diffusion of water and the contractile stimulation of FCS. In order to maintain the target values of circumferential stress and shear stress, the pressure is continually increased and the flow rate is decreased to account for the progressive decrease in loaded outer diameter.

As mentioned in the Methods chapter (Section 3.4.4), the wall thickness was calculated based on the initial no-load dimensions which are known to change during the first 15 hours of culture. In this study, the errors in wall thickness lead to an underestimate of circumferential stress and an overestimate of shear stress during this period. Since the changes of no-load dimensions were consistent for all cultured arteries, it is reasonable to expect that the errors in calculating circumferential stress and shear stress are consistent for arteries with the same target stress values.

Following the adjustment period, when no change in unloaded dimensions occurs, the control of circumferential and shear stress is achieved by significantly varying

pressure and flow rate to account for changes in arterial geometry. A plausible explanation for the observed variation of the vessel outer diameter during this period is a change in vascular tone (*Process 2A*). When shear stress is kept at levels higher than the baseline values, the artery initially dilates, which is consistent with the results of *in vivo* studies on flow-induced remodeling (Kamiya and Togawa 1980; Zarins et al. 1987; Brownlee and Langille 1991). However, the subsequent diminishing of the outer diameter (Figure 4-8) indicates that the vascular tone tends to increase over time. Because the forced diffusion effect is consumed in the first 15 hours of culture, this response is likely due to the contractile stimulation of FCS, as described earlier in this section. Therefore, the non-monotonic changes in outer diameter observed in this study likely result from a balance of the competing effects of a flow-induced relaxation of vascular smooth muscle (*Process 1A*) and the contractile stimulation of FCS (*Process 2A*). The relative magnitude or timescale of each of these responses is unknown. Similar responses were observed in most arteries for all experimental conditions, although the order of dilation and constriction responses was not consistent between different experimental states. Changes in geometry due to remodeling processes, such as the addition or resorption of matrix, may not be observed due to the short timeframe of this experiment (*Process 3A*).

Iterative adjustments of pressure and flow rate were used to achieve control of circumferential stress and shear stress (Figure 4-9). During these adjustments of pressure and flow rate, the outer diameter passively changed in response to the adjusted pressure and then resumed the active response. Iterative adjustments allow for small incremental changes of pressure and flow rate which yield sufficiently small vasoactive responses

compared to the large vasomotor responses observed following large, step changes in pressure and flow rate (Figure 3-3).

The experiment comparing the time course of circumferential stress and shear stress for arteries in which local parameters were controlled with arteries in which global parameters were controlled confirmed that holding global parameters constant will not adequately control the local mechanical environment (Figure 4-10). The changes of no-load dimensions during the early stage of culture, discussed previously in Section 5.1, significantly affected the circumferential stress and shear stress of arteries on which only global parameters were controlled. To achieve a target value of shear stress, traditional organ culture studies typically determine the flow rate at the onset of the experiment using the incompressibility assumption and then hold the flow rate constant throughout the experiment (Chesler et al. 1999; Han and Ku 2001; Clerin et al. 2002). By not accounting for the changes in no-load dimensions over time, traditional organ culture approaches could have significant errors in their estimates of shear stress as shown for the artery in which global parameters were held constant (Figure 4-10).

This experiment also confirmed that holding global parameters constant was not sufficient for maintaining the values of circumferential stress and shear stress. Following the adjustment period ( $t = 15$  h), both arteries experienced changes in the loaded outer diameter. For the artery in which global parameters were held constant, the changes in outer diameter caused errors in local parameters that exceeded the errors in the artery under local control. It is expected that if the culture period were extended to allow for geometric changes due to remodeling, then the differences in the local mechanical environment between the two control methods would be even greater. This difference is

due to the fact that, over time, the artery in which global parameters were controlled would adapt in order to restore circumferential stress and shear stress to baseline levels while artery in which local parameters were controlled would maintain circumferential stress and shear stress at constant levels.

### **5.3 Changes in Pressure-Diameter Response**

The pressure-diameter response was measured during the inflation test which was conducted at the onset of the experiment and during the adjustment period at  $t = 15$  h. The changes in the pressure-diameter relationship were not statistically significant, with the exception of one point in the shear stress experiments. However, the tendency of the pressure-diameter relationship was to change such that the arteries became less distensible after 15 hours of culture (Figure 4-4 and Figure 4-5). Similar changes in pressure-diameter response have been reported elsewhere. For example, Gleason et al. (2007) found that mouse carotid arteries tended to become less distensible after 48 hours in culture. This response was consistent for arteries under different levels of axial stretch. In a different study, Davis (2002) found that the percent change in outer diameter reduced by approximately three-fold over the measured pressure range in porcine carotid arteries following a seven day culture period. This response was observed in control arteries held under physiologic loading conditions as well as experimental arteries under two different levels of axial stretch. Taken together, the trends of the pressure-diameter response observed in this study are in agreement with the results reported by Gleason et al. and Davis.

The tendency of arteries to lose distensibility during culture found in this study and in the work of others suggests that this response is not solely due to remodeling.

Because this response was present in several studies using different animal sources, culture periods, and loading condition, it is likely that the loss of distensibility may result from the organ culture environment. Again, a possible explanation for such as response is the loss of water through forced diffusion as described previously. Presumably, the loss of water could affect the relative composition of collagen and elastin and, therefore, affect the mechanical behavior of cultured arteries. This response is described by *Process 2B* in Figure 5-1.

In the absence of organ culture effects, the pressure-diameter response could be predicted based on the known relationship between local mechanical and vascular tone as well as the relationship between vascular tone and mechanical response. As described earlier, the local mechanical environment affects vascular tone which leads to changes in arterial geometry (*Process 1A*). Briefly, increases in circumferential stress lead to a vasoconstriction known as the Bayliss effect (Bayliss 1902). Reductions in circumferential stress yield the opposite response, a vasodilation, due to the partial or complete loss of basal tone. Further, increases in shear stress lead to a dilation (Kamiya and Togawa 1980; Zarins et al. 1987; Brownlee and Langille 1991), while decreases in shear stress lead to a constriction (Langille and O'Donnell 1986; Langille et al. 1989).

Vascular tone is known to affect the mechanical response of arteries (Cox 1978). The stiffness of canine carotid arteries is reduced in a state of vasoconstriction. In contrast, when relaxed, the stiffness of arteries is increased. By applying these notions to our study, it is possible to determine the outcome for the mechanical response of arteries in the absence of organ culture effects.

An overview of the relationship between vasomotor activity and mechanical response is given as *Process 1B*. As described earlier in this section, an artery subjected to an elevated circumferential stress undergoes a vasoconstriction. Based on the results of Cox (1978), this vasoconstriction results in a decrease in the artery's stiffness. In response to reduced circumferential stress, the stiffness of an artery is increased. An artery subjected to an increased shear stress undergoes a vasodilation which results in an increased stiffness. Whereas, an artery subjected to a decreased shear stress results in a reduced stiffness.

The pressure-diameter responses observed at 15 hours in this study result from the combined effects of changes in vasomotor activity (*Process 1B*) and the forced diffusion of water out of the tissue (*Process 2B*). The reduced distensibility of arteries at 15 hours of culture observed for all load conditions suggests that the forced diffusion effect dominated the pressure-diameter response. Because the forced diffusion is consumed within the first 15 hours of culture (Figure 3-4), it may not dominate the response for time points exceeding 15 hours. Therefore, 15 hours could be a reasonable reference point for use in measuring changes in pressure-diameter response in future experiments.

#### **5.4 Changes in Peterson Elastic Modulus**

The Peterson modulus was calculated using the pressure-diameter measurements taken at the onset of the experiment and at  $t = 15$  h. In accordance with the results for the pressure-diameter response, there were no significant differences in the Peterson modulus in the circumferential stress experiments. However, the trends of the responses were that, at  $t = 15$  h, the modulus was greater in low circumferential stress arteries relative to their initial values and, for the high circumferential stress arteries, the modulus was less than

their initial value. The trends of the changes in Peterson modulus are consistent with the expected response, as described in the previous section (*Process 1B* in Figure 5-1).

For the arteries exposed to high circumferential stress, the expected vasomotor effect which leads to reduced  $E_P$  (*Process 1B*) was opposed by the forced diffusion effect which leads to an increased  $E_P$  (*Process 2B*). In this case, the net result was a reduction in  $E_P$  which suggests that the vasomotor effects dominated the response. For the arteries exposed to low circumferential stress, the vasomotor effects and forced diffusion effects work synergistically to increase  $E_P$  (*Processes 1B* and *2B*) as observed.

Although it is difficult to directly compare these results with the work of others, some studies have reported results that support the trend of a reduced Peterson modulus in hypertensive arteries. In an organ culture study of rabbit carotid arteries, Matsumoto et al. found that the incremental elastic modulus measured at 20 mmHg and 80 mmHg was less for hypertensive arteries than for both normotensive and hypotensive vessels following a six day culture period. However, they found that at 160 mmHg, the trend changed such that the incremental modulus of hypertensive arteries was greater than normotensive and hypotensive vessels. It is important to note that the authors measured incremental modulus rather than Peterson modulus as was calculated in this study. Further, they measured there modulus over a smaller ranges of pressures about three different points. In this study, Peterson modulus was calculated over a pressure range of 50 mmHg to 200 mmHg because only three pressure-diameter data points were required to conduct the inflation test. Therefore, while several factors prevent direct comparison of the results, the findings of Matsumoto et al. (1999) confirm that the trend of the reduced Peterson's modulus in the hypertensive arteries is at least a reasonable finding.



The trend of reduced Peterson modulus in hypertensive arteries was also predicted by a mechanical model of pressure-induced remodeling proposed by Rachev et al. (1996). The authors proposed a model of pressure-induced remodeling that found that the Peterson's modulus of hypertensive arteries is less than normotensive arteries at pressures exceeding 40 mmHg. Qualitatively, the trends of the results for Peterson's modulus in this study agree with the findings of Rachev et al. (1996).

In shear stress studies, there were no significant differences in Peterson's modulus measured at the onset of the experiment. However, at  $t = 15$  h, the modulus of the high shear stress arteries was significantly greater than the modulus of low shear stress arteries. This response is consistent with the response expected due to vasomotor responses (*Process 1B*).

For the arteries exposed to high shear stress, the expected vasomotor and force diffusion effects work synergistically to increase  $E_P$  (*Processes 1B* and *2B*) as observed. However, for the arteries exposed to low shear stress, the vasomotor effects and forced diffusion effects oppose each other. The vasomotor effects are expected to lead to a reduced  $E_P$  (*Process 1B*) as opposed to the increased  $E_P$  expected from the forced diffusion effect (*Process 2B*). Therefore, for arteries exposed to low shear stress, the net result was a reduction in  $E_P$  which suggests that the vasomotor effects dominated the response.

### **5.5 Effects of Local Mechanical Environment of Arterial Remodeling**

This study was focused on the effects of circumferential and shear stress on biological markers of remodeling, specifically matrix synthesis, MMP activity, cell proliferation, and cell death. Biological markers were measured because no recordable

changes in arterial dimensions due to remodeling were observed. Therefore, the results obtained represent the trend of macroscopic changes caused by remodeling (*Processes 3A* and *3B* in Figure 5-1). These results of this study can be compared to the early stage remodeling responses of previous pressure-induced and flow-induced remodeling studies. Because the values of circumferential stress and shear stress vary during these studies, our results should be compared to the results from the early stage of previous studies, well before the values of the local parameters are restored to baseline levels.

### **5.5.1 Circumferential Stress**

Significant differences in each biological marker were detected between arteries cultured at high circumferential stress (*Case A* in Table 3-3) and arteries cultured at low circumferential stress (*Case B*). For matrix synthesis, the increased activity at higher circumferential stress is consistent with the finding that protein synthesis increases in strips of rabbit pulmonary artery cultured at elevated wall stress under no flow conditions for 4 days (Kolpakov et al. 1995). Although cell culture studies generally do not apply circumferential stresses to vascular smooth muscle cells, studies have examined the effect of strain, which is analogous to the circumferential strain experienced by smooth muscle cells in organ culture. These studies have shown that smooth muscle cells increase collagen synthesis when subjected to cyclic strain in culture (Leung et al. 1976; Sumpio et al. 1988; Durante et al. 2000). Although cells were subjected to a dynamic stimulus, these cell culture studies suggest that mechanical loading promotes increased matrix synthesis in smooth muscle cells, a result that is consistent with the findings of this study.

The finding of increased matrix synthesis in response to elevated circumferential stress is also consistent with the macroscopic response observed in animal studies that

show remodeling results in thickening of arterial wall in response to sustained hypertension (Liu and Fung 1989; Vaishnav et al. 1990; Fridez et al. 2001). These findings are consistent because increased matrix synthesis is a means of increasing wall thickness. The mechanical environment in this study, where circumferential stress is held constant, is fundamentally different from hypertension studies because an increase in pressure induces an adaptive remodeling response that restores the baseline value of circumferential stress. However, results of this work can be compared to the results of hypertension studies because it is accepted that remodeling related responses are driven by the elevated circumferential stress (Liu and Fung 1989). It should be noted that, in this study, the circumferential stress is permanently elevated and the remodeling outputs could be limited by the synthetic and proliferative capacity of smooth muscle cells, an issue which needs further investigation.

Arteries reduced MMP-2 and pro-MMP-2 activity in response to elevated circumferential stress while pro-MMP-9 activity was not affected by changes in circumferential stress. The effect of circumferential stress on MMP-2 and pro-MMP-2 activity is consistent with the finding that MMP-2 activity in arteries subjected to a pressure of 200 mmHg is about 70% less than that of arteries held at a 100 mmHg over a 48 hour culture period (Chesler et al. 1999). However, in that study, MMP-9 levels were significantly greater in hypertensive arteries which was not observed in this study where pro-MMP-9 activity was unaffected by circumferential stress. The reason for the discrepancy in the MMP-9 results is unclear, but could be due to the differences in culture time. Because MMPs are involved in matrix degrading processes (Galis and Khatri 2002), the artery is essentially acting to limit tissue degradation by reducing

MMP-2 activity in response to elevated circumferential stress and, therefore, contributing to a net increase in tissue content. When combined, the matrix synthesis and MMP-2 results suggest that these two pathways are working synergistically to promote a net increase in tissue content which is consistent with the macroscopic view of remodeling described earlier.

The proliferation rates of smooth muscle cells and fibroblasts were significantly greater under elevated circumferential stress conditions. These increases are consistent with the finding that overall proliferation rates increased in strips of rabbit pulmonary artery under elevated wall stress in static culture. Further, the percent of proliferating cells was greater for fibroblasts than for smooth muscle cells as observed in this study, although the proliferation rate for endothelial cells was not reported (Kolpakov et al. 1995). This increased proliferation response for endothelial cells and fibroblasts was also reported by Davis et al. (2005).

There are several factors that could contribute to the observation that cell proliferation is higher in endothelial cells and fibroblasts than in smooth muscles cells. Both the intimal and adventitial layers of the artery are in direct contact with nutrient-rich media which contains exogenous growth factors from fetal calf serum. Because the intima and adventitia are in direct contact with media, the nutrients and growth factors could likely trigger a stronger proliferative response in endothelial cells and fibroblasts.

Another source of the increased proliferative response of endothelial cells and fibroblasts could be an increased level of proliferation in response to cellular damage from mechanical insult. During preparation for tissue culture, arteries are gently inflated with air to identify leaks and side branches along the arterial wall. Though this process is

conducted as gently as possible, directly exposing the intima to air could potentially injure the endothelial cells and trigger a cascade of events that results in increased proliferation. In addition, excess adventitia is trimmed away during tissue preparation in order to achieve a clean, cylindrical vessel for the purpose of measuring the outer diameter during culture. This process of handling and trimming the adventitia could also induce damage in fibroblasts that results in the observed increased proliferative response.

Alternatively, the response could be due to the different proliferative capacities of the different cell types in cultured arteries. Fibroblasts and endothelial cells undergo much larger increases in proliferation than smooth muscle cells in rat hilar pulmonary arteries subjected to hypobaric hypoxia (Meyrick and Reid, 1979). These results suggest that endothelial cells and fibroblasts proliferate at a higher rate than smooth muscle cells and could explain the differential cell proliferation results observed in this study. However, a cell culture study directly comparing the proliferation rates of endothelial cells, smooth muscles cells, and fibroblasts should be conducted under identical culture conditions in order to definitively answer this question.

The percentage of non-viable cells was significantly greater in arteries exposed to high circumferential stress. Although the percentage of non-viable cells in high circumferential stress arteries is significantly greater than in arteries at low circumferential stress, the percentage of non-viable cells for both sets of arteries ( $1.8 \pm 0.4$  % for low circumferential stress,  $4.1 \pm 1.0$  % for high circumferential stress) is on the same order of magnitude. Further, both of these rates are on the same order of magnitude of the cell death rates measured in fresh tissue ( $2.2 \pm 1.0$  %). While the increased cell death could indicate that smooth muscle cells are being injured or damaged as a result of

the elevated circumferential stress, cell death is a process involved in normal physiological processes such as apoptosis (Alberts et al. 1994). Therefore, given the general increased remodeling activity of high circumferential stress arteries in this study, it is reasonable to expect that the increased percentage reflects the overall increased activity of these vessels.

### **5.5.2 Shear Stress**

In contrast to circumferential stress, we found that flow-induced shear stress does not have a significant affect on the measured biological markers of remodeling – matrix synthesis, MMP-2/9 activity, cell proliferation, or cell death. For matrix synthesis, this result could be explained by the differential roles of smooth muscle cells and endothelial cells. Smooth muscle cells are primarily responsible for matrix synthesis in arteries. However, endothelial cells, which line the lumen of the artery, are directly exposed to flow-induced shear stress. Therefore, for there to be a synthetic response to changes in shear stress, endothelial cells would have to signal smooth muscle cells. This signaling would likely occur through nitric oxide (NO) – a known regulator of vascular tone, but also a prominent cell signaling molecule (Nathan 1992). Under conditions of elevated shear stress, endothelial cells release nitric oxide which causes a vasodilation in order to increase luminal diameter and restore a normal level of shear stress. However, it is possible that NO also mediates the smooth muscle cell response to changes in shear stress.

Kolpakov et al. (1995) showed that protein synthesis and collagen synthesis were inhibited by nitric oxide in a dose-dependent manner in aortic smooth muscle cells (1995). In our work, arteries are subjected to values of shear stress above and below

physiologic levels. For the low shear stress arteries, NO should not be released due to the reduced shear stress so, presumably, matrix synthesis will continue at a basal rate. However, for the high shear stress arteries, NO should be released and would likely remain constant or even inhibit matrix synthesis as described by Kolpakov et al. Such a process would explain why matrix synthesis was not changed in response to changes in shear stress in this study.

An alternative explanation for the constant level of matrix synthesis is that changing synthesis rates may not be required to change luminal diameter in response to changes in shear stress. In the early stages of remodeling, the artery may initiate the diameter change response through other means such as changing vessel tone, rearranging existing matrix, or matrix degradation. None of these mechanisms require alterations in matrix synthesis in order to change the luminal diameter.

The results for MMP-2 activity in response to changes in shear stress are consistent with the finding that MMP-2 activity was not statistically different in arteries cultured at 0.15 and 1.5 Pa after 48 hours in culture, a response that was independent of pressure. In addition, MMP-9 was not affected by shear stress at a pressure of 100 mmHg, but increased with shear stress at a pressure of 200 mmHg (Chesler et al. 1999). This result suggests that MMP-9 activity in response to shear stress is dependent on pressure. In our study, shear stress was varied while circumferential stress was maintained at a physiologic level of 100 kPa which is roughly analogous to the pressure of 100 mmHg used by Chesler et al. We only explore the MMP response to shear stress at a single level of circumferential stress, so we were not able to observe the pressure dependence of the shear stress response reported by Chesler et al. in our work. Although

we explored the MMP response over a shear stress range of 0.75 Pa to 2.25 Pa, as opposed to 0.15 Pa to 1.5 Pa of Chesler et al., our results for MMP-2 activity are in close agreement.

Cell proliferation was not significantly different between arteries exposed to low and high shear stress. As observed in circumferential stress experiments, cell proliferation was increased in endothelial cells and fibroblasts and much lower for smooth muscle cells. The reasons for this differential proliferation response were described earlier for arteries exposed to different levels of circumferential stress.

The percentage of non-viable cells was relatively low in both sets of arteries in the shear stress experiments. The average percentage of EthD-positive nuclei in the experimental arteries was less than 2% which is similar to the percentage of EthD-positive nuclei for fresh tissue ( $2.2 \pm 1.0$  %), which suggests that the percentage of dead cells is normal and that the loading conditions do not induce cell death.

Overall, the apparent lack of remodeling response to changes in shear stress may be due to several factors. Given the wide range of physiologic shear stresses, it is possible that the values of shear stress used in this study were not extreme enough to induce a remodeling response. Normal physiologic shear stresses can range from 1.0 to 7.0 Pa depending on location within the vasculature (Malek et al. 1999). In this study, arteries were exposed to shear stresses of 0.75 Pa and 2.25 Pa, values that are 50% less and greater than 1.5 Pa, the level of shear stress that is considered physiologic in most experiments. In addition, remodeling in response changes in flow is generally a slower process compared to pressure-induced remodeling. It is possible that a 72 hour culture period is not sufficient to observe detectable changes caused by flow-induced remodeling.



Finally, it is possible that the remodeling response depends on the magnitude of circumferential stress experienced by the smooth muscle cells after flow-induced changes in the shear stress sensed by the endothelial cells. This effect was shown by Chesler et al. (Chesler et al. 1999) for MMP-9 and, therefore, it is likely that similar responses could be observed for other biological markers. In addition, it was speculated that abnormal circumferential stress in combination with flow-induced alterations in the contractile state of vascular smooth muscle cells might elicit a remodeling response (Rachev 2000).

## **5.6 Limitations**

The limitations of this study result from several technical constraints. As described earlier, the lack of a continuous, non-destructive means of measuring the arterial inner diameter limited us to estimating the inner diameter based on the assumption of material incompressibility. Although, we corrected for the observed changes in no-load dimensions, having a non-destructive means of determining the inner diameter would improve the accuracy of the measurement. Ultrasonic transducers have recently been used to measure the inner diameter of arteries in organ culture (Zulliger et al. 2002), but were not included in this study due to technical constraints.

The mechanical response of the artery was determined at the onset of the experiment and during the adjustment period, but not at the end of the culture period. Measuring the pressure-diameter response at the end of culture would increase the time interval between the end of the experiment and the start of the  $^3\text{H}$ -proline assay. Every effort was taken to transfer the tissue section from the loaded artery to the radiolabeled media as quickly as possible, therefore, the pressure-diameter response was not measured at this point. However, measuring the pressure-diameter response following culture

would provide a more comprehensive view of the mechanical response over the entire culture period. In future studies, the time course of the pressure-diameter response could be measured by simultaneously culturing additional arterial segments to prevent potential interference with biological assays conducted following culture. This requires additional experimental chambers to accommodate the need to simultaneously culture more vessels.

The effects of the viscous properties of arteries were not considered in this study. Surprisingly, few experiments have been reported that study the viscous properties of arteries. For example, in Cardiovascular Solid Mechanics (Humphrey 2002), a comprehensive text reviewing cardiovascular biomechanics literature, viscous effects are only briefly mentioned with regard to cardiac tissue, but not vascular tissues. In general, creep and stress relaxation appear when there are step changes in pressure and flow rate or rate dependent loads are applied. However, these effects could be minimized by using a closed-loop control scheme to continuously adjust pressure and flow rate. These viscous effects could contribute to the changes in deformed dimensions and modulate the vasomotor responses of the artery. There is a need for future experiment to investigate the viscous properties of vascular tissues and their effects on the mechanical response of arteries in organ culture.

The functionality of endothelial cells and smooth muscle cells was not measured in this study due to the possibility that the agonists used in the vasomotor assays may interfere with the  $^3\text{H}$ -proline and MMP assays performed following culture. However, our lab has experience conducting organ culture studies under a range of different mechanical loads in experiments lasting up to 7 days and has been able to successfully maintain cell functionality (Han and Ku 2001; Han et al. 2003; Davis et al. 2005). The

use of ring segments in vasoactivity testing would be a viable alternative, but previous attempts to perform these by our lab have been unsuccessful. Given the lab's experience with organ culture methods and considering that the culture period for these experiments was shorter than previously reported studies by our lab (Han and Ku 2001; Han et al. 2003; Davis et al. 2005), it is likely that cell functionality was maintained in these experiments. In addition, considering the presence of synthetic activity at the end of culture, it is likely that the cells retain functionality during the culture period. Further, the use of negative controls demonstrated that the activity measured following culture is due to the synthetic activity of cells rather than the passive retention of  $^3\text{H}$ -proline by the tissue (Figure 3-8).

The  $^3\text{H}$ -proline assay was conducted following the culture period using a tissue segment that was statically incubated. Ideally, the assay would have been performed during the culture period. However, this approach was not pursued due to the potential for contamination if leaks occurred within the flow loop during an experiment. Since the assay was performed post-culture, a study was conducted to determine the duration of synthetic activity of cells following culture (Figure 3-8). Based on these results, it is reasonable to assume that the protocol effectively measured the synthetic activity of cells using the  $^3\text{H}$ -proline assay.

With the exception of EthD incorporation, each of the biological markers used in this study –  $^3\text{H}$ -proline incorporation, MMP-2/9 activity, BrdU incorporation – measures cellular responses over a limited range of time, and thus captures a “snapshot” of these responses. In contrast, the EthD incorporation assay measures cumulative cell death because EthD binds to DNA exposed by the fragmented cell membranes, which could

result from cells that have died at any point during the culture period. By measuring biological markers that give a “snapshot” of remodeling, it is possible that the results are misleading in the sense that some of the observed responses may be transient in nature. To address this limitation, we compared our results to those of others that measured similar biological markers under different experimental conditions to check for agreement. However, future studies should consider investigating the time course of biological responses in order to comprehensively understand their role in the early stages of remodeling.

Although local parameters can be controlled independently in organ culture, such control cannot be achieved *in vivo*. In organ culture, pressure and flow rate can be adjusted independently in order to control circumferential and shear stress. However, pressure and flow cannot be adjusted independently *in vivo*. Therefore, this approach for controlling the local mechanical environment cannot be used in animal studies.

## **CHAPTER 6**

### **CONCLUSIONS AND FUTURE WORK**

#### **6.1 Conclusions**

This thesis proposes a novel approach to study arterial remodeling in organ culture based on response to controlled changes in the local mechanical environment of endothelial and smooth muscle cells. This method offers a fundamentally new approach to studying the role of the mechanical environment in arterial remodeling. By independently controlling local parameters, it is possible to use a systems approach to studying the effects of local parameters on remodeling outputs. This approach can be used for the design and realization of different types of experiments to determine the effects of the local environment on arterial remodeling. For example, studies can be conducted to identify synergistic effects of local parameters, dose responses of arteries to local parameters, or the full extent of the cellular responses to changes in local parameters. It is expected that the results from such experiments can promote a better understanding and prediction of the behavior of arteries during normal physiological conditions and at certain pathological states.

To illustrate the method, experiments were conducted to evaluate the independent effects of circumferential stress and shear stress on biological markers of arterial remodeling. The following major conclusions were revealed from this work:

1. Circumferential stress and shear stress can be independently controlled by simultaneously adjusting pressure and flow rate in perfusion organ culture.

2. The no-load dimensions of arteries change within the first 15 hours of culture which affects the assumption of material incompressibility and possibly changes in the deformed arterial dimensions.
3. Circumferential stress stimulates changes in biological markers. These early stage responses are consistent with the long term responses observed in *in vivo* studies. These early stage responses include:
  - Matrix synthesis, as measured by  $^3\text{H}$ -proline incorporation, is greater in arteries exposed to high circumferential stress.
  - MMP-2 and pro-MMP-2 activity is reduced in arteries exposed to high circumferential stress, while pro-MMP-9 activity is unaffected.
  - The proliferation of smooth muscle cells and fibroblasts is greater in high circumferential stress arteries.
  - Cell death is greater in high circumferential stress arteries.
4. Shear stress does not affect the biological markers measured in this study.

## **6.2 Future Work**

This work established a new approach to investigate the role of the local mechanical environment in arterial remodeling. By controlling the local mechanical environment, this approach facilitates the development of experiments that will add further insights into the mechanisms of arterial remodeling. The following list describes some of the future experiments that can build on the methods and results presented in this study:

1. Explore additional combinations of circumferential and shear stress. Table 3-3 describes the combinations of circumferential stress and shear stress that were

explored in this study. Due to time constraints, we were not able to explore every combination of circumferential stress and shear stress, but it is possible that certain combinations may lead to remodeling results that have applications elsewhere. Such results could be applied to the field of tissue engineering where the mechanical environment could be controlled to optimally promote tissue growth when developing a vascular graft.

2. Investigate remodeling due to axial strain. Recent studies suggest that arteries adapt to changes in axial strain (Jackson et al. 2002; Han et al. 2003; Davis et al. 2005; Nichol et al. 2005; Gleason et al. 2007), but circumferential stress and shear stress were not independently controlled in these studies. Therefore, exploring the effect of axial strain while controlling the other local parameters should offer meaningful insights into the understanding of axial-stretch-induced remodeling.
3. Use a non-destructive means of measuring wall thickness. This would improve the accuracy of the circumferential stress and shear stress calculations and obviate the need to impose the incompressibility assumption. As mentioned in the Discussion section (Section 5.6), ultrasonic transducers have been used by others to measure wall thickness in organ culture (Zulliger et al. 2002). This approach was not pursued for this work due to the technical constraint of integrating the transducers with the current experimental system.
4. Use closed-loop control to further strengthen this experimental approach. By having closed loop control, pressure and flow rate could be adjusted continuously to maintain the target values of circumferential stress and shear stress. In addition, such an approach would eliminate the need to conduct the inflation test

during the experiment which would minimize disturbances to the mechanical environment of the artery.

5. Increase the length of the culture period. By increasing the length of the culture period, it is possible to determine the remodeling capacity of endothelial cells and smooth muscle cells. In previous experiments which subjected arteries to a controlled change of pressure or flow rate, circumferential stress and shear stress were restored to baseline levels over time. Using our method, it is possible to hold circumferential stress or shear stress at fixed levels and observe how the cellular responses change over time. Developing techniques to lengthen the culture period of arteries will allow such responses to be observed.
6. Measure additional biological markers of remodeling. This will provide a broader view of the cellular processes involved in remodeling. The use of molecular biology techniques such as Western blotting and real-time polymerase chain reaction facilitate the measurement of the expression of a wide array of proteins and genes involved in remodeling.
7. Investigate the effects of pulsatility on arterial remodeling. As mentioned in the Discussion chapter, pulsatile pressure and flow rate are significant components of the mechanical environment. Using this new method, the independent role of pulsatility in arterial remodeling can be studied while the rest of the local mechanical environment is held constant.
8. Investigate the role of vascular tone in remodeling. It is known that, during pressure-induced and flow-induced remodeling, the muscular tone of arteries initially changes and then, over time, is gradually restored to baseline levels.



However, the significance of vascular tone in regulating the remodeling response is not well understood. Using the method developed in this study, experiments could be conducted in which the vascular tone is chemically altered while circumferential stress or shear stress is independently varied. The resulting responses would help to reveal the role of tone in arterial remodeling.

## **APPENDIX A**

### **EXPERIMENTAL DATA ACQUISITION PROGRAMS**

## A.1 C++ Code for Inflation Test

```
/* Code modified from Data Translation's source code & Davis 2002 */
/* C++ code compiled using Microsoft Visual Studio 6.0 */

// Standard include files
#include <windows.h>
#include <stdlib.h>
#include <stdio.h>
#include <conio.h>
#include <olmem.h>
#include <olerrors.h>
#include <oldaapi.h>
#include <olwintyp.h>
#include <olfgapi.h>
#include <olimgapi.h>
#include <time.h>
#include "DtColorSdk.h"
#include <dos.h>
#include <string.h>
#include <math.h>
#include <malloc.h>
#include <signal.h>

// This is a macro that dumps on the screen
// the error message if an error occurs.
#define DT_TRY(a) {\
char Message(1000);\
DWORD Error;\
Error = a;\
OlImgGetStatusMessage(Error,Message,1000);\
if (Error)\
{\
printf("\n");\
printf("ERROR: %s\n",Message);\
}\
}

HWND CreateChildWindow(HWND Parent, DWORD x, DWORD y, DWORD w, DWORD
h);
HWND CreateParentWindow(DWORD x, DWORD y, DWORD w, DWORD h);
LRESULT CALLBACK _export MyWindowProc(HWND hWnd,UINT Msg,WPARAM
wParam,LPARAM lParam);

// Parent window dimensions
// Child windows

#define X 10 // Define position of
the main window
#define Y 100

#define WIDTH 640
#define HEIGHT 480

#define SCALE_X 100
// in %
```

```

#define SCALE_Y 100
// in %
#define CHILD_WIDTH 640 * SCALE_X/100
#define CHILD_HEIGHT 480 * SCALE_Y/100
#define UPPER_BACKGROUND_ROW 5
#define LOWER_BACKGROUND_ROW 475
#define MIDDLE_FOREGROUND_ROW 240
#define ROW_START 0
#define COL_START 0
#define ROW 480 /* number of rows to be
read */
#define COLUMN 640 /* number of columns to be read */
#define INCREMENT 30 /* interval between columns to take images */
#define ITERATION 20 /* number of columns used to measure dia */
#define DETECTION_FRAME 5 /* no. of pix to look ahead of
current pixel in order to see if that pixel
value matches the current pixel value. Helps
detect edges more robustly */
#define Y_DIM 480 /* size of image in pixels in vertical
dimension */
#define X_DIM 640

// Parameters for Diameter Calibration
#define REPEAT 5 /*no. of dia measurements to avg during
calibration*/
#define DATA_INTERVAL 15 /* no. of secs between dia readings
*/

void main(){
    int i,j;
    char a = 0,pressure(100);
    float diameter_factor,DIAMETER_STANDARD;
    float average_diameter;
    time_t
current_time,previous_time,initial_time,elapsed_time;
    int is_enter();
    float diameter();
    float diameter_calibration();
    void image();
    void initialization ();
    void ftime(struct timeb *buf); /*structure to
establish sampling frequency*/
    FILE* pTestFile;

    /*get diameter calibration factor, initial artery area,
length, and desired axial stress*/
    system("cls");

    pTestFile = fopen("press_dia_A.txt", "a");
    //'a' is for append file, use 'w' to overwrite

    printf("Diameter calibration.\n\n");
    diameter_factor = diameter_calibration();
    fprintf(pTestFile,"diameter calibration factor (mm/pixel):
%f\n\n",diameter_factor);
    fclose(pTestFile);

```

```

/*****
/* Diameter measurements are made from the number of frames specified
/* by REPEAT. Measured diameter is printed to the screen, and as many
/* as desired can be made.
*****/

/* Provide live video to reposition camera for diameter measurement,
then proceed upon any key strike*/

    printf("Position camera for diameter measurement.\n");
    printf("Strike any key when ready.\n\n");
    image();

    system("cls");
    printf("Diameter measurement initiated...\n");

    while(1){
        average_diameter = 0;
        printf("\n\nEnter pressure (mmHg): ");
        scanf("%s", &pressure);
        printf("\n\n");

        pTestFile = fopen("press_dia_A.txt", "a");
        fprintf(pTestFile, "\nPressure(mmHg):

%s\n", pressure);

        printf("Pressure(mmHg): %s\n\n", pressure);

        fprintf(pTestFile, "Iteration          Diameter

(mm)\n");

        for (j=1; j<6; j++){
            for (i=0; i<REPEAT; i++){
                average_diameter =
average_diameter + diameter()*diameter_factor/(float)REPEAT;
            }
            fprintf(pTestFile, "%d

%f\n", j, average_diameter);
            printf("Iteration = %d   diameter (mm) =

%f\n", j, average_diameter);
            average_diameter = 0;
        }
        fclose(pTestFile);
    }

}

/*****
/* diameter() returns average diameter in pixels
*/
*****/

float diameter()

{
    OLT_IMG_DEV_ID          DevId;
    OLT_FG_FRAME_ID         FrameId;

```

```

        Hwnd
        hChild1, hChild2;
        USHORT
        old;
        //to be used with line containing
function = OlFgSetInputVideoSource
        DWORD
        Count = 0;
        OLT_SCALE_PARAM
        ULNG
        Timeout;
        BYTE*
        pColumnPixelBuffer;
        BYTE*
        pRowPixelBuffer;
        FILE*
        pTestFile;

        scale.hscale = SCALE_X;
        scale.vscale = SCALE_Y;

        int i=0;
        int j=0;
        int k=0;
        int status;
        int count;
        int m=1;
        /* loop
index; m is a counter */
        int upper_max_square(ITERATION);
        int lower_max_square(ITERATION);
        int a(Y_DIM); /* temp array to hold pixel values for
columns */
        int b(X_DIM); /* temp array to hold pixel values for rows
*/

        int dia_pixels =0;
        int upper_bound=0;
        int lower_bound=0;
        int sum_dia=0;
        char
        framegrabber(20);
        long
        sum_pixels=0;
        float
        avg_pixels=0;
        float
        background_value=0,foreground_value=0,threshold=0;
        float
        avg_dia;

        // create user buffers for pixel data
        pColumnPixelBuffer = new BYTE(1*ROW);
        pRowPixelBuffer = new BYTE(COLUMN*1);

        //initial buffers to hold pixel data
        for (i=0; i<Y_DIM; ++i){
            pColumnPixelBuffer(i)=0;
        }

        for (i=0; i<X_DIM; ++i){
            pRowPixelBuffer(i)=0;
        }

```

```

        // Display image in window prior to measuring diameter
        DT_TRY(OLImgOpenDevice("Framegrabber-2",&DevId));
        DT_TRY(OLImgSetTimeoutPeriod(DevId,10,&Timeout));

        // Allocate one frame
        DT_TRY(OLFgAllocateBuiltInFrame(DevId, OLC_FG_DEV_MEM_VOLATILE,
        OLC_FG_NEXT_FRAME,&FrameId))
        DT_TRY(DtColorHardwareScaling(DevId,0,OLC_WRITE_CONTROL,&scale))

        MSG
        msg;
        OLT_SIGNAL_TYPE                signal;

        signal = OLC_COMPOSITE_SIGNAL;

        DT_TRY(DtColorSignalType(DevId, 0, OLC_WRITE_CONTROL,
        &signal)); DT_TRY(OLFgAcquireFrameToDevice(DevId,FrameId));
        OLFgSetInputVideoSource(DevId,0,&old);

        // Determine threshold for background & foreground
        measurements

        //Avg Background Value for a Row in Upper Portion of Frame
        DT_TRY(OLFgReadFrameRect(DevId,FrameId,0,UPPER_BACKGROUND_R
        OW,COLUMN,1,pRowPixelBuffer,COLUMN*1));

        for (i=0;i<COLUMN;++i){
            avg_pixels = avg_pixels + (float)
        pRowPixelBuffer(i)/COLUMN;
        }

        background_value = avg_pixels;
        avg_pixels = 0;

        //Avg Background Value for a Row in Lower Portion of Frame
        DT_TRY(OLFgReadFrameRect(DevId,FrameId,0,LOWER_BACKGROUND_R
        OW,COLUMN,1,pRowPixelBuffer,COLUMN*1));

        for (i=0;i<COLUMN;++i){
            avg_pixels = avg_pixels + (float)
        pRowPixelBuffer(i)/COLUMN;
        }

        background_value = (background_value + avg_pixels)/2;
        avg_pixels = 0;

        //Avg Foreground Value for a Row in Middle Portion of Frame
        DT_TRY(OLFgReadFrameRect(DevId,FrameId,0,MIDDLE_FOREGROUND_
        ROW,COLUMN,1,pRowPixelBuffer,COLUMN*1));

        for (i=0;i<COLUMN;++i){
            avg_pixels = avg_pixels + (float)
        pRowPixelBuffer(i)/COLUMN;
        }

```

```

        foreground_value = avg_pixels;
        avg_pixels = 0;
        threshold = background_value - (background_value-
foreground_value)/4;

        //Obtain pixel values and calculate diameters
        for (i=0;i<ITERATION;++i){

                DT_TRY(OLFgReadFrameRect(DevId,FrameId,m,ROW_START,1,ROW,pC
olumnPixelBuffer,COLUMN*1));

                for (j=0; j<ROW; j++){
                        if
(pColumnPixelBuffer(j)<=threshold){
                                dia_pixels++;
                        }
                }
                sum_dia = sum_dia+dia_pixels;
                dia_pixels = 0;
                m=m + INCREMENT;
        }

        avg_dia = ((float) sum_dia)/(1.0*ITERATION);

        // Delete the user buffer
        free(pColumnPixelBuffer);
        free(pRowPixelBuffer);

        DT_TRY(OLImgCloseDevice(DevId));

        return avg_dia;
}

/*****
/* is_enter returns a 1 if the keyboard hit is a carriage return, 0
/* otherwise
*/
*****/

int is_enter()
{
        char a = 0;
        a = getch();
        if (a == 13){
                return(1);
        }
        else {
                return(0);
        }
}

/*****
/* image() continuously acquires a frame & displays it in a window
/* until keyboard is hit
*/
*****/

```



```

void image()
{
    OLT_IMG_DEV_ID                DevId;
    OLT_FG_FRAME_ID               FrameId;
    HWND                          hWnd,
hChild1, hChild2;
    USHORT                        old;

    //to be used with line containing function =
    OlFgSetInputVideoSource
        OLT_SCALE_PARAM           scale;
        ULNG
        Timeout;

    int    i=0;
           int j=0;
           int k=0;
           char a=0;
           scale.hscale = SCALE_X;
           scale.vscale = SCALE_Y;

    // Display image in window prior to measuring diameter
    DT_TRY(OlImgOpenDevice("Framegrabber-2",&DevId));
    DT_TRY(OlImgSetTimeoutPeriod(DevId,10,&Timeout));

    // Allocate one frame
    DT_TRY(OlFgAllocateBuiltInFrame(DevId, OLC_FG_DEV_MEM_VOLATILE,
    OLC_FG_NEXT_FRAME,&FrameId))
    DT_TRY(DtColorHardwareScaling(DevId,0,OLC_WRITE_CONTROL,&scale))

    // Create a window to display the result
    hWnd = CreateParentWindow(X,Y,1300,600);
    hChild1 =
    CreateChildWindow(hWnd,10,10,CHILD_WIDTH,CHILD_HEIGHT);
    hChild2 = CreateChildWindow(hWnd,CHILD_WIDTH +
    20,10,CHILD_WIDTH,CHILD_HEIGHT);

    MSG                                msg;
    OLT_SIGNAL_TYPE                    signal;

    //This enumerated type specifies the video signal type
    signal = OLC_COMPOSITE_SIGNAL;

    DT_TRY(DtColorSignalType(DevId, 0, OLC_WRITE_CONTROL,
    &signal));

    while(1)
    {
        // Acquire one frame for hChild1 window
        DT_TRY(OlFgAcquireFrameToDevice(DevId,FrameId));

        // Display the whole frame
        DT_TRY(OlFgDrawAcquiredFrame(DevId,hChild1,FrameId));
        OlFgSetInputVideoSource(DevId,0,&old);
    }
}

```

```

// Acquire one frame for hChild2 window
DT_TRY(OFgAcquireFrameToDevice(DevId,FrameId));
// Display the whole frame
DT_TRY(OFgDrawAcquiredFrame(DevId,hChild2,FrameId));
OFgSetInputVideoSource(DevId,0,&old);

if(kbhit()){
    a=getch();
    break;
}

if (PeekMessage(&msg, hWnd, 0,0,PM_REMOVE))
{
    TranslateMessage(&msg);
    DispatchMessage(&msg);
}

DT_TRY(OFgCloseDevice(DevId));
}

/*****
/* diameter_calibration() performs diameter calibration on a diameter*/
/* standard and returns the calibration factor in units of mm/pixel */
*****/

float diameter_calibration()
{
    char a=0;
    char camera(3),exp(100);
    int i,j=1,e,status,known_factor;
    float dia = 0.0;
    float sum_dia,avg_dia,DIAMETER_STANDARD;
    float diameter_factor = 0.0;
    FILE* pTestFile;

    system("cls");

    printf("Position camera to perform diameter
calibration.\n");
    printf("Strike any key when ready.\n\n");

    image(); /* acquire an image */

    printf("Enter Experiment #/Date: ");
    scanf("%s",&exp);
    printf("Enter the camera you are using (1A/2A): ");
    scanf("%s",&camera);
    printf("Do you know calibration factor (Enter 1 if yes, 2
if no): ");
    scanf("%d",&known_factor);

    if (known_factor == 1){

```

```

        printf("Enter calibration factor (mm/pixel):
");

        scanf("%f",&diameter_factor);
        pTestFile = fopen("press_dia_A.txt", "a");

        fprintf(pTestFile,"\n\nExperiment #: %s\n",exp);
        fprintf(pTestFile,"Camera: %s\n",camera);
        fclose(pTestFile);
        system("cls");
        return(diameter_factor);
    }

    printf("Enter the diameter of the standard used for
calibration (mm): "); //allow user to enter calibrated diameter
    scanf("%f",&DIAMETER_STANDARD);
    pTestFile = fopen("press_dia_A.txt", "a");
    fprintf(pTestFile,"\n\nExperiment #: %s\n",exp);
    fprintf(pTestFile,"Camera: %s\n",camera);
    fprintf(pTestFile,"diameter of calibration standard (mm):
%f\n",DIAMETER_STANDARD);

    do{
        sum_dia = 0.0;
        for(i=0;i<REPEAT;i++){
            dia = diameter();
            sum_dia = sum_dia + dia;
        }
        avg_dia = sum_dia/(float)REPEAT;
        printf("\nAverage diameter (pixels):
%f\n",avg_dia);

        diameter_factor =
DIAMETER_STANDARD/(sum_dia/(float)REPEAT);
        printf("Diameter factor (mm/pixel):
%f\n\n",diameter_factor);
        printf("Hit enter to accept, any other key to
redo the calibration.\n");
    }while(!is_enter());

    fprintf(pTestFile,"Average diameter (pixels):
%f\n",avg_dia);
    fclose(pTestFile);

    system("cls");
    return(diameter_factor);
}

HWND CreateParentWindow(DWORD x, DWORD y, DWORD w, DWORD h)
{
    HWND          NewWindow = 0;
    WNDCLASS      wc        = 0;
    DWORD         Error;

    wc.style      = CS_VREDRAW | CS_VREDRAW;
    wc.lpfnWndProc = DefWindowProc;
    wc.cbClsExtra = 0;

```

```

wc.cbWndExtra      = 0;
wc.hInstance       = 0;
wc.hIcon           = 0;
wc.hCursor         = 0;
wc.hbrBackground   = (HBRUSH) (COLOR_WINDOW + 1);
wc.lpszMenuName     = NULL;
wc.lpszClassName   = "DEFAULT_WINDOW";

Error = RegisterClass(&wc);    // may fail if class already exists.
Error = GetLastError();

NewWindow = CreateWindow(
                                "DEFAULT_WINDOW",
                                // Default class
                                "Driver default
window",    // title
                                WS_SYSMENU|WS_OVERLAPPED,    // style
                                x, y,
                                // x, y position
                                w, h,
                                // size
                                NULL,
                                // No Parent
                                NULL,
                                // menu
                                NULL,
                                NULL);

Error = GetLastError();
ShowWindow(NewWindow, SW_SHOWDEFAULT);

return NewWindow;
}

HWND CreateChildWindow(HWND Parent, DWORD x, DWORD y, DWORD w, DWORD h)
{
    HWND      NewWindow = 0;
    DWORD      Error;

    NewWindow = CreateWindow(
                                "DEFAULT_WINDOW",
                                // Default class
                                "Driver default
window",    // title
                                WS_CHILD,
                                // style
                                x, y,
                                // x, y position
                                w, h,
                                // size
                                Parent,
                                // No Parent
                                NULL,
                                // menu
                                NULL,
                                NULL);

```

```
NULL);
```

```
    Error = GetLastError();  
    ShowWindow(NewWindow, SW_SHOWDEFAULT);  
    return NewWindow;  
}
```

```
LRESULT CALLBACK _export MyWindowProc(HWND hWnd, UINT Msg, WPARAM  
wParam, LPARAM lParam)  
{  
    return DefWindowProc(hWnd, Msg, wParam, lParam);  
}
```

## A.2 C++ Code for Calculating Circumferential Stress and Shear Stress

```
/* Code modified from Data Translation's source code & Davis 2002 */
/* C++ code compiled using Microsoft Visual Studio 6.0 */

// Standard include files
#include <windows.h>
#include <stdlib.h>
#include <stdio.h>
#include <conio.h>
#include <olmem.h>
#include <olerrors.h>
#include <oldaapi.h>
#include <olwintyp.h>
#include <olfgapi.h>
#include <olimgapi.h>
#include <time.h>
#include "DtColorSdk.h"
#include <dos.h>
#include <string.h>
#include <math.h>
#include <malloc.h>
#include <signal.h>

// This is a macro that dumps on the screen
// the error message if an error occurs.
#define DT_TRY(a) {\
char Message(1000);\
DWORD Error;\
Error = a;\
OlImgGetStatusMessage(Error,Message,1000);\
if (Error)\
{\
printf("\n");\
printf("ERROR: %s\n",Message);\
}\
}

HWND CreateChildWindow(HWND Parent, DWORD x, DWORD y, DWORD w, DWORD
h);
HWND CreateParentWindow(DWORD x, DWORD y, DWORD w, DWORD h);

LRESULT CALLBACK _export MyWindowProc(HWND hWnd,UINT Msg,WPARAM
wParam,LPARAM lParam);

// Parent window dimensions
// Child windows

#define X 10 // Define position of
the main window
#define Y 100

#define WIDTH 640
#define HEIGHT 480

#define SCALE_X 100 // in %
```

```

#define SCALE_Y          100                      // in %

#define CHILD_WIDTH      640 * SCALE_X/100
#define CHILD_HEIGHT     480 * SCALE_Y/100

#define UPPER_BACKGROUND_ROW      5
#define LOWER_BACKGROUND_ROW     475
#define MIDDLE_FOREGROUND_ROW    240
#define ROW_START 0
#define COL_START 0
#define ROW 480                      /* number of rows to be read */
#define COLUMN 640                  /* number of columns to be read */
#define INCREMENT 30               /* interval between columns to take images */
#define ITERATION 20               /* no. of col from which to measure the dia */
#define DETECTION_FRAME 5          /* no. of pixels to look ahead of the
                                   current pixel in order to see if that
                                   pixel value matches the current pixel
                                   value. Helps detect edges more robustly
                                   */

#define Y_DIM 480                   /* size of image in pixels in y
dimension */
#define X_DIM 640

// Parameters for Diameter Calibration
#define REPEAT 1                   /*no. of dia used to avg during
calibration*/
#define DATA_INTERVAL 30          /* no. of secs betw diameter
readings */

#define STRLEN 80                  /* string size for text manipulation */
char str(STRLEN);                 /* global string for text manipulation */

typedef struct tag_board {
    HDEV  hdrv;                    /* driver handle */
    HDASS hdass;                  /* sub system handle */
    ECOD  status;                 /* board error status */
    HBUF  hbuf;                  /* sub system buffer handle */
    PWORD lpbuf;                 /* buffer pointer */
    char name(STRLEN);            /* string for board name */
    char entry(STRLEN);           /* string for board name */
} BOARD;

typedef BOARD* LPBOARD;

static BOARD board;

BOOL CALLBACK
GetDriver( LPSTR lpszName, LPSTR lpszEntry, LPARAM lParam )
/*
this is a callback function of olDaEnumBoards, it gets the
strings of the Open Layers board and attempts to initialize
the board. If successful, enumeration is halted.
*/
{
    LPBOARD lpboard = (LPBOARD)(LPVOID)lParam;

```

```

/* fill in board strings */

lstrcpy(lpboard->name,lp.szName,STRLEN);
lstrcpy(lpboard->entry,lp.szEntry,STRLEN);

/* try to open board */

lpboard->status = oldaInitialize(lp.szName,&lpboard->hdrvr);
if (lpboard->hdrvr != NULL)
    return FALSE;          /* false to stop enumerating */
else
    return TRUE;           /* true to continue          */
}

void main(){
    int          i,j,t, interval, channel, ch;
    char         a = 0;
    float        diameter_factor, DIAMETER_STANDARD;
    float        average_diameter, pressure;
    float
th;              no_load_length, no_load_dia, no_load_thickness, flow_rate, leng

                float        thickness, hoop_stress, shear_stress;
                time_t
                current_time, previous_time, initial_time, elapsed_time;
                int          is_enter();
                float        diameter();
                float        diameter_calibration();
                float        adjust_flow_rate();
                void         image();
                void         initialization ();
                float        output_voltage(int channel);
                void         ftime(struct timeb *buf); /*structure to
establish sampling frequency*/
                FILE*        pTestFile;

                /*get diameter calibration factor, initial artery area,
length, and desired axial stress*/
                system("cls");

                pTestFile = fopen("press_dia_30s_A.txt", "a");

                printf("Diameter calibration.\n\n");
                diameter_factor = diameter_calibration();
                fprintf(pTestFile,"diameter calibration factor (mm/pixel):
%f\n\n",diameter_factor);

                printf("Enter Transducer Channel: ");
                scanf("%d",&channel);
                printf("Enter No-Load Length (mm): ");
                scanf("%f",&no_load_length);
                printf("Enter No-Load Diameter (mm): ");
                scanf("%f",&no_load_dia);
                printf("Enter No-Load Thickness (mm): ");
                scanf("%f",&no_load_thickness);
                printf("Enter Length (mm): ");

```



```

scanf("%f",&length);
printf("Enter Flow Rate (ml/min): ");
scanf("%f",&flow_rate);

fprintf(pTestFile,"Transducer Channel: %d\n",channel);
fprintf(pTestFile,"No-Load Length (mm):
%f\n",no_load_length);
fprintf(pTestFile,"No-Load Diameter (mm):
%f\n",no_load_dia);
fprintf(pTestFile,"No-Load Thickness (mm):
%f\n",no_load_thickness);
fprintf(pTestFile,"Length (mm): %f\n",length);
fprintf(pTestFile,"Flow Rate (ml/min): %f\n",flow_rate);

fprintf(pTestFile,"\n\n\nElapsed Time (s)          Pressure
(mmHg) Flow Rate (ml/min)          Diameter (mm)          Thickness
(mm) Hoop Stress (kPa)          Shear Stress (dyn/cm2)\n");
fclose(pTestFile);

/*****
/* Diameter measurements are made from the number of frames specified
/* by REPEAT. Measured diameter is printed to the screen, and as many
/* as desired can be made.
*****/

/* Provide live video to reposition camera for diameter measurement,
then proceed upon any key strike*/

system("cls");
printf("\n\nPosition camera for diameter measurement.\n");
printf("Strike any key when ready.\n\n");
image();

system("cls");
printf("Diameter measurement initiated...\n");

/*get the initial time*/
time(&initial_time);
time(&previous_time);
elapsed_time=0;

/*get initial measurement at t = 0 */

average_diameter = 0;
for (i=0;i<REPEAT;i++){
    average_diameter = average_diameter +
diameter()*diameter_factor/(float)REPEAT;
}
pressure=output_voltage(channel)*100;

thickness=0.5*(average_diameter-
sqrt(pow(average_diameter,2)-
4*no_load_length*no_load_thickness*(no_load_dia-
no_load_thickness)/length));
hoop_stress=pressure*0.1333224*(average_diameter-
(2*thickness))/(2*thickness);

```

```

        shear_stress=2.66667*flow_rate/(3.14159265*pow((average_dia
meter/2-thickness),3));

        printf("t (s)=%ld                                P (mmHg)=%f
        Q (ml/min)=%f\n",elapsed_time,pressure,flow_rate);
        printf("d (mm)=%f                                h
(mm)=%f\n",average_diameter,thickness);
        printf("hoop (kPa)=%f    shear
(dyn/cm2)=%f\n\n",hoop_stress,shear_stress);

        pTestFile = fopen("press_dia_30s_A.txt", "a");
        if (pTestFile!=NULL){
            fprintf(pTestFile,"%ld
            %f                                %f
            %f                                %f
            %f\n",elapsed_time,pressure,flow_rate,average_diameter,thic
kness,hoop_stress,shear_stress);
            fclose(pTestFile);
        }

        ch = 0;

        /* Initiate measurement loop */

        while(1){
            time(&current_time);
            elapsed_time = current_time-initial_time;

            // Diameter measurement occurs when
            DATA_INTERVAL seconds have elapsed
            if((current_time-
previous_time)>=DATA_INTERVAL){
                time(&previous_time);

                average_diameter = 0;
                for (i=0;i<REPEAT;i++){
                    average_diameter = average_diameter
+ diameter()*diameter_factor/(float)REPEAT;
                }

                pressure=output_voltage(channel)*100;

                thickness=0.5*(average_diameter-
sqrt(pow(average_diameter,2)-
4*no_load_length*no_load_thickness*(no_load_dia-
no_load_thickness)/length));

                hoop_stress=pressure*0.1333224*(average_diameter-
2*thickness)/(2*thickness);

                shear_stress=2.66667*flow_rate/(3.14159265*pow((average_dia
meter/2-thickness),3));

                printf("t (s)=%ld                                P (mmHg)=%f
                Q (ml/min)=%f\n",elapsed_time,pressure,flow_rate);
                printf("d (mm)=%f                                h
(mm)=%f\n",average_diameter,thickness);

```

```

        printf("hoop (kPa)=%f    shear
(dyn/cm2)=%f\n\n",hoop_stress,shear_stress);

        pTestFile = fopen("press_dia_30s_A.txt", "a");
        if (pTestFile!=NULL){
            fprintf(pTestFile,"%ld
%f          %f          %f          %f
%f\n",elapsed_time,pressure,flow_rate,average_diameter,thic
kness,hoop_stress,shear_stress);
            fclose(pTestFile);
        }

        if(kbhit()){
            printf("\n\n\n\nPROGRAM PAUSED\nEnter 1 to
adjust flow rate or 2 to exit: ");
            scanf("%d",&ch);
            if(ch==1){
                printf("Enter New Flow Rate
(ml/min): ");

                scanf("%f",&flow_rate);
                printf("\nPROGRAM RESUMED\n\n\n\n");
            }
            if(ch==2){
                break;
            }
        }
    }

    /*****
    /* diameter() returns average diameter in pixels
    */
    /*****/

float diameter()

{
    OLT_IMG_DEV_ID                DevId;
    OLT_FG_FRAME_ID              FrameId;
    HWND                          hWnd,
hChild1, hChild2;
    USHORT                        old;

    //to be used with line containing function =
    OlFgSetInputVideoSource
        DWORD
        Count = 0;
        OLT_SCALE_PARAM                scale;
        ULONG
        Timeout;
        BYTE*
        pColumnPixelBuffer;
        BYTE*
        pRowPixelBuffer;

```

```

FILE*
pTestFile;

scale.hscale = SCALE_X;
scale.vscale = SCALE_Y;

int i=0;
int j=0;
int k=0;
int status;
int count;
int m=1;      /* loop index; m is a counter */
int upper_max_square(ITERATION);
int lower_max_square(ITERATION);
int a(Y_DIM);      /* array to hold pixel values for
columns */
int b(X_DIM);      /* array to hold pixel values
for rows */
int dia_pixels =0;
int upper_bound=0;
int lower_bound=0;
int sum_dia=0;
char      framegrabber(20);
long      sum_pixels=0;
float     avg_pixels=0;
float
background_value=0,foreground_value=0,threshold=0;
float     avg_dia;

// create user buffers for pixel data
pColumnPixelBuffer = new BYTE(1*ROW);
pRowPixelBuffer = new BYTE(COLUMN*1);

//initial buffers to hold pixel data
for (i=0; i<Y_DIM; ++i){
    pColumnPixelBuffer(i)=0;
}

for (i=0; i<X_DIM; ++i){
    pRowPixelBuffer(i)=0;
}

// Display image in window prior to measuring diameter

DT_TRY(OLImgOpenDevice("Framegrabber-2",&DevId));
DT_TRY(OLImgSetTimeoutPeriod(DevId,10,&Timeout));

// Allocate one frame
DT_TRY(OLFgAllocateBuiltInFrame(DevId, OLC_FG_DEV_MEM_VOLATILE,
OLC_FG_NEXT_FRAME,&FrameId))
DT_TRY(DtColorHardwareScaling(DevId,0,OLC_WRITE_CONTROL,&scale))

MSG                                msg;
OLT_SIGNAL_TYPE                    signal;
signal =
OLC_COMPOSITE_SIGNAL;

```

```

DT_TRY(DtColorSignalType(DevId, 0, OLC_WRITE_CONTROL,
&signal));

DT_TRY(OlFgAcquireFrameToDevice(DevId,FrameId));
OlFgSetInputVideoSource(DevId,0,&old);

// Determine threshold value for background & foreground
measurements

//Avg Background Value for a Row in Upper Portion of Frame
DT_TRY(OlFgReadFrameRect(DevId,FrameId,0,UPPER_BACKGROUND_R
OW,COLUMN,1,pRowPixelBuffer,COLUMN*1));

for (i=0;i<COLUMN;++i){
    avg_pixels = avg_pixels + (float)
pRowPixelBuffer(i)/COLUMN;
}

background_value = avg_pixels;
avg_pixels = 0;

//Avg Background Value for a Row in Lower Portion of Frame
DT_TRY(OlFgReadFrameRect(DevId,FrameId,0,LOWER_BACKGROUND_R
OW,COLUMN,1,pRowPixelBuffer,COLUMN*1));

for (i=0;i<COLUMN;++i){
    avg_pixels = avg_pixels + (float)
pRowPixelBuffer(i)/COLUMN;
}

background_value = (background_value + avg_pixels)/2;
avg_pixels = 0;

//Avg Foreground Value for a Row in Middle Portion of Frame
DT_TRY(OlFgReadFrameRect(DevId,FrameId,0,MIDDLE_FOREGROUND_
ROW,COLUMN,1,pRowPixelBuffer,COLUMN*1));

for (i=0;i<COLUMN;++i){
    avg_pixels = avg_pixels + (float)
pRowPixelBuffer(i)/COLUMN;
}

foreground_value = avg_pixels;
avg_pixels = 0;
threshold = background_value - (background_value-
foreground_value)/4;

//Obtain pixel values and calculate diameters
for (i=0;i<ITERATION;++i){

DT_TRY(OlFgReadFrameRect(DevId,FrameId,m,ROW_START,1,ROW,pC
olumnPixelBuffer,COLUMN*1));

for (j=0; j<ROW; j++){

```

```

        if
        (pColumnPixelBuffer(j)<=threshold){
            dia_pixels++;
        }
    }

    sum_dia = sum_dia+dia_pixels;
    dia_pixels = 0;
    m=m + INCREMENT;
}

avg_dia = ((float) sum_dia)/(1.0*ITERATION);

// Delete the user buffer
free(pColumnPixelBuffer);
free(pRowPixelBuffer);

DT_TRY(OLImgCloseDevice(DevId));

return avg_dia;
}

/*****
/* is_enter returns a 1 if the keyboard hit is a carriage return, 0
/* otherwise
*****/

int is_enter()
{
    char a = 0;
    a = getch();
    if (a == 13){
        return(1);
    }
    else {
        return(0);
    }
}

/*****
/* image() continuously acquires a frame & displays it in a window
/* until keyboard is hit
*****/

void image()
{
    OLT_IMG_DEV_ID          DevId;
    OLT_FG_FRAME_ID        FrameId;
    HWND                    hWnd,
    hChild1, hChild2;
    USHORT
    old;                    //to be used with line containing
    function = OlFgSetInputVideoSource
    OLT_SCALE_PARAM        scale;
    ULONG
    Timeout;

```

```

int      i=0;
        int j=0;
        int k=0;
        char a=0;
        scale.hscale = SCALE_X;
        scale.vscale = SCALE_Y;

// Display image in window prior to measuring diameter
DT_TRY(OLImgOpenDevice("Framegrabber-2",&DevId));
DT_TRY(OLImgSetTimeoutPeriod(DevId,10,&Timeout));

// Allocate one frame
DT_TRY(OLFgAllocateBuiltInFrame(DevId, OLC_FG_DEV_MEM_VOLATILE,
OLC_FG_NEXT_FRAME,&FrameId))
DT_TRY(DtColorHardwareScaling(DevId,0,OLC_WRITE_CONTROL,&scale))

// Create a window to display the result
hWnd = CreateParentWindow(X,Y,1300,600);
hChild1 =
CreateChildWindow(hWnd,10,10,CHILD_WIDTH,CHILD_HEIGHT);
hChild2 = CreateChildWindow(hWnd,CHILD_WIDTH +
20,10,CHILD_WIDTH,CHILD_HEIGHT);

MSG      msg;
OLT_SIGNAL_TYPE      signal;

DT_TRY(DtColorSignalType(DevId, 0, OLC_WRITE_CONTROL,
&signal));

while(1)
{
// Acquire one frame for hChild1 window
DT_TRY(OLFgAcquireFrameToDevice(DevId,FrameId));

// Display the whole frame
DT_TRY(OLFgDrawAcquiredFrame(DevId,hChild1,FrameId));
OLFgSetInputVideoSource(DevId,0,&old);

// Acquire one frame for hChild2 window
DT_TRY(OLFgAcquireFrameToDevice(DevId,FrameId));
// Display the whole frame
DT_TRY(OLFgDrawAcquiredFrame(DevId,hChild2,FrameId));
OLFgSetInputVideoSource(DevId,0,&old);

if(kbhit()){
a=getch();
break;
}
}

if (PeekMessage(&msg, hWnd, 0,0,PM_REMOVE))
{

```

```

        TranslateMessage(&msg);
    }

    DT_TRY(01ImgCloseDevice(DevId));
    DestroyWindow(hWnd);
}

/*****
/* diameter_calibration() performs diameter calibration on a diameter
/* standard and returns the calibration factor in units of mm/pixel
*****/

float diameter_calibration()
{
    char a=0;
    char camera(3),exp(100);
    int i,j=1,e,status,known_factor;
    float dia = 0.0;
    float sum_dia,avg_dia,DIAMETER_STANDARD;
    float diameter_factor = 0.0;
    FILE* pTestFile;

    system("cls");

    printf("Position camera to perform diameter
calibration.\n");
    printf("Strike any key when ready.\n\n");

    image(); /* acquire an image */

    printf("Enter Experiment #/Date: ");
    scanf("%s",&exp);
    printf("Enter the camera you are using (1A/2A): ");
    scanf("%s",&camera);
    printf("Do you know calibration factor (Enter 1 if yes, 2
if no): ");
    scanf("%d",&known_factor);

    if (known_factor == 1){
        printf("Enter calibration factor (mm/pixel):
");
        scanf("%f",&diameter_factor);

        pTestFile = fopen("press_dia_30s_A.txt", "a");

        fprintf(pTestFile,"\n\nExperiment #: %s\n",exp);
        fprintf(pTestFile,"Camera: %s\n",camera);
        fclose(pTestFile);

        system("cls");
        return(diameter_factor);
    }

    printf("Enter the diameter of the standard used for
calibration (mm): ");
    scanf("%f",&DIAMETER_STANDARD);

```



```

pTestFile = fopen("press_dia_30s_A.txt", "a");
fprintf(pTestFile, "\n\nExperiment #: %s\n", exp);
fprintf(pTestFile, "Camera: %s\n", camera);
fprintf(pTestFile, "diameter of calibration standard (mm):
%f\n", DIAMETER_STANDARD);

do{
    sum_dia = 0.0;
    for(i=0;i<REPEAT;i++){
        dia = diameter();
        sum_dia = sum_dia + dia;
    }
    avg_dia = sum_dia/(float)REPEAT;
    printf("\nAverage diameter (pixels):
%f\n", avg_dia);
    diameter_factor =
DIAMETER_STANDARD/(sum_dia/(float)REPEAT);
    printf("Diameter factor (mm/pixel):
%f\n\n", diameter_factor);
    printf("Hit enter to accept, any other key to
redo the calibration.\n");
    }while(!is_enter());

    fprintf(pTestFile, "Average diameter (pixels):
%f\n", avg_dia);
    fclose(pTestFile);

    system("cls");
    return(diameter_factor);
}

/*****
/* output_voltage returns the voltage measured on the data acquisition
/* boardfor the specified channel

*****/

float output_voltage(int channel)
{
    DBL          min,max;
    float        volts;
    long         value;
    UINT         encoding,resolution;
    DBL          gain = 1.0;

    /* Get first available Open Layers board */

    board.hdrv = NULL;
    oldaEnumBoards(GetDriver, (LPARAM) (LPBOARD)&board);

    /* get handle to A/D sub system */

    oldaGetDASS(board.hdrv, OLSS_AD, 0, &board.hdass);

    /* set subsystem for single value operation */

```

```

    oldDaSetDataFlow(board.hdass,OL_DF_SINGLEVALUE);

    // Added Set Channel Type & Set Range to the next 2 lines
    oldDaSetChannelType(board.hdass,OL_CHNT_DIFFERENTIAL);
    oldDaSetRange(board.hdass,10,0);
    oldDaConfig(board.hdass);

    /* get single value */
    oldDaGetSingleValue(board.hdass,&value,channel,gain);

    /* get sub system information for code/volts conversion */
    oldDaGetRange(board.hdass,&max,&min);
    oldDaGetEncoding(board.hdass,&encoding);
    oldDaGetResolution(board.hdass,&resolution);

    /* convert value to volts */

    if (encoding != OL_ENC_BINARY) {
        /* convert to offset binary by inverting the sign bit */

        value ^= 1L << (resolution-1);
        value &= (1L << resolution) - 1;      /* zero upper bits */
    }

    volts = ((float)max-(float)min)/(1L<<resolution) * value +
(float)min;

    /* release the subsystem and the board */

    oldDaReleaseDASS(board.hdass);
    oldDaTerminate(board.hdrv);

    return(volts);
}

HWND CreateParentWindow(DWORD x, DWORD y, DWORD w, DWORD h)
{
    HWND          NewWindow = 0;
    WNDCLASS      wc        = (0);
    DWORD          Error;

    wc.style          = CS_VREDRAW | CS_VREDRAW;
    wc.lpfnWndProc    = DefWindowProc;
    wc.cbClsExtra     = 0;
    wc.cbWndExtra     = 0;
    wc.hInstance      = 0;
    wc.hIcon          = 0;
    wc.hCursor        = 0;
    wc.hbrBackground  = (HBRUSH) (COLOR_WINDOW + 1);
    wc.lpszMenuName   = NULL;
    wc.lpszClassName  = "DEFAULT_WINDOW";

    Error = RegisterClass(&wc);    // may fail if class already exists.

```

```

Error = GetLastError();

NewWindow = CreateWindow(
                                "DEFAULT_WINDOW",
                                // Default class
                                "Driver default
window", // title
                                WS_SYSMENU|WS_OVERLAPPED, // style
                                x, y,
                                // x, y position
                                w, h,
                                // size
                                NULL,
                                // No Parent
                                NULL,
                                // menu
                                NULL,
                                NULL);

Error = GetLastError();
ShowWindow(NewWindow, SW_SHOWDEFAULT);

return NewWindow;
}

HWND CreateChildWindow(HWND Parent, DWORD x, DWORD y, DWORD w, DWORD h)
{
    HWND NewWindow = 0;
    DWORD Error;

    NewWindow = CreateWindow(
                                "DEFAULT_WINDOW",
                                // Default class
                                "Driver default
window", // title
                                WS_CHILD,
                                // style
                                x, y,
                                // x, y position
                                w, h,
                                // size
                                Parent,
                                // No Parent
                                NULL,
                                // menu
                                NULL,
                                NULL);

    Error = GetLastError();
    ShowWindow(NewWindow, SW_SHOWDEFAULT);

    return NewWindow;
}

```

```
LRESULT CALLBACK _export MyWindowProc(HWND hWnd,UINT Msg,WPARAM  
wParam,LPARAM lParam)  
{  
    return DefWindowProc(hWnd, Msg, wParam, lParam);  
}
```

## **APPENDIX B**

### **PROTOCOLS FOR BIOLOGICAL ENDPOINTS**

## **B.1 MTT Protocol**

*(Adapted from protocol of Hai-Chao Han)*

### Products

MTT: Sigma # M5655

1. Make solution of 1 mg/ml solution of MTT in PBS (need 0.5 ml per segment).
2. Place 0.5 ml of MTT solution in 1.5 ml Eppendorf tubes.
3. Remove excess connective tissue from artery.
4. Cut approximately 5 mm segment and place in solution.
5. Incubate segment 37 °C for 1 – 2 hours.
6. Take pictures of the segments.

## **B.2 H & E Stain Protocol**

*(Adapted from protocol of Tracey Couse)*

Prior to staining, tissue samples should be fixed overnight in 10% neutral buffered formalin (Fisher SF100-4) and placed in 70% alcohol for long-term storage. Samples should then be embedded in paraffin, then cut into 5 mm sections and placed on microscope slides (SuperFrost Plus slides, available in IBB Histology Lab).

Note: The deparaffinization and staining procedure can be completed using the Autostainer in the IBB Histology Lab.

1. Deparaffinize and rehydrate to distilled water using the following schedule:  
Xylene x 3 for 3 minutes each.  
100% alcohol x 3 for 2 minutes each.  
95% alcohol x 2 for 2 minutes each.  
75% alcohol x 1 for 2 minutes.
2. Rinse in distilled water for 2 minutes.
3. Stain in hematoxylin for 0.5-1 minute.
4. Rinse in water until excess dye is removed.
5. Differentiate in 0.5% acid alcohol (0.5% HCl in 70% alcohol) for 1 dip.
6. Quickly transfer to water and rinse for 1 minute.
7. Blue slides in Scott's tap water for 30 seconds.
8. Rinse in water for 1 minute.
9. Immerse in 95% alcohol for 1 minute.

10. Stain in 1% alcoholic eosin for 30 seconds.
11. Rinse in 95% alcohol for 30 second.
12. Dehydrate in 100% alcohol x 3 for 1 minute each.
13. Clear in xylene x 3 for 1 minute each.
14. Coverslip and mount in permanent mounting medium.

Results:

Nuclei\_\_\_\_\_

\_\_\_\_\_blue-purple

Connective tissue elements\_\_\_\_\_various shades of pink

Notes:

Avoid drying of sections.

If progressive method of staining is used then skip step #5.

If using the regressive method of stain, and over differentiation of the nuclei results after checking the sections at step #8, return the slides to hematoxylin and repeat.

If using the regressive method of stain, and under differentiation of the nuclei results after checking the sections at step #8, return the slides to acid alcohol and proceed.

### B.3 <sup>3</sup>H-Proline Incorporation

(Adapted from protocols of Dr. Levenston and Dr. Yoganathan's Lab)

Materials: <sup>3</sup>H-proline (L-(5-<sup>3</sup>H)Proline; Amersham Biosciences, #TRK323)

1. Autoclave all instruments, chambers, etc. as you would for a typical experiment. Prepare the amount of culture media required for the experiment + at least 2 mL extra. This media should come from the medium reservoir for each artery.
2. When handling radioactive materials, always wear a lab coat and plastic gloves. It is a good idea to remove your watch and any jewelry from your hands. Tape the sleeves of your labcoat tight around your wrists. Always hold radioactive materials away from your body. Clear your workspace of any unnecessary clutter. Liquid radioactive materials must always be handled in a tray/bin with absorbent paper that will contain any spills. When at all possible, pre-set your pipettor before beginning to handle the radiolabel.
3. Compute the total amount of radiolabeled culture medium required. Add 2 mL to this total and set aside (if you prepared more in Step 1).
4. Compute the present concentration of your radiolabel.

<sup>3</sup>H-proline: The half-life of <sup>3</sup>H-proline is about 23.5 years, so in a year there is only about a 5% loss of radioactivity. If the calibration date is within the last year, you don't need to bother recalculating the activity (the error is probably equivalent to your experimental error). If the stock is very old then calculate the stock as follows:

$$C = C_{calibrated} * 0.5^{x/23.5}$$

where  $C$  is the actual concentration of <sup>3</sup>H-proline in mCi/mL,  $C_{calibrated}$  is the calibrated concentration in mCi/mL, and  $x$  is the amount of time expired (in years) since the calibration date.

5. <sup>3</sup>H-proline Labeling: Add enough <sup>3</sup>H-proline to the culture medium to bring the total concentration to 10 µCi/mL of culture medium.

*Example:* To label 30 mL of medium, we need 300 µCi of <sup>3</sup>H-proline. For a stock solution at 1mCi/mL, we need 300 µL of <sup>3</sup>H-proline.

- a) Loosen the cap on the container with your medium.
- b) Uncap the vial containing the <sup>3</sup>H-proline. Using an aerosol-filtered pipettor tip, carefully remove the appropriate volume and add it to your medium. Cap the source vial and the medium container. Dispose of the radioactive pipette tip.



- c) Mix the medium by gently shaking/stirring it (make sure that the top is secured first).
  - d) Transfer 1 ml of the dual-labeled medium to a labeled cryovial. Dispose of the pipette tip (or retain it for adding medium to the bioreactors).
6. Load the tissue culture well plate with the artery segment and medium as you normally would. Be careful not to drip radioactive medium or contaminate anything with the pipette tip. If contamination occurs, wipe the area with an alcohol swab and dispose of it as radioactive waste.
  7. *Clean up*: Wipe your work area and perform a wipe test to ensure no contamination is present. Decontaminate any hot areas (subject to ALARA). Dispose of any solid wastes in the solid radioactive wastes container. Dispose of any liquid medium as liquid radioactive wastes.
  8. Fill in the inventory sheet with the amount of radiolabel removed and all other info. Fill in the disposal sheets on solid/liquid waste containers with the appropriate amount of radiolabel removed.

#### Radiolabeling Protocol (following culture)

Materials: Scintillation Fluid (Ecolume, ICN Biomedical, #882470)

- 1) Wash sample with sulfate solution (see sulfate solution protocol) 4 times, each for 30 mins at 4 °C
- 2) Collect spent media and washing liquid, clean the yellow tray, the metal tray and the forceps with ethanol 4 times
- 3) After washing, put samples in small vials (weight the vials before putting samples in). Put vials in lyophilizer to dry the tissue (usu. 2 days)
- 4) Weight the vials to get the dry weight of tissue
- 5) Digest tissue with Proteinase K (see protocol) for overnight at 55 °C
- 6) After digestion, do scintillation counting as follows:
  - a) 100 µl sample + 2 ml ecolume for each scintillation vial (make 2 duplicates for each sample)
  - b) Do the same with the sample media (1X, 2X, 4X, 8X, 16X, 2 duplicates for each)
  - c) Vortex
  - d) Put scintillation vials in small glass bottles and do scintillation counting in Room 1420
- 7) Normalize results using dry tissue weight

### Sulfate Solution

Materials: Sodium Sulfate (Sigma S-2804)  
L-Proline (Sigma P-0380)  
PBS without  $\text{Ca}^{2+}$  and  $\text{Mg}^{2+}$  (Sigma D-1408)

To 1 L of PBS, add:  
113.6 mg of Sodium Sulfate  
115 mg of L-proline

Adjust pH to 7.4.  
Store at 4 °C

### Proteinase K Digestion

*(Adapted from protocol of Janna Mouw in Dr. Marc Levenston's Lab)*

Materials: Proteinase K  
Ammonium Acetate (Sigma A-2706)

1. Read through this entire protocol before starting. Make up the entire amount of Ammonium Acetate buffer (pH 7.0). (Rule of thumb: 1 mg Proteinase K can digest 80 mg of tissue) The amount of Ammonium Acetate buffer may need to be increased due to the small amount of Proteinase K that will need to be added (and thus hard to measure).
2. Add Proteinase K to the Ammonium Acetate buffer and mix. (This amount may need to be changed according to the size of your sample, following the *rule of thumb*.)
3. Activate solution by heating it up to 60 °C for 10 minutes.
4. Add 1 ml of solution to a 10 mg wet weight (or less) sample of tissue.
5. Digest at 60 °C for 18-24 hours, periodically vortexing samples.
6. The enzyme is inactivated by heating the samples at 100 °C for 5 minutes.
7. Undigested tissue debris is removed by centrifugation (15,000 X g, 10 minutes, room temperature).

#### **B.4 Tissue Homogenization**

1. Place frozen tissue samples (stored in 1.5 ml Eppendorf tubes) in ice chest.
2. Place tissue sample in plastic vial (Wheaton Omni-Vial) with 500  $\mu$ l of cold lysis buffer (see protocol).
3. Homogenize tissue in 500  $\mu$ l of lysis buffer (see below) using IKA Ultra Turrax T25 homogenizer. (Rinse homogenizer with DI before first use)
4. Store vial on ice while homogenizing other samples.
5. Rinse homogenizer after each use by turning homogenizer on in DI water.
6. Using a 1000  $\mu$ l pipettor (with tip cut off), transfer homogenate to 1.5 ml tubes.
7. Centrifuge for 10 minutes @ 10,000 RPM in a low-temperature centrifuge.

#### Lysis Buffer Formulation for Tissue Homogenization (Ivan et al, Circulation, 2002)

10 mM Sodium Phosphate, pH 7.2 (FW 163.94)  
150 mM NaCl (MW 58.44)  
1% Triton X-100  
0.1% SDS (1 mg/ml)  
0.5% Sodium Deoxycholate (5 mg/ml)  
0.2% Sodium Azide (2 mg/ml)

## B.5 MMP Zymography Protocol

*(Adapted from protocol used in the lab of Dr. Jo)*

### Renaturing Buffer

For 100 ml:  
2.5% Triton X-100

### Assay Buffer

For 50 ml:  
50 mM Tris-HCl, pH 7.4  
10 mM CaCl<sub>2</sub>  
50 mM NaCl  
0.05% Triton X-100

### Non-reducing SDS-PAGE (10%) – Makes 4 – 0.75 mm gels

4.66 ml of 3 mg/ml gelatin in DI water  
(Final Conc. – 1 mg/ml; Heat DI to dissolve gelatin in stock solution)  
3.06 ml of DI H<sub>2</sub>O  
5.33 ml of protogel  
3.2 ml of separating buffer  
800 µl of 1.5% ammonium persulfate  
160 µl of 10% SDS  
15 µl of TEMED

1. Make 10% polyacrylamide gels with 1 mg/ml gelatin in 0.75 mm plates (see protocol for making gels)
2. Cool running buffer (can be purchased from Bio-Rad) to 4 °C
3. Add samples at equal concentrations using the protocol for preparing SDS-PAGE gels
4. Let gels run in cold room at 80 mV for about 2 hours
5. Wash gels 2 X 15 minutes each with renaturing buffer at room temperature
6. Incubate overnight at 37 °C in assay buffer
7. Wash with DI H<sub>2</sub>O for 10 minutes
8. Stain at room temperature with Coomassie stain until signal is bands are apparent (approximately 1 hour)
9. Destain 2 X 15 minutes each
10. Place gels in a sheet protector and scan
11. Analyze image intensity of lysis band using Scion Image

***If considering doing Western Blots, a good primer is available online at  
[www.abcam.com/ps/pdf/protocols/WB-beginner.pdf](http://www.abcam.com/ps/pdf/protocols/WB-beginner.pdf)***

## B.6 Solutions for MMP Assay

*(Adapted from protocol used in the lab of Dr. Jo)*

### 5X Buffer Formulation

(Kleiner & Stettler-Stevenson)

For 10 ml:

8 ml	0.5 M Tris, pH 6.8
2 ml	Glycerol
3 mg	Bromophenol Blue
500 mg	SDS

### 5X Separating Buffer

pH 8.9

113.3 g Tris base

500 ml DI H<sub>2</sub>O

### Coomassie Stain

Total volume – 10 L (probably only need to make 1 L at a time)

6.5 L DI H<sub>2</sub>O

1L Acetic Acid

2.5 L Isopropanol

4.5 g Coomassie Blue R250

### Destain Solution

Total volume – 10 L (probably need to make 1 L at a time)

6.5 L DI H<sub>2</sub>O

1L Acetic Acid

2.5 L Isopropanol

## B.7 Protocol for making SDS-PAGE Gels

*(Adapted from protocol used in the lab of Dr. Jo)*

Note: Be sure to wear gloves  
This protocol requires that you already have protein samples (using tissue homogenization protocol) and have done a protein assay to determine protein concentration.  
Protocol uses Bio-Rad electrophoresis system.

1. Get clear gel stand (each stand allows for two gels)
2. Get green gel holders (one for each gel)
3. Get glass plates with edges that appear green when viewed from the side. Use one flat plate and one “spacer” plate per gel. (0.75 mm plates are used for MMP zymography; 1.5 mm plates are used for Western Blots)
4. Clean all plates with ethanol and dry with Kimwipes
5. Insert flat plate and spacer plate into green gel holder with the spacer plate behind the flat plate. The “feet” of the green gel holder should be facing you. Secure clamps.
6. Insert holders with plates into each stand on the gray pad and secure; make sure they are level
7. Fill each side with DI H<sub>2</sub>O to check for leaks; dry after couple of seconds if no leaks (plates do not need to be completely dry)
8. Get two 50 ml beakers. Use one of the beakers to make separating gel; combine ingredients according the protocol. Be sure to add TEMED last. Right after adding TEMED, swirl contents gently to mix for a couple of seconds. Quickly inject separating gel solution in between glass plates using 1000 µl pipet. Fill the gel setup to approximately the level of the of the green gel holder seen through the glass plates. Add about 200 µl of 1-butanol to remove bubbles and even gel surface. Allow gel to harden for at least 15 minutes.
9. Wash out each set of glass plates with DI H<sub>2</sub>O. Dry gently using flat edge of paper towel.
10. Make stacking gel in second 50 ml beaker. Add TEMED last. Swirl contents gently to mix for a couple of seconds.
11. Using 1000 µl pipet, add approximately 2 ml of stacking gel solution to each gel. Slowly push combs (10 columns; 0.75 mm thick for MMP zymography, 1.5 mm thick for western blot) down completely in between glass plates. Wipe excess stacking gel solution with Kimwipes. Make sure there are as few bubbles as possible to ensure the best possible gel columns. Allow gel to harden for at least 15 minutes.
12. Gently pull combs out; rinse away bubbles with running buffer. If using 1.5 mm plates, suction out running buffer and air bubbles using small pipet tip attached to vacuum.

13. Put each “gel rack” (gel and both glass plates surrounding it) in beige holder with gold rods and green seal. Make sure that the side with the higher glass plate faces outside and the side with the shorter glass plate faces the inside of the beige holder. Place a gel rack on each side of the beige holder. If only using one gel, then insert the clear plastic “dummy” gel on the other side of the beige holder. Insert beige holder inside beige housing unit and close clear tightening flaps until they snap shut. Put the holder/housing unit into clear rectangular transfer tanks (the ones with the removable green top with red/black wires).
14. Pour Running Buffer into middle of gel holder (in between “gel racks”) so that it overflows the lower glass panels. Fill the rest of the tank with Running Buffer to the level of the buffer inside the gel holder.
15. Get protein samples and put them in an ice bucket. You should already have protein assay information telling you how much sample and 5X sample buffer to add to each lane.
16. Get as many empty 1.5 ml centrifuge tubes as you have samples. Label each tube with the corresponding label as found on each sample.
17. Add the required amount of 5X sample buffer to each of the new tubes and then the required amount of sample (according to the results of the protein assay).
18. Add 10 ml of Molecular Weight marker to the leftmost lane.
19. Add required amount of sample to each lane left to right; try not to inject bubbles. Use careful pipetting techniques.
20. Add an equal amount of 5X sample buffer (according to the results of the protein assay).
21. Put on green lid with red-black connections. Connect red to red and black to black.
22. Move tank to cold room.

## B.8 Protocol for Protein Assay

*(Adapted from protocol used in the lab of Dr. Jo)*

### 1. Equipment

- a. Plastic tubes that will hold at least 8 ml
  - i. 6 for standard curve
  - ii. x for number of samples (2x if duplicates, recommended)
- b. 1 mg/ml BSA standard
- c. 96-well plate
- d. Spectrophotometer

### 2. Standard curve

- a. Mark tubes 0, 5, 10, 25, 50, 75
- b. Add 0 (this is your blank), 5, 10, 25, 50, or 75  $\mu\text{l}$  of BSA standard to the corresponding tubes
- c. Add 8  $\mu\text{l}$  of lysis buffer to each standard tube
- d. Add DI  $\text{H}_2\text{O}$  to standard tubes according to table below
- e. Each standard tube should have a total volume 100  $\mu\text{l}$

Standard Tube ( $\mu\text{l}$ BSA)	Sample Buffer ( $\mu\text{l}$ )	DI $\text{H}_2\text{O}$ ( $\mu\text{l}$ )
0 (Blank)	8	92
5	8	87
10	8	82
25	8	67
50	8	42
75	8	17

### 3. Standard curve

- a. Mark sample tubes to identify them with your sample
- b. Add 8 ml of sample to each tube
- c. Add 92 ml of DI  $\text{H}_2\text{O}$  to each sample tube
- d. Each sample tube should have a total volume 100  $\mu\text{l}$

### 4. Addition of Reagents A and B (available from Bio-Rad)

- a. To all tubes (standards and samples) add 500  $\mu\text{l}$  of Reagent A
- b. To all tubes add 4 ml of Reagent B and vortex

### 5. Reading samples

- a. Add 300  $\mu\text{l}$  of each tube to a well of a 96-well plate (use duplicates)
- b. Read absorbance of samples using plate reader at a wavelength of 750 nm
- c. Use a linear regression to relate the absorbance and protein amount for the standards
- d. Using the linear regression, determine the amount of protein in the samples



## B.9 BrdU Stain Protocol

*(Adapted from the protocol of Hai-Chao Han)*

Materials: BrdU Kit (Molecular Probes, product # 1 296 736)

Note: Use 5 µm sections mounted & dried on Superfrost Plus microscope slides.

1. Deparaffinize sections using Autostainer in the Histology lab.
2. Boil slides using the HIER protocol.
3. Permeabilize sections by covering sections with ~ 100 ml of 0.5% Triton X-100 for 30 min at 37 °C.
4. Wash in PBS for 5 min.
5. Cover sections in BSA solution (1% BSA in PBS) for 5 min at room temp. Drain & wipe the blank on the slide leave a square with the sections untouched.
6. 1° (primary) antibody  
Dilute 1:10 (antibody:buffer) in incubation buffer (included in kit)  
Use ~100 ml/section, incubate in humidified chamber for 30 min at 37 °C.
7. Wash in 2X in PBS for 5 min each time.
8. 2° (secondary) antibody  
Dilute 1:10 (antibody:buffer) in incubation buffer (included in kit)  
Use ~100 ml/section, incubate in humidified chamber for 30 min at 37 °C.
9. Wash in PBS for 5 min.
10. Place slides in DAPI solution (0.25 µg/ml) in PBS by placing slide rack in staining dish. Incubate for 5 min at room temp in the dark (DAPI is light sensitive/DAPI is available in the histology lab).
11. Wash in PBS for 5 min.
12. Coverslip using Gel/Mount.

## **B.10 DAPI Stain Protocol**

*(Adapted from protocol used of Tracey Couse)*

Note: Use this protocol to counterstain EthD sections.

1. Deparaffinize sections using Autostainer in the Histology lab.
2. Place slides in DAPI solution (0.25 µg/ml) in PBS by placing slide rack in staining dish. Incubate for 5 min at room temp in the dark (DAPI is light sensitive/DAPI is available in the histology lab).
3. Wash in PBS for 5 min.
4. Coverslip using Gel/Mount.

## **B.11 HIER Protocol using Princess Electric Pressure Cooker and Citrate Buffer**

*(Adapted from protocol of Tracey Couse)*

Note: HIER – Heat Induced Epitope Retrieval

1. Plug the pressure cooker base into an outlet.
2. Remove the lid from the pressure cooker pot. Ensure the steel rack resting the pot is prong side up.
3. Add about 2 staining dishes worth of water to the pot (about 400 ml).
4. Fill the staining dish with 200 ml of 10 mM citrate buffer, pH 6.0 (see below). Add slide rack containing slides and cover with staining dish lid.
5. Place slides and staining dish into the pressure cooker pot. Lock the pressure cooker lid in place atop pressure cooker. Be sure that the vent (rapid release) is in the closed position (up position).
6. Set the pressure mode to high by pressing the “Pressure Mode” button twice.
7. Set the time for 15 minutes by using the “up” arrow. Press the start button.
8. The time will begin once the pot reaches the correct pressure and temperature (this takes ~ 10 min)
9. When the timer reaches zero, push the “off” button.
10. After waiting 5 minutes, push the “Rapid Release” tap to the down position. This releases the pressure within the pot. The red pin will descend once all the pressure has been released. The lid can now be removed.
11. Let slides cool to room temperature for 20 minutes.
12. Transfer slide rack to PBS and proceed with the IHC protocol.

For 200 ml Citrate Buffer, add:

3.6 ml of Solution A  
16.4 ml of Solution B  
180 ml of DI H<sub>2</sub>O

Note: Solutions A & B (and their formulations) are available in the histology lab.

## REFERENCES

- Alberts, B., D. Bray, J. Lewis, M. Raff, K. Roberts and J. D. Watson (1994). *Molecular biology of the cell*. New York, Garland Publishing.
- Bakker, E. N., E. T. van Der Meulen, J. A. Spaan and E. VanBavel (2000). Organoid culture of cannulated rat resistance arteries: effect of serum factors on vasoactivity and remodeling. *Am J Physiol* 278(4): H1233-40.
- Bardy, N., R. Merval, J. Benessiano, J. L. Samuel and A. Tedgui (1996). Pressure and angiotensin II synergistically induce aortic fibronectin expression in organ culture model of rabbit aorta. Evidence for a pressure-induced tissue renin-angiotensin system. *Circ Res* 79(1): 70-8.
- Bayliss, W. M. (1902). On the local reactions of the arterial wall to changes of internal pressure. *J Physiol* 28(3): 220-231.
- Binko, J., S. Meachem and H. Majewski (1999). Endothelium removal induces iNOS in rat aorta in organ culture, leading to tissue damage. *Am J of Physiol* 276(1 Pt 1): E125-34.
- Birukov, K. G., N. Bardy, S. Lehoux, R. Merval, V. P. Shirinsky and A. Tedgui (1998). Intraluminal pressure is essential for the maintenance of smooth muscle caldesmon and filamin content in aortic organ culture. *Arterioscler Thromb Vasc Biol* 18(6): 922-7.
- Birukov, K. G., S. Lehoux, A. A. Birukova, R. Merval, V. A. Tkachuk and A. Tedgui (1997). Increased pressure induces sustained protein kinase C-independent herbimycin A-sensitive activation of extracellular signal-related kinase 1/2 in the rabbit aorta in organ culture. *Circ Res* 81(6): 895-903.
- Boonen, H. C., P. M. Schiffers, G. E. Fazzi, G. M. Janssen, M. J. Daemen and J. G. De Mey (1991). DNA synthesis in isolated arteries. Kinetics and structural consequences. *Am J Physiol* 260(1 Pt 2): H210-7.
- Brant, A. M., M. F. Teodori, R. L. Kormos and H. S. Borovetz (1987). Effect of variations in pressure and flow on the geometry of isolated canine carotid arteries. *J Biomech* 20(9): 831-8.

- Brownlee, R. D. and B. L. Langille (1991). Arterial adaptations to altered blood flow. *Can J Physiol Pharmacol* 69(7): 978-83.
- Carew, T. E., R. N. Vaishnav and D. J. Patel (1968). Compressibility of the arterial wall. *Circ Res* 23(1): 61-8.
- Chen, Y. C. and A. Hoger (2000). Constitutive functions of elastic materials in finite growth. *J Elasticity* 59(1-3): 175-193.
- Chesler, N. C., D. N. Ku and Z. S. Galis (1999). Transmural pressure induces matrix-degrading activity in porcine arteries ex vivo. *Am J Physiol* 277(5 Pt 2): H2002-9.
- Chuong, C. J. and Y. C. Fung (1984). Compressibility and constitutive equation of the arterial wall in radial compression experiments. *J Biomech* 17(1): 35-40.
- Clerin, V., R. J. Gusic, J. O'Brien, P. M. Kirshbom, R. J. Myung, J. W. Gaynor and K. J. Gooch (2002). Mechanical Environment, Donor Age, and Presence of Endothelium Interact to Modulate Porcine Artery Viability Ex Vivo. *Ann Biomed Eng* 30: 1117-1127.
- Clerin, V., J. W. Nichol, M. Petko, R. J. Myung, J. W. Gaynor and K. J. Gooch (2003). Tissue engineering of arteries by directed remodeling of intact arterial segments. *Tissue Eng* 9(3): 461-72.
- Cowin, S. C. (1996). Strain or deformation rate dependent finite growth in soft tissues. *J Biomech* 29(5): 647-9.
- Cox, R. H. (1978). Passive mechanics and connective tissue composition of canine arteries. *Am J Physiol* 234(5): H533-41.
- Davis, C., J. Fischer, K. Ley and I. J. Sarembock (2003). The role of inflammation in vascular injury and repair. *J Thromb Haemost* 1(8): 1699-709.
- Davis, N. P. (2002). Axial Stretch as a Means of Lengthening Arteries: An Investigation in Organ Culture. Georgia Institute of Technology, Ph. D. Thesis.
- Davis, N. P., H. C. Han, B. Wayman and R. Vito (2005). Sustained axial loading lengthens arteries in organ culture. *Ann Biomed Eng* 33(7): 867-77.

- De Mey, J. G., M. P. Uitendaal, H. C. Boonen, M. J. Vrijdag, M. J. Daemen and H. A. Struyker-Boudier (1989). Acute and long-term effects of tissue culture on contractile reactivity in renal arteries of the rat. *Circ Res* 65(4): 1125-35.
- Del Rizzo, D. F., M. C. Moon, J. P. Werner and P. Zahradka (2001). A novel organ culture method to study intimal hyperplasia at the site of a coronary artery bypass anastomosis. *Ann Thorac Surg* 71(4): 1273-9; discussion 1279-80.
- Durante, W., L. Liao, S. V. Reyna, K. J. Peyton and A. I. Schafer (2000). Physiological cyclic stretch directs L-arginine transport and metabolism to collagen synthesis in vascular smooth muscle. *Faseb Journal* 14(12): 1775-83.
- Earley, J. J., X. Su and R. S. Moreland (1998). Caldesmon inhibits active crossbridges in unstimulated vascular smooth muscle: an antisense oligodeoxynucleotide approach. *Circ Res* 83(6): 661-7.
- Epstein, M. and G. A. Maugin (2000). Thermomechanics of volumetric growth in uniform bodies. *Int J Plasticity* 16(7-8): 951-978.
- Fischer, G. M. and J. G. Llauro (1966). Collagen and Elastin Content in Canine Arteries Selected from Functionally Different Vascular Beds. *Circ Res* 19(2): 394-399.
- Fridez, P., A. Makino, D. Kakoi, H. Miyazaki, J. J. Meister, K. Hayashi and N. Stergiopoulos (2002). Adaptation of conduit artery vascular smooth muscle tone to induced hypertension. *Ann Biomed Eng* 30(7): 905-16.
- Fridez, P., A. Makino, H. Miyazaki, J. J. Meister, K. Hayashi and N. Stergiopoulos (2001). Short-Term biomechanical adaptation of the rat carotid to acute hypertension: contribution of smooth muscle. *Ann Biomed Eng* 29(1): 26-34.
- Fung, Y. C. (1990). *Biomechanics: Motion, Flow, Stress, and Growth*. New York, Springer.
- Galis, Z. S. and J. J. Khatri (2002). Matrix metalloproteinases in vascular remodeling and atherogenesis: the good, the bad, and the ugly. *Circ Res* 90(3): 251-62.

- Gambillara, V., C. Chambaz, G. Montorzi, S. Roy, N. Stergiopoulos and P. Silacci (2006). Plaque-prone hemodynamics impair endothelial function in pig carotid arteries. *Am J Physiol* 290(6): H2320-2328.
- Glagov, S., C. Zarins, D. P. Giddens and D. N. Ku (1988). Hemodynamics and atherosclerosis. Insights and perspectives gained from studies of human arteries. *Arch Pathol Lab Med* 112(10): 1018-31.
- Gleason, R. L., S. P. Gray, E. Wilson and J. D. Humphrey (2004). A multiaxial computer-controlled organ culture and biomechanical device for mouse carotid arteries. *J Biomech Eng* 126(6): 787-95.
- Gleason, R. L. and J. D. Humphrey (2005). Effects of a sustained extension on arterial growth and remodeling: a theoretical study. *J Biomech* 38(6): 1255-61.
- Gleason, R. L., Jr. and J. D. Humphrey (2005). A 2D constrained mixture model for arterial adaptations to large changes in flow, pressure and axial stretch. *Math Med Biol* 22(4): 347-69.
- Gleason, R. L., L. A. Taber and J. D. Humphrey (2004). A 2-D model of flow-induced alterations in the geometry, structure, and properties of carotid arteries. *J Biomech Eng* 126(3): 371-81.
- Gleason, R. L., E. Wilson and J. D. Humphrey (2007). Biaxial biomechanical adaptations of mouse carotid arteries cultured at altered axial extension. *J Biomech* 40(4): 766-76.
- Gotlieb, A. I. and P. Boden (1984). Porcine aortic organ culture: a model to study the cellular response to vascular injury. *In Vitro* 20(7): 535-42.
- Han, H. C. and D. N. Ku (1999). Contractility in arteries subjected to hypertensive pressure in 7-day organ culture. *Am J Physiol* Submitted.
- Han, H. C. and D. N. Ku (2001). Contractile responses in arteries subjected to hypertensive pressure in seven-day organ culture. *Ann Biomed Eng* 29(6): 467-75.
- Han, H. C., D. N. Ku and R. P. Vito (2003). Arterial wall adaptation under elevated longitudinal stretch in organ culture. *Ann Biomed Eng* 31: 403-411.

- Holt, C. M., S. E. Francis, S. Rogers, P. A. Gadsdon, T. Taylor, C. Clelland, A. Soyombo, A. C. Newby and G. D. Angelini (1992). Intimal proliferation in an organ culture of human internal mammary artery. *Cardiovasc Res* 26(12): 1189-94.
- Humphrey, J. (2002). *Cardiovascular solid mechanics: cells, tissues, and organs*. New York, Springer-Verlag.
- Humphrey, J. D. (1999). Remodeling of a collagenous tissue at fixed lengths. *J Biomech Eng* 121(6): 591-7.
- Jackson, Z. S., A. I. Gotlieb and B. L. Langille (2002). Wall tissue remodeling regulates longitudinal tension in arteries. *Circ Res* 90(8): 918-25.
- Kaiser, L., S. J. Hull and H. J. Sparks (1986). Methylene blue and ETYA block flow-dependent dilation in canine femoral artery. *Am J Physiol* 250: H974-981.
- Kamiya, A. and T. Togawa (1980). Adaptive regulation of wall shear stress to flow change in the canine carotid artery. *Am J Physiol* 239(1): H14-21.
- Kleiner, D. E. and W. G. Stetler-Stevenson (1994). Quantitative zymography: detection of picogram quantities of gelatinases. *Anal Biochem* 218(2): 325-9.
- Kolpakov, V., M. D. Rekhter, D. Gordon, W. H. Wang and T. J. Kulik (1995). Effect of mechanical forces on growth and matrix protein synthesis in the in vitro pulmonary artery. Analysis of the role of individual cell types. *Circ Res* 77(4): 823-31.
- Koo, E. W. and A. I. Gotlieb (1991). Neointimal formation in the porcine aortic organ culture. I. Cellular dynamics over 1 month. *Lab Invest* 64(6): 743-53.
- Labadie, R. F., J. F. Antaki, J. L. Williams, S. Katyal, J. Ligush, S. C. Watkins, S. M. Pham and H. S. Borovetz (1996). Pulsatile perfusion system for ex vivo investigation of biochemical pathways in intact vascular tissue. *Am J Physiol* 270(2 Pt 2): H760-8.
- Langille, B. L., M. P. Bendeck and F. W. Keeley (1989). Adaptations of carotid arteries of young and mature rabbits to reduced carotid blood flow. *Am J Physiol* 256(4 Pt 2): H931-9.



- Langille, B. L. and F. O'Donnell (1986). Reductions in arterial diameter produced by chronic decreases in blood flow are endothelium-dependent. *Science* 231(4736): 405-7.
- Leung, D. Y., S. Glagov and M. B. Mathews (1976). Cyclic stretching stimulates synthesis of matrix components by arterial smooth muscle cells in vitro. *Science* 191(4226): 475-7.
- Ligush, J., Jr., R. F. Labadie, S. A. Berceci, J. B. Ochoa and H. S. Borovetz (1992). Evaluation of endothelium-derived nitric oxide mediated vasodilation utilizing ex vivo perfusion of an intact vessel. *J Surg Res* 52(5): 416-21.
- Lindqvist, A., B. O. Nilsson and P. Hellstrand (1997). Inhibition of calcium entry preserves contractility of arterial smooth muscle in culture. *J Vasc Res* 34(2): 103-8.
- Lindqvist, A., I. Nordstrom, U. Malmqvist, P. Nordenfelt and P. Hellstrand (1999). Long-term effects of Ca(2+) on structure and contractility of vascular smooth muscle. *Am J Physiol* 277(1 Pt 1): C64-73.
- Liu, S. Q. (1998). Influence of tensile strain on smooth muscle cell orientation in rat blood vessels. *J Biomech Eng* 120(3): 313-20.
- Liu, S. Q. and Y. C. Fung (1989). Relationship between hypertension, hypertrophy, and opening angle of zero-stress state of arteries following aortic constriction. *J Biomech Eng* 111(4): 325-35.
- Lowry, O. H., N. J. Rosebrough, A. L. Farr and R. J. Randall (1951). Protein measurement with the Folin phenol reagent. *J Biol Chem* 193(1): 265-75.
- Malek, A. M., S. L. Alper and S. Izumo (1999). Hemodynamic shear stress and its role in atherosclerosis. *J Am Med Assoc* 282(21): 2035-2042.
- Masuda, H., H. Bassiouny, S. Glagov and C. K. Zarins (1989). Artery wall restructuring in response to increased flow. *Surg Forum* 40: 285-286.
- Masuda, H., K. Kawamura, K. Tohda, T. Shozawa, M. Sageshima and A. Kamiya (1989). Increase in endothelial cell density before artery enlargement in flow-loaded canine carotid artery. *Arteriosclerosis* 9(6): 812-23.

- Matsumoto, T. and K. Hayashi (1994). Mechanical and dimensional adaptation of rat aorta to hypertension. *J Biomech Eng* 116(3): 278-83.
- Matsumoto, T., E. Okumura, Y. Miura and M. Sato (1999). Mechanical and dimensional adaptation of rabbit carotid artery cultured in vitro. *Med Biol Eng Comput* 37(2): 252-6.
- Melkumyants, A. M. and S. A. Balashov (1990). Effect of blood viscosity on arterial flow induced dilator response. *Cardiovasc Res* 24(2): 165-8.
- Melkumyants, A. M., S. A. Balashov and V. M. Khayutin (1989). Endothelium dependent control of arterial diameter by blood viscosity. *Cardiovasc Res* 23(9): 741-7.
- Merrilees, M. J., B. W. Beaumont and L. J. Scott (1995). Fluoroprobe quantification of viable and non-viable cells in human coronary and internal thoracic arteries sampled at autopsy. *J Vasc Res* 32(6): 371-7.
- Nathan, C. (1992). Nitric oxide as a secretory product of mammalian cells. 6(12): 3051-3064.
- Nichol, J. W., M. Petko, R. J. Myung, J. W. Gaynor and K. J. Gooch (2005). Hemodynamic conditions alter axial and circumferential remodeling of arteries engineered ex vivo. *Ann Biomed Eng* 33(6): 721-32.
- Nichols, W. W. and N. F. O'Rourke (1998). *McDonalds's Blood Flow in Arteries: Theoretical, Experimental, and Clinical Principles*. London, Arnold.
- Olivetti, G., P. Anversa, M. Melissari and A. V. Loud (1980). Morphometry of medial hypertrophy in the rat thoracic aorta. *Lab Invest* 42(5): 559-65.
- Osol, G. (1995). Mechanotransduction by vascular smooth muscle. *J Vasc Res* 32(5): 275-92.
- Peterkofsky, B. and D. J. Prockop (1962). A method for the simultaneous measurement of the radioactivity of proline-C14 and hydroxyproline-C14 in biological materials. *Anal Biochem* 4: 400-6.

- Rachev, A. (1997). Theoretical study of the effect of stress-dependent remodeling on arterial geometry under hypertensive conditions. *J Biomech* 30(8): 819-27.
- Rachev, A. (2000). A model of arterial adaptation to alterations in blood flow. *J Elasticity* 61: 83-111.
- Rachev, A., E. Manoach, J. Berry and J. E. Moore, Jr. (2000). A model of stress-induced geometrical remodeling of vessel segments adjacent to stents and artery/graft anastomoses. *J Theor Biol* 206(3): 429-43.
- Rachev, A., N. Stergiopulos and J. J. Meister (1996). Theoretical study of dynamics of arterial wall remodeling in response to changes in blood pressure. *J Biomech* 29(5): 635-42.
- Rachev, A., N. Stergiopulos and J. J. Meister (1998). A model for geometric and mechanical adaptation of arteries to sustained hypertension. *J Biomech Eng* 120(1): 9-17.
- Rodriguez, E. K., A. Hoger and A. D. McCulloch (1994). Stress-dependent finite growth in soft elastic tissues. *J of Biomech* 27(4): 455-67.
- Ruiz-Razura, A., J. L. Williams, C. L. Reilly, B. E. Cohen, V. B. Schini, P. M. Vanhoutte and S. Thomsen (1994). Acute intraoperative arterial elongation: histologic, morphologic, and vascular reactivity studies. *Journal of Reconstructive Microsurgery* 10(6): 367-73.
- Schwartz, L. B., C. M. Purut, M. F. Massey, J. C. Pence, P. K. Smith and R. L. McCann (1996). Effects of pulsatile perfusion on human saphenous vein vasoreactivity: a preliminary report. *Cardiovasc Surg* 4(2): 143-9.
- Shi, S. R., B. Chaiwun, L. Young, R. J. Cote and C. R. Taylor (1993). Antigen retrieval technique utilizing citrate buffer or urea solution for immunohistochemical demonstration of androgen receptor in formalin-fixed paraffin sections. *J Histochem Cytochem* 41(11): 1599-604.
- Skalak, R., G. Dasgupta, M. Moss, E. Otten, P. Dullumeijer and H. Vilmann (1982). Analytical description of growth. *J of Theor Biol* 94(3): 555-77.

- Sumpio, B. E., A. J. Banes, W. G. Link and G. Johnson (1988). Enhanced collagen production by smooth muscle cells during repetitive mechanical stretching. *Arch Surg* 123(10): 1233-6.
- Surowiec, S. M., B. S. Conklin, J. S. Li, P. H. Lin, V. J. Weiss, A. B. Lumsden and C. Chen (2000). A new perfusion culture system used to study human vein. *J Surg Res* 88(1): 34-41.
- Taber, L. A. and D. W. Eggers (1996). Theoretical study of stress-modulated growth in the aorta. *J Theor Biol* 180(4): 343-57.
- Takamizawa, K., K. Hayashi and T. Matsuda (1992). Isometric biaxial tension of smooth muscle in isolated cylindrical segments of rabbit arteries. *Am J Physiol* 263(1 Pt 2): H30-4.
- Thom, T., N. Haase, W. Rosamond, V. J. Howard, J. Rumsfeld, T. Manolio, Z. J. Zheng, K. Flegal, C. O'Donnell, S. Kittner, D. Lloyd-Jones, D. C. Goff, Jr., Y. Hong, R. Adams, G. Friday, K. Furie, P. Gorelick, B. Kissela, J. Marler, J. Meigs, V. Roger, S. Sidney, P. Sorlie, J. Steinberger, S. Wasserthiel-Smoller, M. Wilson and P. Wolf (2006). Heart disease and stroke statistics--2006 update: a report from the American Heart Association Statistics Committee and Stroke Statistics Subcommittee. *Circulation* 113(6): e85-151.
- Vaishnav, R. N., J. Vossoughi, D. J. Patel, L. N. Cothran, B. R. Coleman and E. L. Ison-Franklin (1990). Effect of hypertension on elasticity and geometry of aortic tissue from dogs. *J Biomech Eng* 112(1): 70-4.
- Voisard, R., J. von Eicken, R. Baur, J. E. Gschwend, U. Wenderoth, K. Kleinschmidt, V. Hombach and M. Hoher (1999). A human arterial organ culture model of postangioplasty restenosis: results up to 56 days after ballooning. *Atherosclerosis* 144(1): 123-34.
- Vorp, D. A., D. G. Peters and M. W. Webster (1999). Gene expression is altered in perfused arterial segments exposed to cyclic flexure ex vivo. *Ann Biomed Eng* 27(3): 366-71.
- Vorp, D. A., D. A. Severyn, D. L. Steed and M. W. Webster (1996). A device for the application of cyclic twist and extension on perfused vascular segments. *Am J Physiol* 270(2 Pt 2): H787-95.

- Wilson, D. P., L. Saward, P. Zahradka and P. K. Cheung (1999). Angiotensin II receptor antagonists prevent neointimal proliferation in a porcine coronary artery organ culture model. *Cardiovasc Res* 42(3): 761-72.
- Zarins, C. K., M. A. Zatina, D. P. Giddens, D. N. Ku and S. Glagov (1987). Shear stress regulation of artery lumen diameter in experimental atherogenesis. *J Vasc Surg* 5(3): 413-20.
- Zulliger, M. A., G. Montorzi and N. Stergiopulos (2002). Biomechanical adaptation of porcine carotid vascular smooth muscle to hypo and hypertension in vitro. *J Biomech* 35(6): 757-65.